# Linear and Star-Shaped Poly(Ethylene Oxide) Grafted Surfaces: Grafting Density and Protein Adsorption

by

Susan J. Sofia Allgor

B.S. Chemical Engineering
Cornell University, 1990

SUBMITTED TO THE DEPARTMENT OF CHEMICAL ENGINEERING IN PARTIAL FULFILLMENT OF THE REQUIREMENTS FOR THE DEGREE OF

DOCTOR OF PHILOSOPHY IN CHEMICAL ENGINEERING
AT THE
MASSACHUSETTS INSTITUTE OF TECHNOLOGY

JUNE 1996



Signature of Author: _____
Department of Chemical Engineering
May 20, 1996

Certified by: _____
Edward W. Merrill
C.P. Dubbs Professor of Chemical Engineering
Thesis Supervisor

Accepted by: _____
Robert E. Cohen
Professor of Chemical Engineering
Chairman, Committee for Graduate Students

# LINEAR AND STAR-SHAPED POLY(ETHYLENE OXIDE) GRAFTED SURFACES: GRAFTING DENSITY AND PROTEIN ADSORPTION

SUSAN J. SOFIA ALLGOR

Submitted to the Department of Chemical Engineering on May 20, 1996
in Partial fulfillment of the Requirements for the Degree of Doctor of Philosophy
in Chemical Engineering

Abstract

Poly(ethylene oxide) polymer, in linear and star form, was covalently grafted to various surfaces by two different methods. The first method involved the coupling of PEO molecules via terminal hydroxyl groups activated by tresyl chloride to aminosilane-treated silicon wafers. Linear PEG of molecular weights 3400, 10 000, and 20 000 g/mol, and PEO star molecules 228 and 3510, were grafted to the surfaces. The amount of PEO coupled to the surface was varied by changing the concentration of the tresyl-PEO solution. The dry PEO thickness on the surface was measured using X-ray photoelectron spectroscopy (XPS) and ellipsometry, from which the grafting density was calculated.

The PEO surfaces were exposed to solutions of each of three proteins: cytochrome-c (12 kD), albumin (68 kD), and fibronectin (500 kD). The degree of adsorption of each protein was determined by XPS and ellipsometry, and recorded as a function of PEO grafting density. All three proteins were found to reach zero adsorption at the highest grafting densities on all three PEG surfaces. On both star PEO surfaces, albumin and fibronectin decreased to zero adsorption at intermediate values of grafting density, whereas cytochrome-c continued to adsorb at all grafting densities, although with a decreasing trend. A model was developed to explain the protein adsorption behavior, which was based on the spatial arrangement of PEO chains on the surface. For linear PEG surfaces, extensive overlap of chains was found to be necessary for the prevention of protein adsorption. PEO stars are sufficiently dense in PEO segments to prevent protein adsorption without the need for overlap. Therefore, it is the open spaces between star molecules where proteins adsorb; these spaces need to be smaller than the effective size of the protein to prevent adsorption. This condition was achieved for albumin and fibronectin, but not for cytochrome-c.

The second method for binding PEO to surfaces involved the use of electron beam irradiation in two steps. In the first, methacrylic acid was grafted and polymerized to a polymer surface, changing it from hydrophobic to hydrophilic. Exposure of this surface to PEO aqueous solutions resulted in strong hydrogen bonding of the PEO which in the second radiation step was covalently grafted. Since terminal hydroxyl groups were not involved in the grafting, PEO of much higher molecular weight could be studied. The PEO grafts were stable; they could not be removed with extensive washing with water, soaking in basic solution, or gentle mechanical scraping. Both monolayers and multilayers of PEO were formed. The density of the monolayers were found to have little dependence on the molecular weight or concentration of the PEO solution; multilayers could be controlled by varying the viscosity of the PEO solution and the method of application. The PEO-grafted monolayers were tested for their ability to prevent protein adsorption, using the same proteins as above. Monolayers of PEO stars were the most effective, at best showing a 60% decrease in adsorption from untreated controls. One million molecular weight linear PEO monolayers were almost as effective as star monolayers, and 35 000 g/mol linear PEO was bound too closely to the surface, due to its small size, to have much impact in preventing protein adsorption. The reason for the continued protein adsorption was believed to be due to the grafted methacrylic acid chains being long enough to extend through the PEO layer, thus being accessible on the surface.

Thesis Advisor:
Edward W. Merrill
C.P. Dubbs Professor of Chemical Engineering

Thesis Committee:
Professor Robert Cohen
Professor Linda Griffith-Cima
Professor Paul Laibinis

# Acknowledgments

I would like to first thank Professor Merrill for being a wonderful advisor. Your patience, wealth of knowledge, and endless enthusiasm made working for you a pleasure and a great learning experience. I would also like to thank the members of my thesis committee, for without their knowledge and guidance, I would not have reached this point when I did.

My thanks to Ambuj for being such a great friend, roommate, labmate, and for taking me under your wing when I joined the lab and for sharing with me the contents of your overstuffed, overeducated brain; to Premnath, for also sharing your extensive knowledge with me, especially for your help on the model, and for being a good friend -- I'll always remember our philosophical discussions -- So when are you getting married? To Diane, hopefully my attempt at giving advice and guidance didn't lead you astray too often, and thanks for being such a good friend and listener.

To Stephanie Lopina and Phil Kuhl for your help with issues on PEO coupling and protein adsorption; to Kenneth Wright, for all your time and effort is doing the irradiations for me -- I truly appreciate it; To Kane Jennings, for sharing your knowledge of surface analysis with me, the younger teaching the older; to Yuan Lu, for all your efforts in teaching me how to optimize my use of the XPS, especially for your patience at those times, and there were more than I'd like to admit, when I seemed to have lost all common sense.

Many, many thanks to all those friends I made here over the years, who made being at MIT tolerable and even enjoyable: To Rick, you're a great friend -- We'll have to get together for coffee in Edmonton sometime; to M.J. and your many fun get-togethers, Lloyd and your goofy yet endearing ways, Andrena, Colin, Cath and Tobi for being great roommates as well as friends, Tim and Ed, to the crowd at lunch who made lunchtime conversation oh so interesting; to my soccer buddies Cheryl, Marcy, Cindy, Terrence, Jason -- thanks for keeping me in shape, albeit a bit tired, in the final months of thesis work and writing. And to my best friend from home: thanks for helping me keep my sanity, even when you were in luxurious Central America; Welcome back!!

And last, but most importantly, I'd like to thank my family: to Mom and Dad for your constant, boundless love and support, and for believing in me! To my sisters Karen and Debbie: Karen, you were always there for me as you have been all my life -- a simple thanks just doesn't seem like enough; and Deb, thanks for your love and support, and for typing what was probably the most difficult to decipher, yet personally important, technical report of your career.

And to Russ -- these have been difficult months for both of us, but you still managed to give me the love, support, understanding, and help that I needed to get this thing done. Thanks for being there, and I promise that I'll do the same for you next year when your time comes round, even if I won't understand a word I'm reading.

TABLE OF CONTENTS

## LIST OF TABLES

## LIST OF FIGURES

# CHAPTER 1

## Motivation and Literature Review

### 1.1 PEO and Biocompatibility

Despite the great strides that have been made in the biomedical field in the area of artificial devices, there still remains the problem of achieving a high level of biocompatibility with artificial surfaces, especially those used in contact with blood. Problems of protein and platelet deposition, platelet activation and thrombus formation, complement activation, etc., still exist in the use of current biomaterials. Many researchers are still searching for a material that is more inert in a biological environment.

An end to the search for this ideal material may be made with the use of poly(ethylene oxide) polymer, $(-CH_2CH_2O-)_n$. PEO is probably the most biocompatible material known thus far and is gaining wider recognition as such. It was first noted for its non-adsorption of proteins and platelets over twenty years ago by Hiatt et al.[1] and Wasiewski et al.[2], which lead to its use for concentrating proteins in blood[3] and precipitating proteins from solution[4]. In each of these cases, the PEO was either used in or taken from free solution, and it was the complete non-interaction of the proteins with the PEO that was the key to the experimental successes. This initial work has now been greatly expanded to include nonthrombogenic, non-protein-adsorbing PEO surfaces with significant success[5,6].

It is still not clearly known why PEO is so non-adsorptive. In fact, for many years the answer to the question of what are the characteristics of a truly biocompatible surface has been sought without much success. Many surface characteristics have been investigated, such as surface wettability[7], surface tension[8], crystalline vs. amorphous structure[9], fluid vs. rigid structure[9], and surface charge[9,10].

However, no real conclusive results were obtained[9]. Most materials possess some of the "right" characteristics but not all of them, and chain mobility causes surface characteristics to change depending on the environment in which it is in contact. In the case of PEO, it is believed that its fluid-like behavior when hydrated, and the small hydrophobic (ethylene) and hydrophilic (ether) subunits provide only weak binding sites for proteins[11]. The spatial distance between these subunits, as well as their size, is apparently important since poly(propylene oxide) and poly(tetramethylene oxide) do not exhibit the same non-adsorptive characteristics[5]. The accepted hypothesis for why PEO surfaces are resistant to protein adsorption is that there is a steric repulsion that arises from the loss of configurational entropy as the PEO chains are compressed by an approaching protein.[12,13] In addition, the PEO-water interface has a low interfacial free energy and thus a low driving force for protein adsorption.[14] The protein does not perceive the PEO-water interface much differently than the surrounding solution.

In order for PEO to be used as a biomaterial, it must first be immobilized into a network with another material, since PEO is soluble nearly without limit in aqueous solution and is not mechanically strong in pure form (i.e., as a cross-linked hydrogel). Two ways of achieving immobilization are by covalent binding of one or both ends of the PEO chain to an insoluble substrate, surface, or by incorporating PEO into a network with another polymer, either as an interpenetrating network (IPN) or covalently through a block copolymer network. Both are schematically shown in Figure 1-1. Nagoaka and coworkers[15] end-linked one end of PEO via a methacrylate to various insoluble polymers. PEO end-linked at both ends, either to a surface or in a network, has been achieved with a wide variety of materials: segmented polyurethanes (where the PEO constitutes the "soft segment" continuous phase)[16-21], polysiloxanes[11,22,23], polystyrenes[24-26], polyfunctional isocyanates[27], poly(ethylene

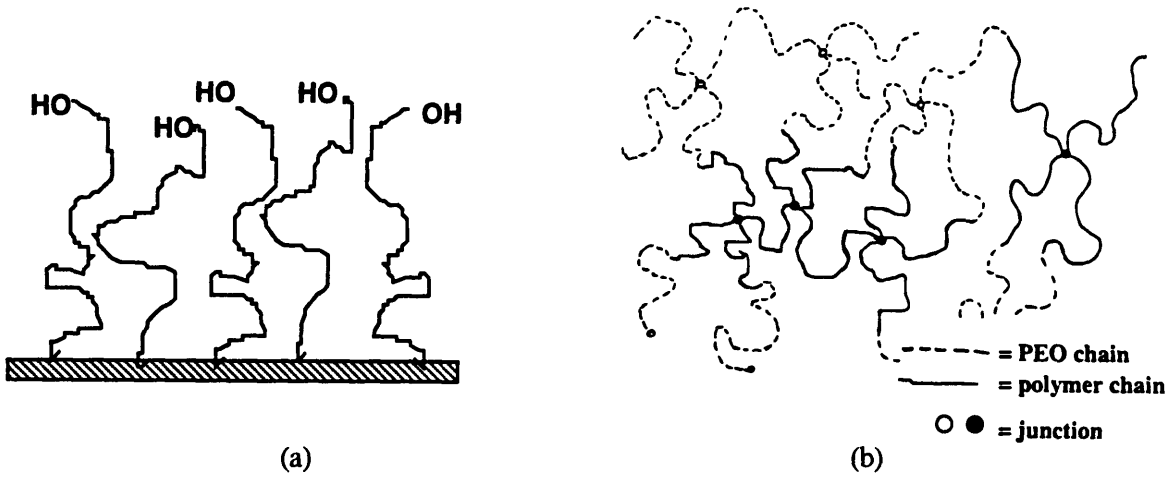


Figure 1-1. Linear PEO (a) end-linked to surfaces, (b) incorporated into networks.

terephthalates)[19,28], poly(methyl methacrylates)[19,29,30], poly(lactic-glycolic acids)[31], poly(tetramethylene oxide)[32], and poly(vinyl chloride)[33]. An important outcome of these studies is the common trend of decreasing adsorption and biological activity with increasing PEO content. Sa da Costa et al.[17] found that an extrapolation to zero platelet adhesion would correspond to pure amorphous PEO on the surface. Desai and Hubbell[28] and several others[11,13,34] reported similar results of greatly reduced protein and platelet adhesion to surfaces as the PEO content and/or PEO molecular weight was increased. Some conflicting results, however, were shown by Chaikof and Merrill[22] in their work with PEO/siloxane networks. In these studies, PEO networks were shown to have actually enhanced thrombogenicity. PEO/siloxane networks with 65 percent, 2000 molecular weight PEO content exhibited greatly increased levels of platelet and fibrinogen deposits as well as a marked increase in complement activation over the respective pure PEO and pure siloxane materials. It was believed that the increased bioactivity was due to the PEO/siloxane juctions being more reactive with biological entities than the control materials alone. A clear result of the above studies is that the highest level of

biocompatibility for a bio-contacting surface can only be achieved when the surface consists solely of amorphous PEO polymer.

Two effective ways of attaining PEO as the sole component exposed on a surface are by coating a layer of PEO hydrogel on a surface by radiation cross-linking[35], or by covalently binding PEO to the surface. As for the former, problems arise where the hydrogel will not bind to the underlying substrate material, and will eventually delaminate from the surface. It is believed that this is caused by the inherent hydrophilic/hydrophobic difference between PEO and the substrate polymer, such that there is not a close enough association between the two for them to bind. So an effective coverage of the surface could be achieved, but the layer is not stable.

As for covalently binding linear PEO to surfaces, there are several critical hurdles to overcome. First, in order to end-link the PEO to a surface, that surface must first be functionalized with a specific group to which the PEO can bind. Various methods have been tried, such as direct chemical treatment or plasma processes, but these methods can be highy destructive to the surface, either creating significant surface roughness or fragmentation (see Appendix A).[36] In addition, any functionalization will usually be specific to a certain polymer material, so extending a method to other polymers, as an intended use may dictate, would not be possible. Second, the inherent roughness, dynamics, and heterogeneity of a polymer surface probably make it difficult to obtain complete, dense coverage of a surface through endlinking PEO. It has been observed in the above referenced studies that greater reduction in protein adsorption or biological activity occurred with increased PEO content and/or molecular weight. This is probably because smaller PEO contents or molecular weights were not present in sufficient density to effectively cover the surface. It is not known, however, from any of these studies, what specific PEO content on the surface (i.e., spacing between chains and/or PEO

molecular weight) is sufficient for the non-adsorption of proteins and cells, since polymer surfaces are complex and difficult to characterize with a high degree of detail and accuracy.

## 1.2 Linear vs. Star-Shaped PEO

One of the key issues investigated in this thesis deals with exploiting the inherent differences between linear PEO molecules and star-shaped PEO molecules in their use in enhancing surface biocompatibity, since there are important structural differences between the two PEO types. In general, in the last thirty years, there has been a steady increase in the interest and investigation of star-shaped polymer molecules. As a general definition, star molecules are species consisting of a central core region with linear chains, or "arms", radiating outward from that core. The number and length of these arms can vary. The first star molecules were synthesized by Schaefgen and Flory[37] in 1948 using step polymerization, but with the advent of anionic polymerization in the 1950's, the field has grown rapidly. There are many reasons for the increased interest in star molecules, such as gaining a better understanding of branching architecture in how it affects polymer solution properties, or in using star molecules as micelles, or as drug delivery systems, or to test current macromolecular theories on branched molecules. It is well known that branched polymer molecules (star molecules being the "ideal" branched molecule) have different properties than their linear counterparts due to the high segment densities and restricted segmental motion. The study presented in this thesis takes advantage of star molecule properties, as well as the extensive biocompatibility of PEO, and combines them to create biocompatible, non-protein adsorptive, "inert" surfaces for biomedical applications, ultimately comparing their efficacy to linear PEO surfaces.

PEO star molecules are synthesized by anionic polymerization using a "core first" method.[38-40] In this procedure, divinyl benzene (DVB) monomer, used to form the core of the star, is added dropwise to a cooled (-40°C) solution of potassium naphthalene initiator ($K^+$) in THF. Once the cores have formed, oxirane (or ethylene oxide, EO) is added and the temperature slowly increased to 30°C to allow for the polymerization of the PEO arms. The active ends are then terminated with acidified methanol to produce a hydroxyl terminus on each arm. The [DVB]/[$K^+$] ratio theoretically determines the functionality, f, of the stars, and the [EO]/[$K^+$] ratio is used to theoretically determine the molecular weight of the PEO arms, $M_{arm}$. It has been found, however, that samples with varying polydispersity result from the synthesis.[38,41] It is believed that this polydispersity results mainly from a large distribution in core functionality and not arm molecular weight.[38]

A second way PEO star molecules can be formed is in using an "arm first" method. In this way, the PEO arms are synthesized first, leaving the active end of each arm to bind to the DVB monomer, and then the DBV to each other to form the star. The "arm-first" method is commonly used in the synthesis of polystyrene[42-44], polyisoprene[45-47], and polybutadiene[48] stars where the cores are a polyfunctional chlorosilane, and significant success in making near monodisperse samples has been achieved. However, for PEO stars, a great advantage of the "core first" method is lost, and that is the presence of the hydroxyls at each arm end. It is currently not possible to anionically polymerize PEO such that the initiating end has a hydroxyl group, or can be easily converted to a hydroxyl group. With such a high hydroxyl concentration per molecule (exactly f/2 greater than a linear molecule), these molecules have great potential for attachment of biological molecules, or for attachment to a surface (see Figure 1-2). For example, by binding heparin to a surface of PEO stars, one could form an actively anti-thrombogenic surface. A second example is in the binding of a biomolecule to star-coated

beads in a packed column, where through antigen/antibody or substrate/ligand interactions, very specific protein separations could be achieved. Therefore, the presence of the hydroxyl groups is a key advantage in the potential applications of PEO star (and linear) molecules.

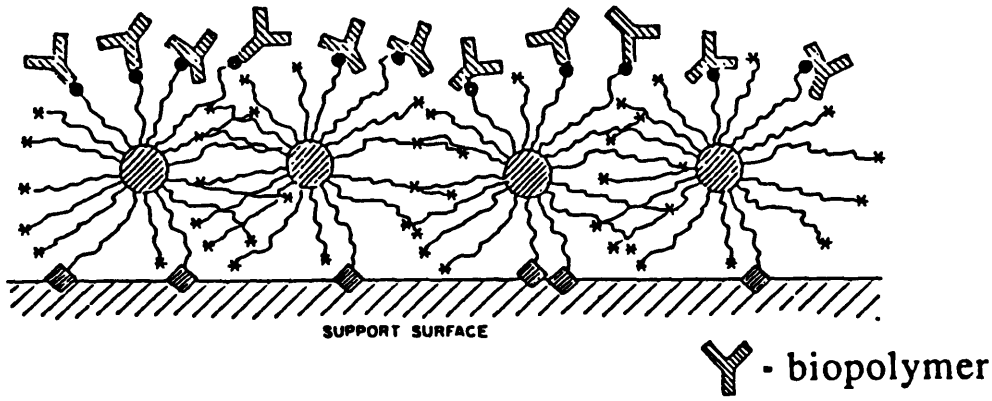


Figure 1-2: A biologically active surface using star molecules.

In addition to PEO stars having a greater number of chain end hydroxyl groups per molecule compared to linear PEO, stars are also more dense in PEO than linear molecules due to their structure. This is clearly observed when samples are analyzed using gel permeation chromatography coupled to light scattering (GPC-LS, see Appendix B).[49] As a small volume of dilute polymer solution passes through the packed columns of a GPC, the molecules are separated based on their hydrodynamic size; the larger molecules pass through (elute) first and the smaller ones elute last. When GPC is coupled to LS, a direct, on-line measurement of molecular weight can be made as the molecules elute. Figure 1-3 shows a plot of log(MW) vs. elution time for a linear PEO sample along with a star PEO sample. The star molecules having a hydrodynamic volume equal to linear molecules (i.e., eluting at the same elution time) have a greater molecular weight, as the plot for PEO stars lies above that of the linear PEO until very high elution times where the stars are of such low functionality (i.e., $f \approx 3$) that they are

essentially linear. For example, a linear molecule eluting at 18 minutes has an approximate molecular weight of 160,000 g/mol, whereas the star molecule at the same elution time has a molecular weight of approximately 560,000 g/mol. Therefore, the star molecule is over three times more dense than the linear molecule having equivalent hydrodynamic size. This is the basis behind the observation that, with increasing functionality, star molecules behave increasingly as hard spheres in solution. It has been observed that for functionalities grater than 20, star molecules have a Huggin's coefficient, $k_H$, near the hard-sphere value of 0.99, and have a value for the ratio of thermodynamic radius to radius of gyration near the hard-sphere value of 1.291.[45]

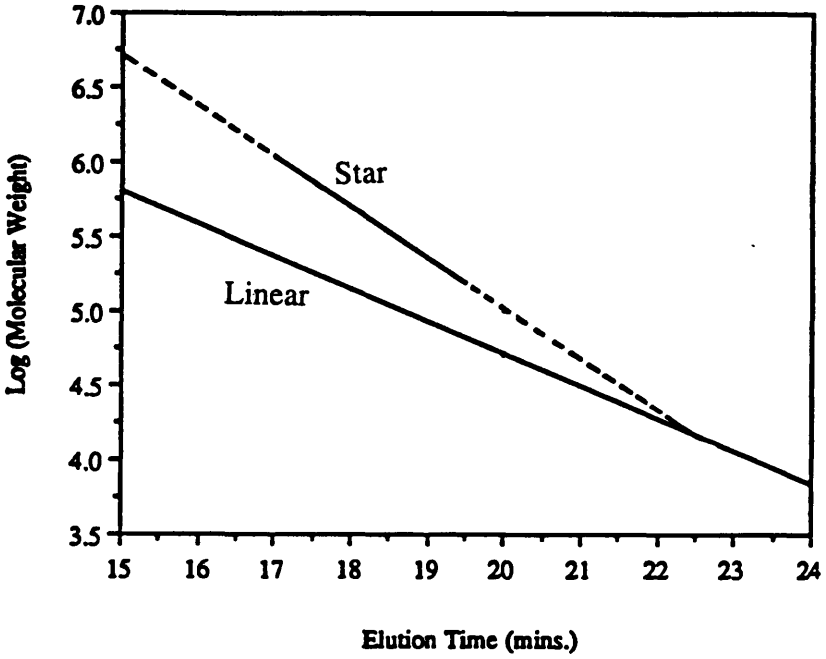


Figure 1-3: Plot of log(MW) vs. elution time for linear and star PEO obtained from GPC-LS.

The dense character of PEO star molecules is important from the standpoint of a layer of PEO covalently grafted to a surface for the purpose of preventing non-specific adsorption of proteins. With PEO stars being more dense in PEO than linear, they naturally offer better protection of the surface in

preventing proteins from reaching it and adsorbing. (This also applies to cell adsorption and activity, since cells interact with their environment through proteins.) Improved effectiveness via a denser PEO layer was brought to attention in the recent theoretical study by Jeon et al[12,50]. They investigated the prevention of protein adsorption to a PEO grafted surface through an analysis of attractive and repulsive forces as a protein approaches an end-linked PEO surface. One of the important conclusions to come of this study was that the critical parameter for the prevention of protein adsorption was the PEO density on the surface (i.e., chain spacing), where the denser the PEO coverage, the higher the probability the protein would be repelled. This general conclusion is in agreement with the experimental results of Prime and Whitesides.[51] In this study, self-assembled monolayers (SAMs) of an alkanethiol on gold were formed where a varying fraction of the SAM had a terminal PEG unit. The length of the PEG unit varied from 1 to 17 monomers. It was found that SAMs having a PEG unit of greater than two monomers were sufficient, at sufficient densities on the surface (i.e., fraction of SAM that was PEG-SAM), to prevent protein adsorption.

Lastly, in keeping with the hard-sphere character of star molecules, another important property of star molecules that is quite different from linear forms is the increased accessibility of the chain end hydroxyl groups. For a linear, randomly coiling PEO molecule, the chain ends could be anywhere within the volume of the molecule, as the molecule has a low segment density throughout the entire volume when hydrated (greater then 95% water). Star molecules, on the other hand, are much more dense in polymer segments, as seen in Figure 1-3. This density, however, is not constant throughout the volume of the molecule. As Daoud and Cotton[52] describe in their theoretical model of star polymers, there are three distinct regions of a star: 1) a close-packed, "melt-like" core region of constant segment density, 2) a high segment concentration intermediate region, and 3) a semi-dilute

concentrated outer region. Therefore, because of the steric hinderance in the inner regions of the star, the arms of the star are more extended than if they were a free, random coil. This has been noted in many theoretical studies of star molecules[53-58], as well as experimental studies.[43,45,46,56] The arm extension increases as the functionality, f, of the star polymer increases, as the stars become more like hard spheres.[45,55,57,58] A result of this arm extension is the greater accessibility of the arm chain ends to the outer regions of the molecule. This high accessibility of the chain end hydroxyl groups greatly increases the probability of binding a specific biomolecule, such as an enzyme or antibody, to the star molecules, or in binding star molecules to a surface. With the fact that many biomolecules could potentially bind to a single star, the biological activity could be highly concentrated and enhanced as opposed to using linear PEO molecules.

## 1.3 Focus of the Thesis

The question of what densities and molecular weights of PEO on a surface are sufficient to result in a surface that does not adsorb proteins, and therefore not cause any adverse biological reactions, is addressed in Chapters 2 and 3. Linear PEO molecules of differing molecular weights, and star-shaped PEO molecules of differing properties (f and $M_{arm}$), were end-linked to amine-functionalized silicon wafers in a range of grafting densities. The protein adsorption on these surfaces was then observed as a function of the PEO form, molecular weight, grafting density, and protein size. Silicon wafers provided a very stable, smooth surface (down to atomic levels) with which an accurate characterization of the surface could be made.

The grafting of PEO molecules, star and linear form, to polymer surfaces is addressed in Chapters 4 and 5. A method was developed where, by using electron beam irradiation, PEO could be

successfully grafted to polymer surfaces, forming a stable layer and in sufficient density such that it is possible to achieve the complete non-adsorption of proteins. This method provides extreme versatility, both in the amount of PEO grafted in the layer, and in the possibility of binding the PEO to a wide range of polymer materials. Therefore, there is significant potential for the use of this method in industrial/biomedical applications.

## 1.4 References for Chapter 1


1. C.W. Hiatt, A. Shelvkov, E.J. Rosenthal, and J.N. Galimore, *J. Chromatogr.*, 56, 362 (1971).

2. W. Wasiewski, M.J. Rasco, B.M. Martin, J.C. Detwiler, and J.W. Fenton, *Thromb. Res.*, 8, 881 (1976).

3. M. Fried and P.W. Chun, *Meth. in Enzymol.*, 22, 238 (1971).

4. K.C. Ingham, *Meth. in Enzymol.*, 182, 301 (1990).

5. E.W. Merrill and E.W. Salzman, *Am. Soc. Artif. Intern. Organs*, 6, 60 (1983).

6. J.M. Harris, Poly(Ethylene Glycol) Chemistry: Biotechnical and Biomedical Applications, Chapter 14, Plenum Press, New York, 1992.

7. H. Lampert, Die Physikalische Seite des Blutgerunnings Problems, Leipzig, George Thieme Verlag, 1931.

8. D.J. Lyman, J.L. Brash, and S.W. Chaikin, *Trans. Am. Soc. Artif. Intern. Organs*, 14, 250 (1968).

9. E.W. Salzman and E.W. Merrill. Hemostasis and Thrombosis, Chapter 69, J.B. Lippincott Company, Philadelphia, PA, 1982.

10. P.N. Sawyer and J.W. Pate, *Am. J. Physiol.*, 175, 103 (1953).

11. S.L. Verdon, E.L. Chaikof, J.E. Coleman, L.L. Hayes, R.J. Connolly, K. Ramberg, E.W. Merrill, and A.D. Callow, *Scanning Microscopy*, 4, 341 (1990).

12. S.I. Jeon, J.H. Lee, J.D. Andrade, and P.G. De Gennes, *J. Coll. Interface Sci.*, 142, 149 (1991).

13. J.H. Lee, P. Kopeckova, J. Kopecek, and J.D. Andrade, *Biomaterials*, 11, 455 (1990).

14. D.L. Coleman, D.E. Gregonis, and J.D. Andrade, *J. Biomed. Mater. Res.*, 16, 381 (1982).

15. S. Nagoaka, Y. Mori, H. Takuchi, K. Yokota, H. Tanyawa, and S. Nishiumi, *Polymer Preprints*, 24, 67 (1983).

16. J.L. Brash and S. Uniyal, *J. Polym. Sci.*, 66, 377 (1979).

17. V. Sa da Costa, D. Brier-Russell, G.Trudell, D.F. Waugh, E.W. Salzman, and E.W. Merrill, *J. Coll. Interface Sci.*, 76, 594 (1980).

18. N. Mahmud, S. Wan, V. Sa da Costa, V. Vitale, D. Brier-Russell, L. Kuchner, E.W. Salzman, and E.W. Merrill. Physical Chemical Aspects of Polymer Surfaces, Vol. 2, K.L. Mittall ed., Plenum Press, New York, 1983.

19. N.P. Desai and J.A. Hubbell, *Biomaterials*, 12, 144 (1991).

20. J.G.F. Bots, L. van der Does, and A. Bantjes, *Biomaterials*, 7, 393 (1986).

21. J.H. Silver, C.W. Myers, F. Lim, and S.L. Cooper, *Biomaterials*, 15, 695 (1994).

22. E.L. Chaikof, E.W. Merrill, A.D. Callow, R.J. Connolly, S.L. Verdon, and K. Ramberg, *J. Biomat. Mater. Res.*, 26, 1163 (1992).

23. C. Sung, M.R. Sobarzo, and E.W. Merrill, *Polymer*, 31, 556 (1990).

24. K. Furusawa, Y. Shimura, K. Otobe, K. Atsumi, and K. Tsuda, *Kobanshi Ronbunshu*, 34, 309 (1977).

25. D. Grainger, T. Okano, and S.W. Kim. Advances in Biomedical Polymers, pp. 229-247, Plenum Press, New York, 1987.

26. K. Bergstrom, K. Holmberg, A. Safrani, A.S. Hoffman, M.J. Edgell, A. Kozlowski, B.A. Hovanes, and J.M. Harris, *J. Biomat. Mater. Res.*, 26, 779 (1992).

27. J.E. Mark. Elastomers and Rubber Elasticity, J.E. Mark and J. Lal eds., American Chemical Society, Washington DC, ACS Symposium Series, 193, 1982.

28. N.P. Desai and J.A. Hubbell, *J. Biomed. Mater. Res.*, 25, 829 (1991).

29. A.G. Shard, M.C. Davies, S.J.B. Tendler, C.V. Nicholas, M.D. Purbrick, and J.F. Watts, *Macromolecules*, 28, 7855 (1995).

30. P.D. Drumheller, and J.A. Hubble, *J. Biomat. Mater. Res.*, 29, 207 (1995).

31. P. Ferruti, M. Penco, P. D'Addato, E. Ranucci, and R. Deghenghi, *Biomaterials*, 16, 1423 (1995).

32. Y. Ikeda, S. Kohjiya, S. Takesako, and S. Yamashita, *Biomaterials*, 11, 553 (1990).

33. S. Nagoaka and A. Nakao, *Biomaterials*, 11, 119 (1990).

34. V. Sa da Costa, D. Brier-Russell, E.W. Salzman, and E.W. Merrill, *J. Coll. Interface Sci.*, 80, 445 (1981).

35. K.A. Dennison, *Radiation Crosslinked Poly(ethylene oxide) Hydrogel Membranes*, Ph.D. thesis, Department of Chemical Engineering, MIT, 1986.

36. S.J.S. Allgor and E.W. Merrill, AIChE Annual Meeting, Paper No. 197i, San Francisco, CA, November, 1994.

37. J. Schaefgren and P.J. Flory, *J. Am. Chem. Soc.*, 70, 2709 (1948).

38. Y. Gnanou, P. Lutz, and P. Rempp, *Makromol. Chem.*, 189, 2885 (1988).

39. P. Lutz and P. Rempp, *Makromol. Chem.*, 189, 1051 (1988).

40. D. Rein, J.P. Lamps, P. Rempp, P. Lutz, D. Papanogopoulos, and C. Tsitsilianis, *Acta Polymer*, 44, 225 (1993).

41. S.J. Sofia Allgor and A. Sagar, preliminary research, MIT, March, 1992.

42. J.W. Mays, N. Hadjichristidis, and L.J. Fetters, *Polymer*, 29, 680 (1988).

43. J.E.L. Roovers and S. Bywater, *Macromolecules*, 7, 443 (1974).

44. J. Roovers and P.M. Toporowski, *J. Polym. Sci. Polym. Phys. Ed.*, 18, 1907 (1980).

45. B.J. Bauer, L.J. Fetters, W.W. Graessley, N. Hadjichristidis, and G.F. Quack, *Macromolecules*, 22, 2337 (1989).

46. N. Hadjichristidis and J.E.L. Roovers, *J. Polym. Sci. Polym. Phys. Ed.*, 12, 2521 (1974).

47. N. Hadjichristidis. A. Guyot and L.J. Fetters, *Macromolecules*, 11, 668 (1978).

48. N. Hadjichristidis and J. Roovers, *Polymer*, 26, 1087 (1985).

49. A.D. Sagar, S.J. Sofia, and E.W. Merrill, *J. Chromatog.*, 635, 132 (1993).

50. S.I. Jeon and J.D. Andrade, *J. Coll. Interface Sci.*, 142, 159 (1991).

51. K.L. Prime and G.M. Whitesides, *J. Am. Chem. Soc.*, 15, 10714 (1993).

52. M. Daoud and J.P. Cotton, *J. Phys.* (Paris, Fr.), 43, 531 (1982).

53. K. Huber, W. Burchard, S. Bantle, and L.J. Fetters, *Polymer*, 28, 1997 (1987).

54. A.T. Boothroyd, G.L. Squires, L.J. Fetters, A.R. Rennie, J.C. Horton, and A.M.B.G. de Vallera, *Macromolecules*, 22, 3130 (1989).

55. A. Miyake and K.F. Freed, *Macromolecules*, 16, 1228 (1983).

56. J.F. Douglas, J. Roovers, and K.F. Freed, *Macromolecules*, 23, 4168 (1990).

57. G.S. Grest, K. Kremer, and T.A. Witten, *Macromolecules*, 20, 1376 (1987).

58. G.S. Grest, *Macromolecules*, 27, 3493 (1994).

# CHAPTER 2

## Protein Adsorption to PEO-Grafted Silicon Surfaces

### 2.1. Introduction

As reported in previous studies in the literature, the accurate experimental characterization of linear PEO chains grafted to a substrate surface has been difficult accomplish. This is mainly due to the fact that the surfaces on which the PEO was grafted, or incorporated onto, were polymers (see Chapter 1), and polymers can have very rough, non-uniform and dynamic surfaces that make their accurate characterization quite a challenge. To describe protein adsorption behavior on such surfaces is made that much more difficult.

The characterization of protein adsorption on PEO surfaces was achieved with self-assembled-monolayers (SAMs) on gold substrates.[1] These surfaces can be characterized very accurately with techniques such as ellipsometry, XPS, and ATR-FTIR, to name a few.[1,2] However, despite the fact that, in references 1 and 2, the PEG surfaces were well characterized, there were several issues that were not addressed. First, the study showed convincingly that only very short lengths of PEO (PEGs of only 2 to 6 monomer units) can succeed, at sufficient densities, to prevent protein adsorption. (This dispels the notion that very small molecular weight PEG loses its "ability" to repel proteins.[3]) The question of what grafting densities are required for longer PEG chains, such as 100 monomer units or more, is still open. Second, the method of assembling the PEG-SAMs is very well defined and specific to gold, on which high grafting

densities can be achieved. There is still the question of what maximum grafting densities can be achieved by end-linking longer PEG chains, and whether these densities are sufficient to prevent protein adsorption. Third, the means in which the protein adsorption was measured in reference 1 was ellipsometry. In theory, this is a very direct method. In practice, however, there is a large uncertainty in the value of $n_p$ the index of refraction of the protein layer, which precludes quantitative results from being achieved. The value of $n_p$ can vary quite a bit, depending on the specific protein, how much adsorbs, and possibly on the degree of denaturing that occurs when it adsorbs. Due to this uncertainty, the error in the measurements was approximated to be ±25%, and therefore only the general trend, and not the specific amount, could be accepted.

The procedure and results presented in this chapter provide methods of grafting, adsorption, and analysis that result in a fairly accurate depiction of the dependence of protein adsorption behavior on PEO linear and star grafted surfaces in a range of PEO grafting densities. Silicon wafers were used as a model substrate material, where the surface is stable and extremely flat. A triaminosilane was covalently coupled to the surface, which provided a high concentration of grafting sites (both primary and secondary amines) for the attachment of the PEO. Tresyl chloride chemistry was used to couple the PEO hydroxyl chain ends to the amines on the surface.[4,5] Tresyl chloride (trifluoroethanesulfonyl chloride, $CF_3CH_2SO_2Cl$) binds to hydroxyl groups in the reaction

$$CF_3CH_2SO_2Cl + HO\text{-}(CH_2CH_2O)_n\text{-} \rightarrow CF_3CH_2SO_2O\text{-}(CH_2CH_2O)_n\text{-} + HCl$$

Triethylamine (TEA) is used as an acid scavenger to ensure that the reaction keeps proceeding forward, far from equilibrium. The resulting end-group $CF_3CH_2SO_3$- is a good leaving group in the reaction with primary and secondary amines.

$$CF_3CH_2SO_2O\text{-}(CH_2CH_2O)_n\text{-} + H_2N\text{-} \rightarrow \text{-}NH\text{-}(CH_2CH_2O)_n\text{-} + CF_3CH_2SO_3H$$

The sulfonic acid byproduct is scavenged by carbonate buffer to prevent the solution from becoming acidic and halting the reaction by protonation of the amines. The resulting chemical group between the amine and PEO is a very stable secondary amine. High pHs are preferred in the reaction (pH 9-10) as the majority of amines are not protonated. However, in using the aminosilane-silicon substrates, the pH had to be kept below pH 8 to prevent the silane from being hydrolyzed from the silicon surface. Thus, the coupling reaction was always performed at pH 7.4 which is still satisfactory for tresyl chloride coupling.[4,5]

The PEO surfaces were made with various molecular weight linear and star PEO at varying grafting densities. The PEO surfaces were contacted with protein solutions of cytochrome-c, albumin, and fibronectin and the respective adsorptions measured. These three proteins were chosen because they span a wide range of sizes, from 12 kD for cytochrome-c (spherical in shape, diameter 34Å), 68 kD for albumin (spherical in shape, diameter 72Å), to 500 kD for fibronectin (rod-like shape, 600Å long and 25Å wide). This is so adsorption as a function of protein size could also be tested.

Both linear and star-shaped PEO molecules were grafted to the silicon surfaces to study the difference in their grafting densities and effectiveness at preventing protein adsorption. Linear PEO random coils have a very loose, non-dense structure with only two chain ends per molecule.

These chain ends could be located anywhere within the volume of the molecule, thus causing its grafting probability to decrease with increasing molecular weight. Star molecules, on the other hand, have very dense, hard-sphere character, with a large number of chain ends per molecule that are located at the outer regions of the molecule due to the steric hindrance within the center of the molecule. Thus, its probability of grafting to a surface is extremely high and would only decrease with a return to more random-coil characteristics (i.e., with increasing arm molecular weight or decreasing functionality). Analysis of the surfaces was performed using X-ray photoelectron spectroscopy (XPS) and ellipsometry. This chapter mainly presents the procedures and results from the experiments, and a more thorough discussion of the results is located in Chapter 3.

## 2.2. Experimental

### 2.2.1 Sample Preparation

#### 2.2.1.1 Aminosilane Coupling to Silicon

Test-grade silicon wafers (1 0 0) were obtained from Silicon Sense Inc. (Nashua, NH). Trimethoxysilylpropyldiethylenetriamine ($(MeO)_3\ Si(CH_2)_3NH(CH_2)_2NH(CH_2)_2NH_2$) was obtained from United Chemical Technologies (Bristol, PA) and used as received. Ultrapure water was provided from a Millipore Inc. (Bedford, MA) RO-60/Milli-Q water purification system (resistance = 18 MOhm-cm). Anhydrous methanol was used as received.

The aminosilane procedure was the same as that used by Stenger et al.[6] Silicon wafer pieces were first cleaned by soaking in a 1:1 (v:v) methanol/concentrated HCl solution for a minimum of 30 minutes. They were rinsed thoroughly with water, then placed in concentrated sulfuric acid (ca. 96%) for a minimum of 30 minutes. Once rinsed thoroughly with water, they

were quickly rinsed in methanol to remove the water. The silane solution consisted of 94% mildly acidified methanol (1 mM acetic acid in methanol), 5% water, and 1% silane by volume. When preparing the silane solution, the silane was first added to the acidified methanol, and then the water, one milliliter at a time. The water was added to the solution as soon as possible after the silane, and then the solution was immediately contacted with the silicon. Delays beyond several minutes between these steps can lead to inhomogeneities and inconsistencies in the resulting surface.[6] The samples were reacted for 15 minutes, rinsed thoroughly three times with methanol, then baked in a convection oven at 120 °C for 5 to 10 minutes. The wafers were coupled to tresylated PEO no more than 48 hours after they were prepared to avoid dust contamination on the surface and oxidation of the amines.

#### 2.2.1.2 Tresylation of Linear PEG and Star PEO

Linear poly(ethylene glycol) (PEG) standards were obtained from Scientific Polymer Products (Ontario, NY), molecular weights 10,000 g/mol ( $\overline{M}w$=9760 g/mol, PDI = 1.05) and 20,000 g/mol ( $\overline{M}w$= 19800 g/mol, PDI = 1.05). PEG 3400 ( $\overline{M}w$= 3350 g/mol, PDI = 1.1) was a gift provided by Shearwater Polymers, Inc. (Huntsville, AL). PEO star polymers were a gift from Dr. Pierre Lutz at the Institut Charles Sadron in Strasbourg, France. Two types were used in these studies: #228: $\overline{M}w$ = 200,000 g/mol, $\overline{M}_{arm}$= 10,000 g/mol, $\bar{f}$ = 20; PDI ≈ 2; #3510,: $\overline{M}w$ = 350,000 g/mol, $\overline{M}_{arm}$ = 5200 g/mol, $\bar{f}$ = 70, PDI ≈ 3.5. The weight average molecular weights were measured using gel permeation chromatography - light scattering. Trifluoroethanesulfonyl chloride (tresyl chloride, TrCl), and triethylamine (TEA) were obtained

from Aldrich Chemical Inc. (Milwaukee, WI) and used as received. Dichloromethane ($CH_2Cl_2$) and methanol were used without any further purification.

The tresylation reaction procedure was the same as that published by Nilsson and Mosbach.[4,5] The reaction vessel (100 ml round-bottom flask) with stir bar was dried in a convection oven at 120 °C for a minimum of 24 hours before reaction. The PEO to be tresylated was dissolved in dichloromethane (5-10% (w/v), usually 2 g PEO in 20-25 ml $CH_2Cl_2$) before molecular sieves were added. The solution was allowed to finish bubbling, lightly capped, (ca. 30 minutes) before being sealed and stored at 4 °C for a minimum of 24 hours. Molecular sieves were added to a small aliquot (ca. 10 ml) of TEA, allowed to bubble, then sealed and also stored at 4 °C for a minimum of 24 hours. It is important that all solutions and glassware involved in the tresylation reaction are as water free as possible; otherwise the reaction will not proceed to a high yield.

The PEO/dichloromethane solution is quickly decanted into the reaction vessel, and the stir bar set to stir at a slow to medium rate. The TEA is pipetted dropwise into the reaction vessel, then the TrCl. When the TrCl is added, a white cloud will sometimes appear over the solution. The amounts of TEA and TrCl to be added were determined by first calculating the approximate number of moles of hydroxyl groups present for tresylation (no. moles OH = [2][mass PEO added] ÷ [ $\overline{Mn}$ PEO]). The number of moles of hydroxyl groups for the star polymer was approximated as [1][mass star PEO added] ÷ [ $\overline{M}_{arm}$]. The amount of TEA and TrCl to be added was then 1.5 times the number of moles of OH calculated. The reaction was allowed to proceed for 90 minutes before the dichloromethane was evaporated off using a liquid nitrogen trap. The polymer was then redissolved in 50 ml acidified methanol (250 µl concentrated

HCl in 50 ml methanol), and placed at -20 °C to precipitate out the tresylated PEO. The solution was then centrifuged at 7000 rpm (~3600g) at -20 °C for 25 minutes, the supernatant poured off, and the PEO redissolved in an additional 50 ml of acidified methanol (now 50 µl concentrated HCl in 50 ml methanol). The procedure of precipitation, centrifugation, and redissolving in 50 ml acidified methanol (50 µl concentrated HCl in 50 ml methanol) was repeated until a total of 4 precipitations were performed (at least six if sent out for elemental analysis). Once the polymer was recovered from the last centrifugation, the methanol was evaporated off, and the tresylated polymer either used immediately, or was stored under nitrogen, dessicated, at -10 °C and used as soon as could be arranged. When a sample of a tresylated PEG 3400 standard was sent out for elemental analysis (Galbraith Labs, Knoxville, TN), it was found that the yield was 75%.

#### 2.2.1.3 Coupling Tresyl-PEO to Aminosilane-Silicon

Varying amounts of tresylated-PEO were added to 3 mls of sodium bicarbonate buffer solution (0.12 M, pH adjusted to pH 7.4). Immediately after the polymer dissolved fully, pieces of aminosilane-treated silicon were added. Despite the fact that the coupling is rapid and probably occurs within the first hour, the silicon pieces were kept in the solution overnight, at 25°C on a rocker table, before being removed and rinsed thoroughly with water. This ensured the greatest extent of reaction onto the surface, and that all unreacted tresyl groups were hydrolyzed off to restore the hydroxyl groups on the PEO. Concentrations of tresyl-PEO ranged from 0.05% to 15% (w/v) for the star PEO's, and 0.05% to 19% (w/v) for the linear PEGs. Generally, six different concentrations were prepared for each PEO sample, and two samples were made at each concentration.

#### 2.2.1.4 Protein Adsorption

Proteins cytochrome-c (equine, MW=12 kD), albumin (human, MW=68 kD), and fibronectin (human, MW=500 kD) were obtained from Sigma Chemical (St. Louis, MO) as was phosphate buffered saline (PBS) solution. The PBS was pH adjusted to pH 7.4, and sodium azide (0.02% (w/v)) was added as bacteriostat. The proteins were dissolved in the PBS at concentrations 2 mg/ml for cytochrome-c, 2 mg/ml for albumin, and 0.1 mg/ml for fibronectin. PEO-coupled pieces were rinsed in PBS to rehydrate the surface, then placed in the protein solutions. Adsorption took place at 25 °C for 24 hours. Samples were then removed from the solution, rinsed 3 times with ca. 1.5 ml PBS from a Pasteur pipette, and once with pure water. The water rinse was to remove any PBS salts from the samples, since the samples were to be analyzed by XPS.

### 2.2.2 Analytical Techniques

#### 2.2.2.1 Ellipsometry

A Gaertner L116a ellipsometer was used to make the thickness measurements on the silicon wafer pieces. Baseline substrate values were taken immediately after the cleaned samples were rinsed the final time in water and then in methanol. A nitrogen stream was used to dry the methanol from the pieces. Total thickness measurements were made at each step after coupling with aminosilane, coupling with PEO and adsorption of protein. A value of 1.44 was used for the index of refraction (n) for all measurements. This is a good estimate for the aminosilane[5] and PEO[2] layers. For the protein layer, however, it is only an average value, as n for proteins can vary widely[1]. Despite the fact that the ellipsometry measurements are not very sensitive to small

variations in n, these larger differences, as may exist for the protein layers, could mean an error of ±25%.[1] Therefore, the ellipsometric data for the protein adsorption can only be accepted for the general trends in the curves, not the actual thickness values presented, as stated previously. For all silicon samples, five to eight measurements were made on each sample.

#### 2.2.2.2 X-Ray Photoelectron Spectroscopy (XPS)

An SSX-100 x-ray photoelectron spectrometer (Surface Sciences, Inc.) was used to make the XPS measurements (analyzing the top ca. 50 Å of the surface) which has a monochromatized Al Kα X-ray source. Survey scans (spot 600 μm, resolution 4) were used to obtain elemental compositions of the surfaces. High resolution scans of the carbon 1s region (spot 600 μm, resolution 2, window 20 eV) were used to obtain the intensity of the ether (C-O) carbon peak (as PEO consists solely of ether carbon). Intensities of the silicon 2p photoelectrons were measured (spot 600 μm, resolution 4, window 20 eV) and used in the calculations to obtain the thickness of the protein layer (through the attenuation of the silicon signal). In all scans, a flood gun setting of 5 eV was used, as well as a nickel wire mesh held approximately 5 mm over the sample stage, to help prevent charging of the samples. All scans of carbon 1s and silicon 2p photoelectrons were peak-fitted using software provided with the instrument. The lowest energy peak in the high resolution carbon 1s scans was referenced to 285 eV.

#### 2.2.2.3 Contact Angle Measurements

Advancing and receding contact angles with a droplet of water were measured on the aminosilane-treated as well as linear and star-grafted silicon surfaces using a Rame-Hart

goniometer. The linear PEO surface was a PEG 10k sample grafted from a 5% (w/v) coupling solution, and the star PEO surface was a star 3510 sample grafted from a 7% (w/v) coupling solution. A small droplet of water (ca. 5 μl) was placed on the sample while still adhered to the pipette tip, and advancing and receding angles were measured quickly once the droplet moved across the surface. At least 4 measurements were taken on each sample.

## 2.3 Results

### 2.3.1 Aminosilane Coupled Surfaces

Results from ellipsometry show that the aminosilane layer is 7±2Å. This indicates that there are approximately two aminosilane molecules per $nm^2$, or that the amine concentration is four secondary and two primary amines per $nm^2$. Tresylchloride is more reactive towards primary amines but will also react with secondary amines, so they are all included in the surface amine content. A spacing between amines of 4.1 Å is certainly sufficient to provide for a high grafting density on the surface, since the size of a PEO monomer unit is approximately 3 Å. The silane layer was found to be stable for two weeks in PBS solution (pH 7.4), as deduced by XPS survey scans which showed a constant ratio of N/Si intensities.

### 2.3.2 PEO-Coupled Surfaces

#### 2.3.2.1 Contact Angle Measurements on Treated Silicon Surfaces

The advancing ($\theta_a$) and receding ($\theta_r$) contact angles of water measured on an aminosilane-treated surface, and linear PEO and star PEO grafted surfaces are given in Table 2-1. The aminosilane surface shows greater wettability than both the PEO surfaces, as indicated by its

lower advancing and receding angles. This is not surprising since amines are more hydrophilic than PEO; PEO is considered to be only moderately hydrophilic.[2] The advancing angle for the stars is slightly larger than that of the linear PEG. It is possible that this could be caused by the DVB cores of the star PEO being exposed to the air when the surface is dry, thus lending a

Table 2-1: Contact angle measurements of water on treated silicon surfaces

| | $\theta_a$ | $\theta_r$ |
|---|---|---|
| Aminosilane | 30-32 | < 10 |
| Linear PEO | 36-39 | 25-26 |
| Star PEO | 41-43 | 25-26 |

hydrophobicity to the surface as the water droplet advances over them. A second hypothesis is that it could be due to surface roughness, where the stars could form a bumpier surface when dehydrated, a result of their dense, hard-sphere structure compared to linear PEO. This hypothesis is compatible with the receding angles for both linear and star PEO surfaces being the same, as now the surfaces are fully hydrated and the water encounters only hydrated PEO as it recedes across the surface.

The advancing and receding contact angles measured on the aminosilane-treated surfaces agree with those reported by Stenger et al.[6] The contact angles for the linear PEO surfaces are in agreement with those reported by Pale-Grosdemarge et al.[2] In their study, they measured contact angles of PEG-SAMs where the PEG content on the surface varied. As the PEG content increased, the advancing and receding contact angles of water asymptotically reached values of 34-38° and 24-25°, respectively. Therefore, our agreement with these values suggests that the

PEO surfaces are entirely PEO as seen by water. Any further details on the surface are probably on too small a scale to be resolved using this method.

#### 2.3.2.2 Thickness of Dried PEO Layer

XPS high resolution carbon 1s scans were used to quantify the presence of the PEO on the surface when compared to the aminosilane control. Figure 2-1 shows the high resolution carbon scan for an aminosilane control surface. The peak shifted 1.1 eV positive of the main (C-C) peak is indicative of carbon bonded to nigrogen atoms (primary, secondary, and tertiary amines all shift the carbon peak equally). The smallest higher energy peak is probably due to the presence of carbon dioxide complexed onto the surface. Figures 2-2 and 2-3 show the scans for linear PEG 20k and star 3510 at three different coupling concentrations of tresylated PEO. These scans clearly show the growing intensity of the (C-O) peak (shifted 1.5 eV from the C-C peak) as the coupling concentration increases, indicating the increasing grafting density of PEO on the surface. It is important to remember that it is the dried (dehydrated) PEO layer that is being analyzed in XPS and ellipsometry, where any inhomogeneities on the surface are averaged out as if the surface had a uniform layer. The intensity of the ether peak can be used to estimate the dried thickness of the PEO layer through the relation:

$$\frac{I}{I_O} = 1 - \exp\left(\frac{-d}{\lambda \sin(\theta)}\right) \qquad (2\text{-}1)$$

where I is the intensity of the ether peak at a certain PEO thickness,

$I_0$ is the intensity of an infinitely thick layer,

d is the thickness of a PEO layer (Å)

$\lambda$ is the attenuation length of the carbon 1s photoelectron through an organic layer (Å),

and $\theta$ is the take-off-angle used when taking the XPS measurements ($\theta = 35°$).

The attenuation length $\lambda$ was found using the results of Laibinis et al.[7]

$$\lambda(\text{Å}) = 9.0 - 0.022\ \text{KE(eV)} \qquad (2\text{-}2)$$

KE is the kinetic energy of the photoelectron found by

$$\text{KE(eV)} = 1486.6 - \text{BE} \qquad (2\text{-}3)$$

where BE is the binding energy of the photoelectron, and 1486.6 eV is the energy of the X-rays.

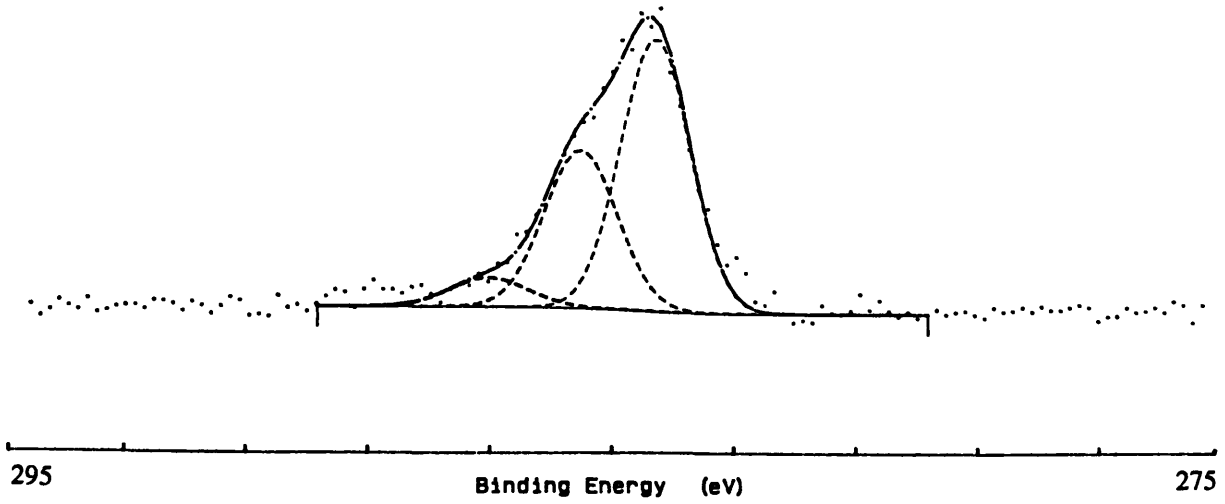


Fig. 2-1: High resolution carbon scan of aminosilane-coupled silicon surface.

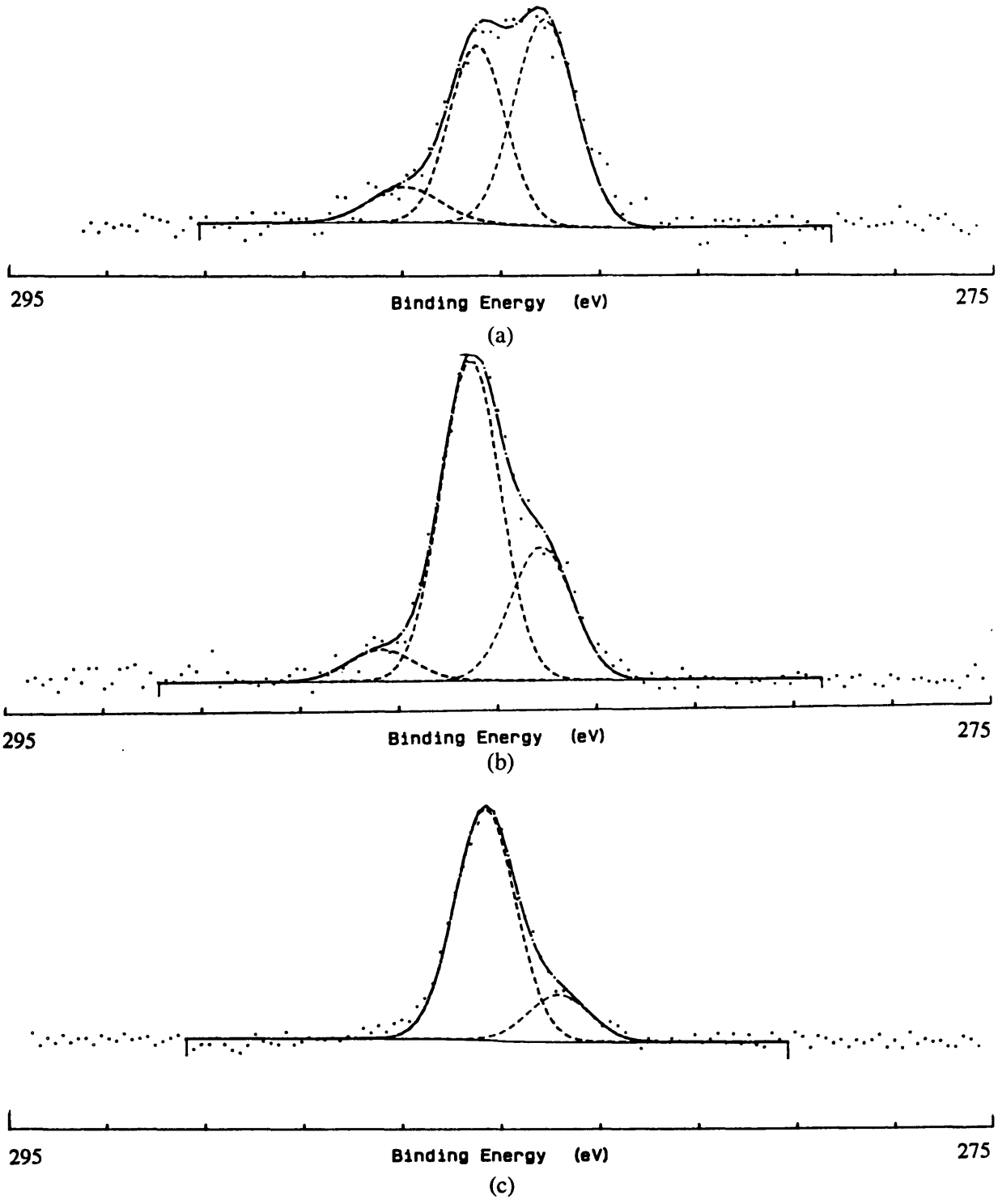


Fig. 2-2: High resolution carbon scans of PEG 20k grafted surfaces from three different coupling concentrations: (a) 0.5%, (b) 2%, (c) 15%.

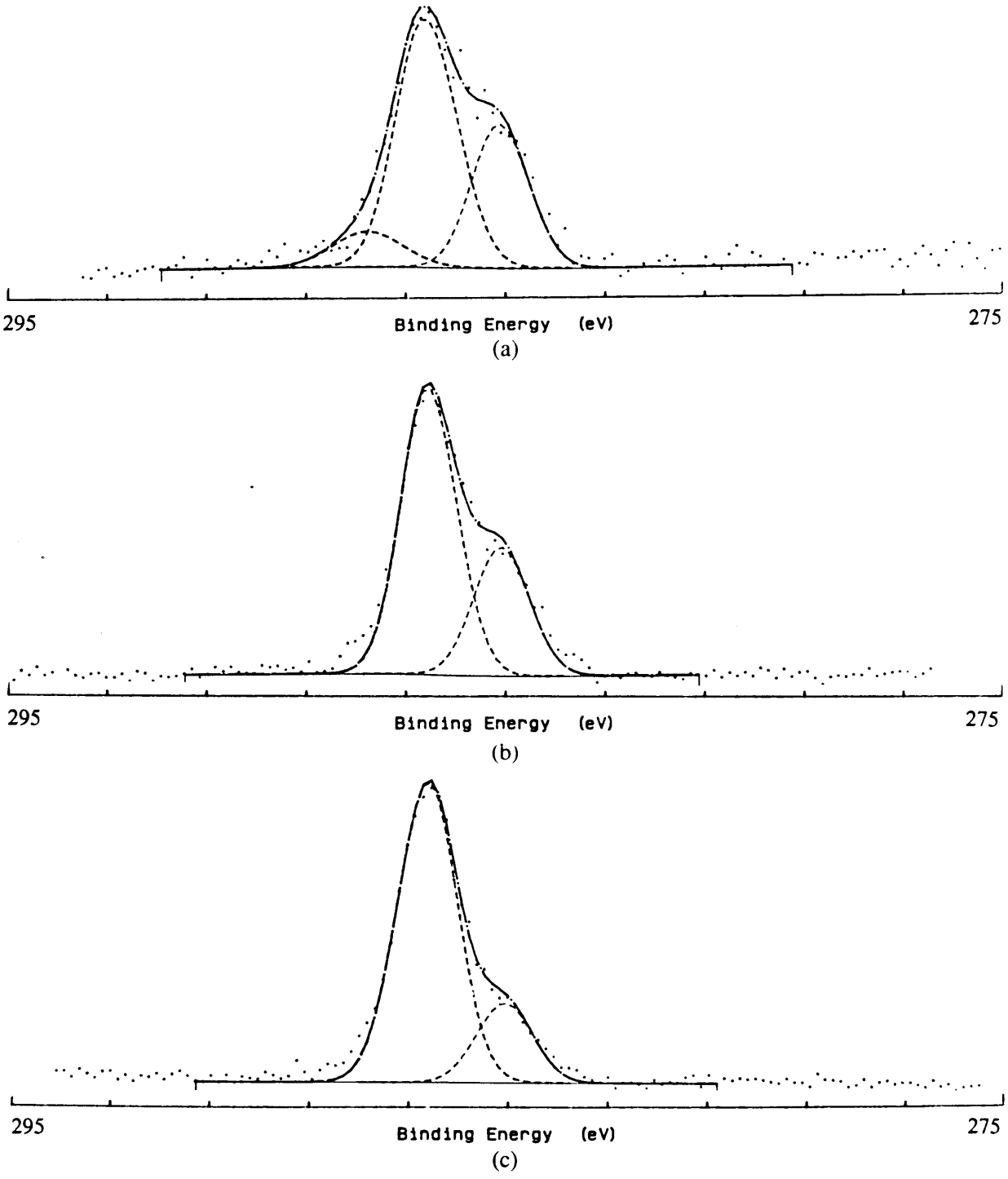


Fig. 2-3: High resolution carbon scans of star 3510 grafted surfaces from three different coupling concentrations: (a) 0.05%, (b) 7%, (c) 12%.

The intensity $I_o$ was estimated by measuring the intensity I of a PEG-SAM where the PEG unit consisted of six monomer units. As reported by Pale-Grosdemange et al.,[2] the PEG thickness of such a SAM was found to be 15 Å. Therefore, knowing d, $\theta$, $\lambda$, and measuring I, an estimate of $I_o$ was calculated. This value of $I_o$ agreed to within 15% of the measured intensity from a pure PEO sample. The only other consideration in calculating the thickness of the PEO layer was accounting for the intensity of the amine carbon peak at low PEO grafting densities, since nitrogen shifts the carbon peak to a similar degree as oxygen. This was handled by looking at the nitrogen signal as PEO grafting density increased. On samples to which PEO was coupled from tresyl-PEO coupling concentrations of 1% (w/v) or greater, the nitrogen signal was less than 10% of that measured on the aminosilane-treated controls. Therefore, only for those samples exposed to tresyl-PEO coupling concentrations of less than 1% (w/v) was a fraction of the (C-O) peak intensity accounted for being (C-N). This fraction was estimated to be equal to the ratio of the nitrogen signal measured from the PEO-coupled samples relative to the signal from the aminosilane control. The error in the calculations of PEO thickness is therefore higher for the samples of lower grafting density, an error of ±2Å, compared to an error at the higher grafting densities of ±1Å.†

The values of the PEO thickness calculated from the XPS data for both the star and linear PEO surfaces were compared to the values obtained from ellipsometry. For the star PEO, the values agreed to within ±2Å at the low grafting densities and to within ±1Å at the higher grafting densities. For the linear PEG, there was a much larger discrepancy of ±3-4Å at all grafting

† The error is using Eq. 2-1 was minimal in that the highest $I/I_o$ measured was ~0.5, still in the region of the function of large slope, far from where it begins to plateau near $I/I_o = 1$.

densities, where ellipsometry was consistently underestimating the thickness compared to XPS. Since there is a larger error associated with ellipsometry than XPS, and XPS is a direct detection of exactly what is present on the surface (made easier since the PEO is the top layer and not being attenuated), the XPS results were used for the PEO thicknesses for the linear PEG surfaces. As seen when applied to the protein adsorption results, this seems to be a reasonable estimation. Figure 2-4 shows the dry PEO measured thicknesses as a function of tresyl-PEO coupling concentration.

#### 2.3.2.3 Calculation of Linear PEG Grafting Density

The values of the dry thickness of PEO can be used to calculate the grafting density, $\sigma$, of the PEO molecules on the surface. Grafting density, used extensively in polymer brush theory, is a more useful parameter than dry PEO thicknesses when discussing PEO coverages and their affect on protein adsorption.

First, the average distance between PEG chains (L) can be estimated from the dry thickness by

$$L(\text{Å}) = \left( \frac{M}{\rho_{dry}\, h\, N_A} \right)^{1/2} \qquad (2\text{-}4)$$

where M is the molecular weight of the PEG chain

$\rho_{dry}$ is the density of the dry PEG layer (assumed constant at $1 g/10^{24}$ Å$^3$)

h is the thickness of the PEG layer (Å)

$N_A$ is Avogadro's number.

$L^2$ is defined to be the average area occupied by a single, hydrated PEO molecule on the surface.

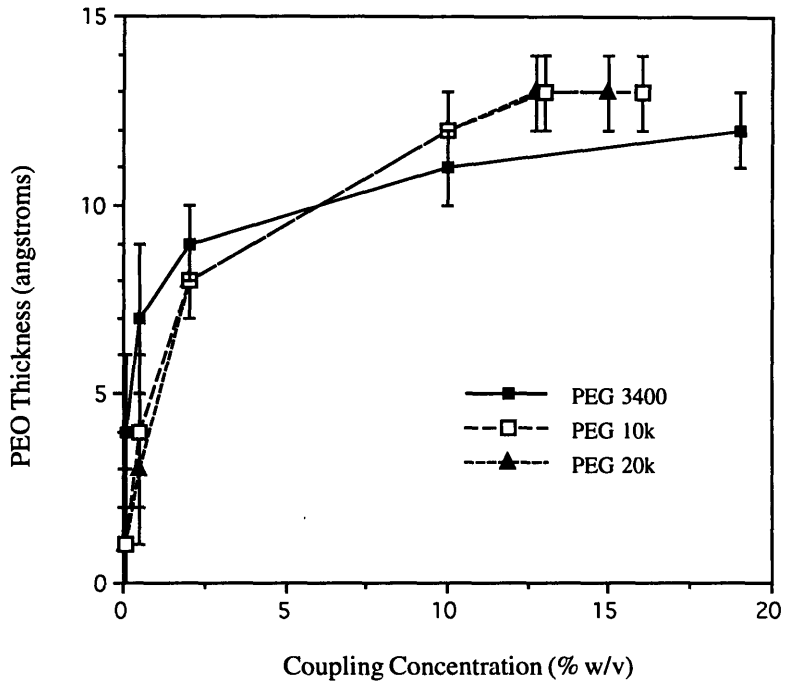


(a)

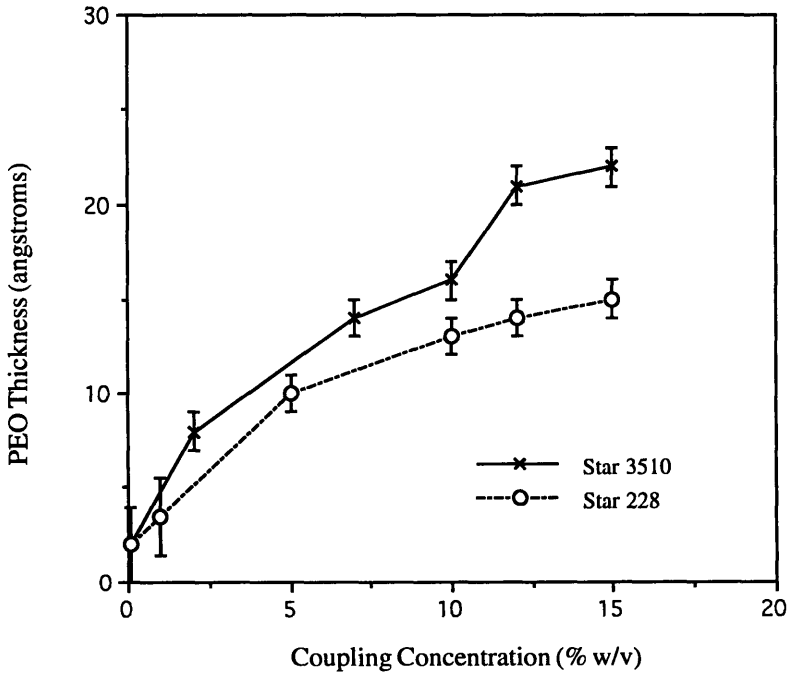


(b)

Figure 2-4: Dry PEO thickness as a function of tresyl-PEO coupling concentration for: (a) linear PEG, and (b) star PEO.

The definition of grafting density for linear molecules is defined to be[8]

$$\sigma \text{ (linear)} = \left(\frac{a}{L}\right)^2 \tag{2-5}$$

where a is the size of a monomer ($a \approx 3$ Å).[1,9] This relation is essentially the area occupied by a single grafted chain relative to the area of a single monomer unit, the latter of which would represent a maximum chain density, or minimum spacing between chains. Therefore, combining Eqs. 2-4 and 2-5, a relationship of $\sigma$ as a function of M and h is obtained.

$$\sigma \text{ (linear)} = \left(\frac{\rho_{dry}\, h\, N_A\, a^2}{M}\right) \tag{2-6}$$

From this relationship, grafting density is directly proportional to the dry thickness at constant molecular weight, and inversely proportional to molecular weight at constant dry thickness.

The relationship between attained grafting density and tresylated-PEO coupling concentration for the three linear PEG molecules is shown in Figure 2-5. All three PEG molecules show the same general behavior of a rapid rise in grafting density at low coupling concentrations, with a leveling off such that a maximum grafting density is attained. This asymptotic behavior was expected. The critical concentration, $c_{crit}$, marking the onset of chain overlap in solution can be estimated by

$$c_{crit} = \left(\frac{M}{N_A \frac{4}{3}\pi R_G^3}\right) \tag{2-7}$$

where $R_G$ is the radius of gyration of the linear PEO molecule, calculated from the well-known Flory equation[10]:

$$\left(\overline{R}_G^{\,2}\right)^{1/2} = \frac{\alpha l}{\sqrt{6}}\left(C_\infty \frac{M}{M_o} 3\right)^{1/2} \qquad (2\text{-}8)$$

where $\alpha$ is the expansion coefficient for PEO in water, l is the average bond length in a PEO monomer unit (l [PEO] =1.47 Å, calculated as the weighted average of two C-O bonds, 1.54 Å, and one C-C bond, 1.44 Å), $C_\infty$ is the polymer constant for PEO ($C_\infty$ [PEO] = 4), M is the molecular weight of the PEO, and $M_O$ is the molecular weight of a monomer unit ($M_O$ [PEO] = 44 g/mol). The value of $\alpha$ is calculated from[10]

$$\alpha^5 - \alpha^3 = 2\, C_M(1/2 - \chi)\, M^{1/2}. \qquad (2\text{-}9)$$

where

$$C_M = \left(\frac{27}{2^{5/2}\,\pi^{3/2}}\right)\left(\frac{\bar{v}^2}{N_A\, V_1}\right)\left(\frac{M}{\bar{r}_o^2}\right)^{3/2} = 0.175 \text{ for PEO in water,}$$

$\bar{v}$ is the specific volume of PEO,

$N_A$ is Avogadro's number,

$V_1$ is the molar volume of water,

$\chi$ is the polymer-solvent interaction parameter (PEO in water at 25°C, $\chi$ =0.43),

and $\left(\bar{r}_o^{\,2}\right)$ is the unperturbed root-mean-square end-to-end distance of PEO.[10]

$$\left(\bar{r}_O^{\,2}\right) = C_\infty \left(3\frac{M}{M_o}\right) l^2 \qquad (2\text{-}10)$$

Therefore, the critical concentrations for the three PEG solutions are $c_{crit}(3400) \approx 8$ %, $c_{crit}(10k) \approx 5$ %, and $c_{crit}(20k) \approx 3$ % (w/v). The highest coupling concentrations used in the experiments

were 2.5 to 5 times larger than these $c_{crit}$ values, indicating there was significant chain overlap in solution. The concentration of PEO at the surface is not necessarily the same as that in the bulk solution, but it is likely that significant chain overlap on the surface was also achieved. With the asymptotic behavior shown in Figure 2-5, it is evident that the surface becomes saturated in PEO such that steric hindrance and excluded volume effects come into play.[11] Additional PEO chains can no longer penetrate into the PEO layer and bind to the surface. The PEG chains on the surface are now in a stretched chain regime where the concentration of PEO within the layer, $\phi$, can be approximated by $\phi \cong \sigma^{2/3}$.[8] The data also clearly show the dependence of grafting density on PEG molecular weight, with PEG 3400 attaining the highest densities and PEG 20k attaining the lowest densities. This is again due to excluded volume effects, where a larger PEG molecule has a larger excluded volume and can't pack as tightly on the surface as a smaller PEG molecule (i.e., to the same grafting density).

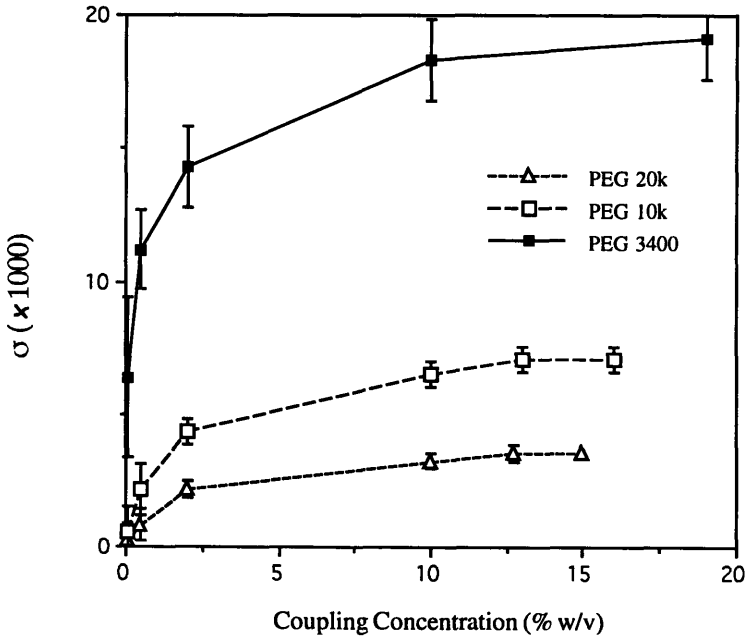


Figure 2-5: Grafting density as a function of tresylated-PEO coupling concentration for linear PEG 3400, 10k, and 20k.

2.3.2.4 Calculation of Star PEO Grafting Density

Defining grafting density for the PEO star molecules is not as straightforward as it is for linear PEO molecules, since the size of a monomer unit is not feasible to use in the reference of grafting density for stars, due to the large structural difference between linear and star PEO molecules. The most appropriate parameter to replace the monomer size "a" in grafting density for star PEO surfaces would be the size of the core of the star molecules. However, the core region of a star molecule is very difficult to define, as indicated in much of the literature cited in Chapter 1. Therefore, for star molecules, a reference state representing a near-maximum density on the surface is defined as a chain spacing equaling the radius of gyration of the star molecules, $R_G$. As the distance L between grafted linear molecules cannot be less than the size of a monomer unit, then it is unlikely that the distance L between star molecules be less than its radius of gyration, since that would mean the arms of one star would be extended through the core region of a neighboring star. This is not to say that grafting densities greater than 1 for star molecules could not be achieved, but it would be very difficult considering the large osmotic pressure and steric crowding within a star molecule. Therefore, grafting density for a star is defined as

$$\sigma\,(\text{star}) = \left( \frac{R_G^{\text{star}}}{L} \right)^2 \tag{2-11}$$

and the relationship between $\sigma$, h, and M for a star is

$$\sigma\,(\text{star}) = \left( \frac{\rho_{dry}\, h\, N_A\, R_G^{\,2}}{M} \right) \tag{2-12}$$

The radius of gyration of a star molecule can be estimated using the empirical results set forth by Bauer et al[12]. A relation of $\log(R_G^{star}/R_G^{arm})$ vs. log(f) for star polymers in a good solvent was presented, and from these data, we get:

$$\log(R_G^{star}/R_G^{arm}) = 0.1312 \log(f) + 0.1910 \qquad (2\text{-}13)$$

The value of $R_G^{arm}$ can be calculated from Eq. 2-8. The average molecular weight of the stars divided by the arm molecular weight yields f. $R_G^{star}$ was then calculated from Eq. 2-13.

Figure 2-6 shows the attained grafting density as a function of tresyl-star coupling concentration for both star 228 and star 3510. Unlike the behavior of linear PEO, there is no leveling off at a maximum grafting density at large concentrations. Instead, $\sigma$ appears to almost linearly increase for star 3510, and star 228 shows similar behavior but has a bit more curvature. One hypothesis to account for these results again has to do with the critical concentration: $c_{crit}(228) \approx 15\%$ and $c_{crit}(3510) \approx 13.5\%$. At the highest coupling concentration of 15%, both stars have just reached the point of overlap. Therefore, from this point onward is where we would expect grafting density to reach a maximum due to steric repulsion and excluded volume effects on the surface. The extremely large values of $c_{crit}$ for the stars are testimony to how dense the stars are, where such high concentrations are needed before the stars are forced to interpenetrate one another. The slope for star 3510 is slightly larger than for star 228. It is possible that this has to due with the arm molecular weight of star 3510 being half that of star 228 ($\overline{M}_{arm}[3510] = 5\,200$ g/mol *vs.* $\overline{M}_{arm}[228] = 10\,000$ g/mol), as well as the functionality of star 3510 being over three times that of star 288 ($\bar{f}\,[3510] = 70$ *vs.* $\bar{f}\,[228] = 20$). As stated

previously, the arms of a star are in an extended conformation due to the steric crowding in the core region, this arm extension increasing with increasing functionality.

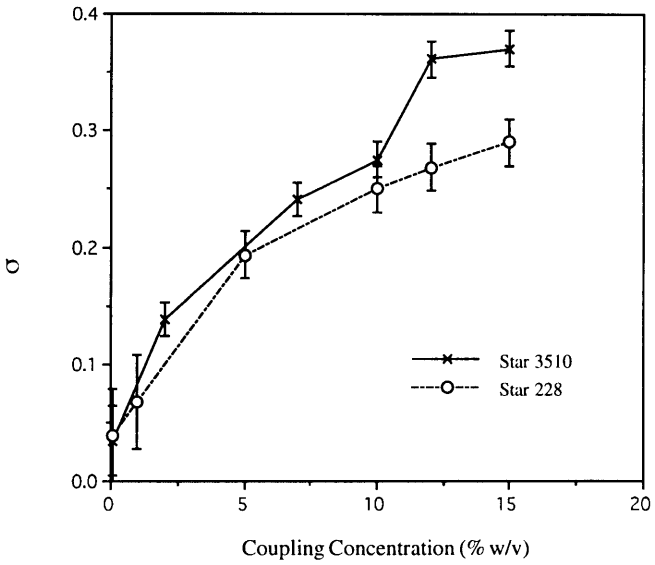


Figure 2-6: Grafting density as a function of tresylated-PEO coupling concentration for stars 228 and 3510.

The arms of star 3510 being shorter and more extended than those of star 228 results in the greater accessibility of the arm-end tresyl groups of star 3510 for binding to the surface. Therefore star 3510 binds more easily to the surface. This also could explain the slight curvature exhibited in the data of star 228, these molecules possessing more linear characteristics since they have both a lower functionality and increased arm molecular weight.

### 2.3.3 Protein Adsorption on PEO Surfaces

#### 2.3.3.1 Thickness of Adsorbed Protein Layer

The thickness of the layer of adsorbed protein was determined by analyzing the attenuation of the silicon 2p photoelectron signal in an XPS scan, as referenced to the equivalent

PEO surface not contacted with protein. The attenuation of a photoelectron due to an overlayer is described by the equation

$$\frac{I}{I_o} = \exp\left(\frac{-d}{\lambda \sin\theta}\right) \tag{2-14}$$

where I is the intensity of the Si 2p with a protein overlayer

$I_o$ is the intensity of the Si 2p with no protein overlayer

d(Å) is the thickness of the protein overlayer

λ(Å) is the attenuation length of Si 2p through an organic overlayer (estimated to be 38.5 Å from Eqs. 2-2 and 2-3), and

θ is the take-off-angle used in taking the measurements (θ = 35°).

Therefore, by measuring I and $I_o$ in an XPS scan, the protein thickness, d, was calculated.

2.3.3.2 Protein Adsorption on Linear PEG Surfaces

Protein adsorption to surfaces depends on many things, such as surface tension, wettability, surface charge, and surface roughness. In addition, different proteins can exhibit varying adsorption behavior on the same surface due to inherent characteristics specific to the protein. For example, albumin tends to have greater adsorption on hydrophobic surfaces,[13] and fibrinogen shows increased adsorption on sulfonated polyurethanes (PU) than on untreated PU, probably due to an affinity for the negatively charged sulfate group.[14] Proteins tend to adsorb to a surface in a monolayer, where over time they slowly unfold and spread over the surface. They generally adsorb via hydrophobic interactions, wanting to maximize the hydrophobic contact with

the surface, thus leaving the hyrophilic portion of the protein exposed to the surrounding environment. This results in a surface with decreased affinity for further protein adsorption.

As discussed in Chapter 1, the presence of PEO on a surface results in decreased protein adsorption; the greater the PEO content, the greater the reduction in protein adsorption. Following this trend, the expected behavior of proteins adsorbing to a series of surfaces with varying PEO content is illustrated in Figure 2-7. There are three distinct regions of adsorption. From point A to point B on the curve, PEO coverage is sparse. A significant fraction of the surface is not covered with PEO, so the degree of adsorption shows relatively little dependence on PEO content. At point B, however, PEO coverages are such that the open space is much diminished, and proteins have difficulty penetrating to the underlying surface. Adsorption then starts to fall off. From point B to point C, the PEO coverage increases, and the decline in adsorption continues until, at point C and beyond, the coverage on the surface is sufficiently dense

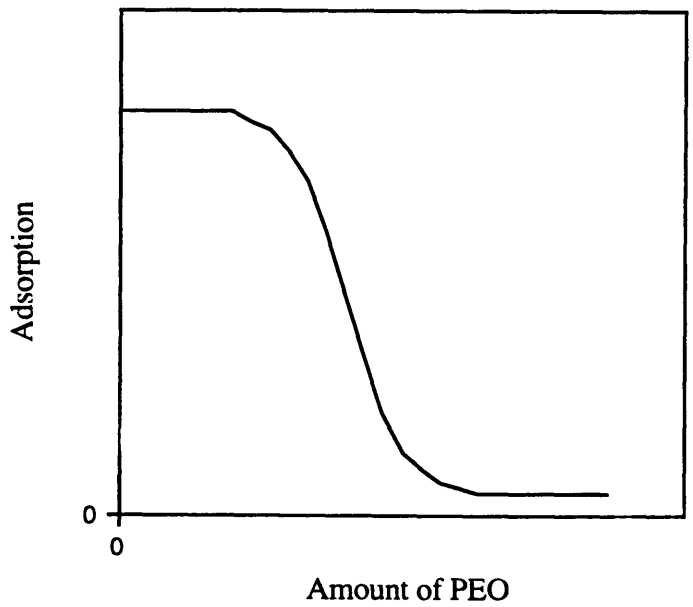


Figure 2-7: General curve of protein adsorption as a function of PEO surface concentration.

that the surface is non-adsorbing. This curve and its points of interest will be referred to in this section and the following section on protein adsorption on star PEO surfaces.

Figures 2-8 to 2-10 show adsorption as a function of PEG grafting density for cytochrome-c, albumin, and fibronectin on surfaces grafted with linear PEG 3400, 10k, and 20k. Again, these three proteins were chosen because they span a wide range of protein size, such that adsorption as a function of protein size could be studied. There are several notable features of the adsorption. First, there is almost no region of high adsorption at low PEO coverage, equivalent to region A-B in Figure 2-7. This is because the PEG readily binds to the amines on the surface, even at low tresyl-PEG coupling concentrations, making it difficult to obtain low coverages. Second, region B-C in Figure 2-7, delineating the rapid decline in adsorption with PEO coverage, is clearly defined in Figures 2-8 to 2-10. What is interesting to note is that the three proteins change from maximum to minimum adsorption in roughly the same range of grafting densities on each PEG surface (corresponding to points B to C), despite the large difference in protein size. in fact, albumin and fibronectin show very similar adsorption, despite the large difference in their molecular weights. This is probably due to the small 25 Å width characteristic of fibronectin, causing it to behave as a protein whose size is similar to that of albumin. Third, there is a definite distinction in the rate of decline of adsorption for the three proteins (i.e., slope of the line from points B to C): fibronectin and albumin decline rapidly, at approximately the same rate, on all three PEG surfaces, while cytochrome-c shows the slowest decline with the smallest slope. Fourth, on all three PEG surfaces, the amount of protein adsorbed at a given grafting density generally correlates with the size of the protein, with fibronectin showing the greatest adsorption, followed by albumin and then cytochrome-c. For an equal area, a large protein adsorbed to the

surface in a monolayer is more total adsorbed protein than a monolayer of a small protein. The fact that fibronectin does not exhibit much larger thicknesses when compared to albumin and cytochrome-c, despite its much larger mass, suggests that fibronectin, a rod-like molecule where the other two are spherical, lies down on the surface with its long axis parallel to the surface.

An important conclusion to draw from the results in Figures 2-8, 2-9, and 2-10 is that there is no specific PEO molecular weight, or universal range of PEO grafting densities, that are

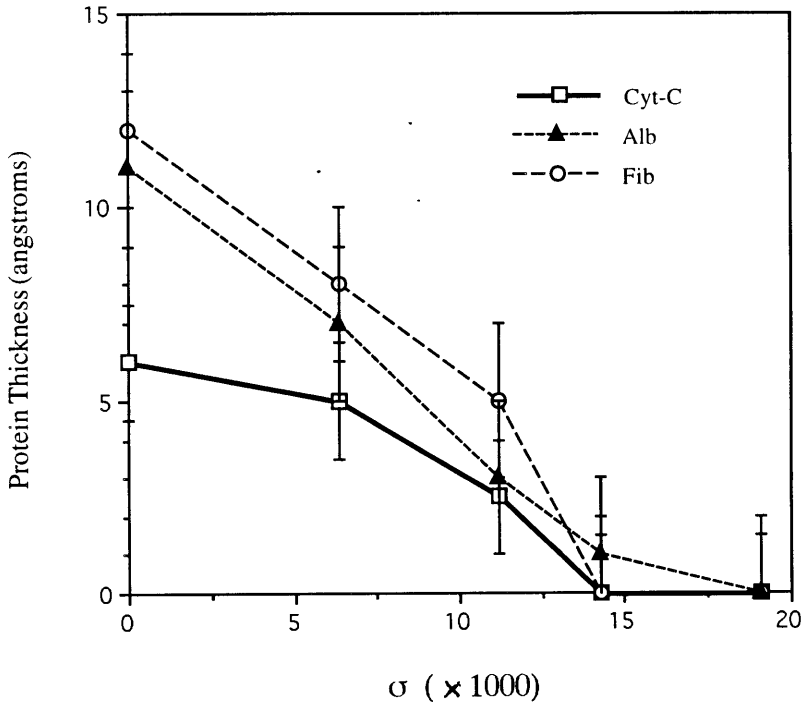


Figure 2-8: Protein adsorption, as measured by XPS, as a function of PEG 3400 grafting density.

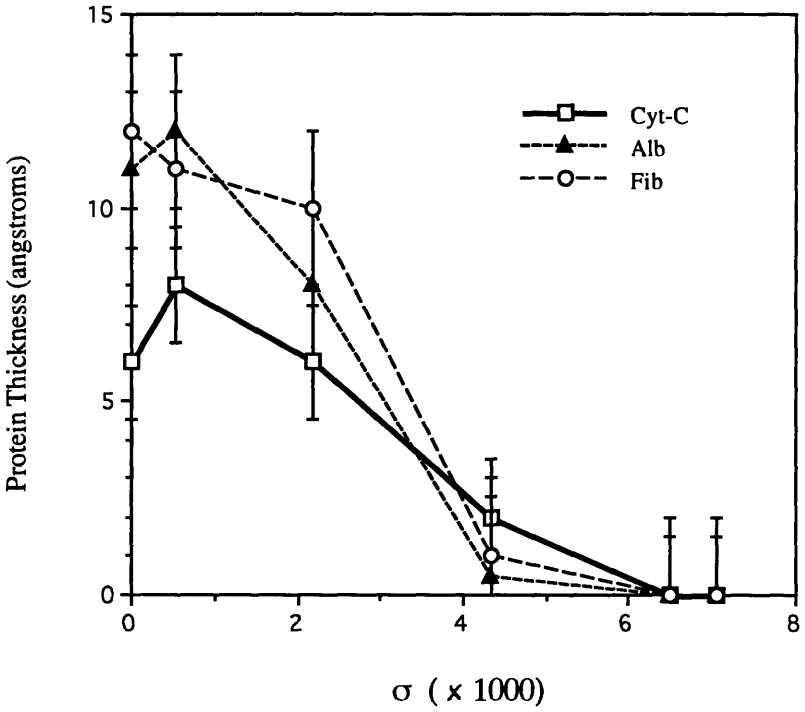


Figure 2-9: Protein adsorption, as measured by XPS, as a function of PEG 10k grafting density.

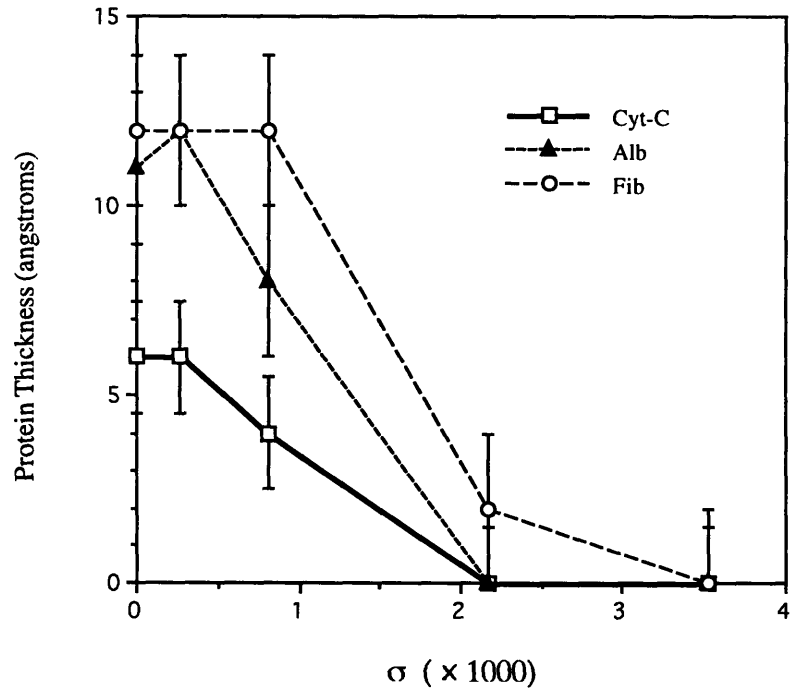


Figure 2-10: Protein adsorption, as measured by XPS, as a function of PEG 20k grafting density.

necessary for the prevention of protein adsorption, at least in the ranges of protein sizes and PEG molecular weights studied. Instead, there is a specific range of grafting densities for a given PEO molecular weight that are required to prevent protein adsorption.

Protein adsorption of the three proteins on each of the three PEG surfaces as deduced by ellipsometry are shown in Figures 2-11 to 2-13. As stated previously in the introduction to this chapter, ellipsometry measurement of protein layers involves some error in the absolute value of the thicknesses, whereas the general trends in the data are correct. Therefore, the results shown in Figures 2-11 to 2-13 are in concordance with the XPS results of Figures 2-8 to 2-10, where maximum adsorption is at the lowest grafting densities which declines to nearly zero adsorption at the highest grafting densities.

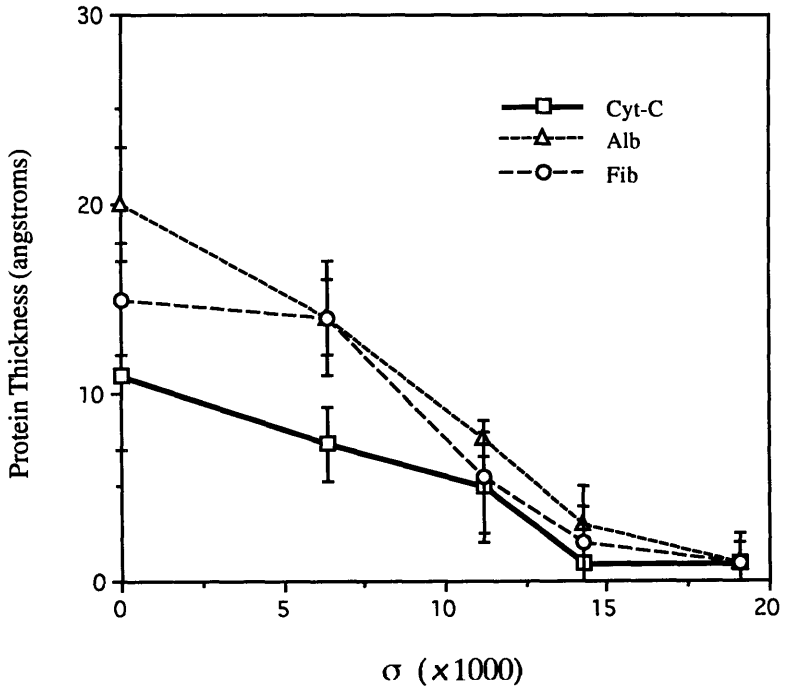


Figure 2-11: Protein adsorption on PEG 3400 surfaces as measured by ellipsometry.

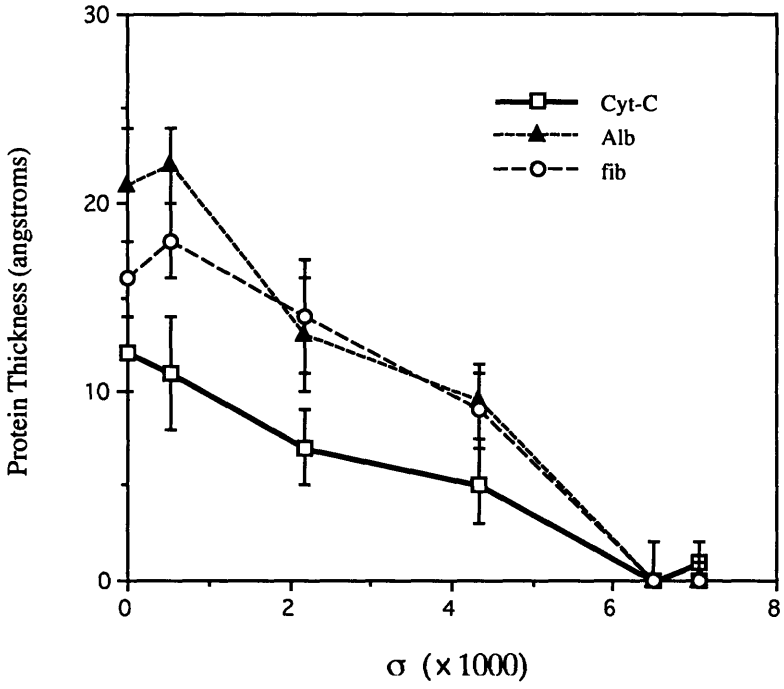


Figure 2-12: Protein adsorption on PEG 10k surfaces as measured by ellipsometry.

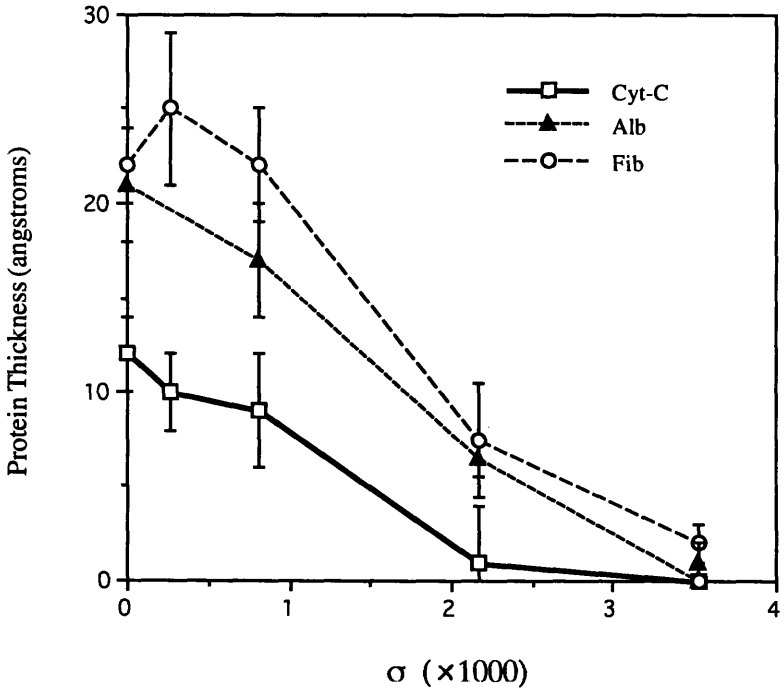


Figure 2-13: Protein adsorption on PEG 20 k surfaces as measured by ellipsometry.

2.3.3.3 Protein Adsorption on Star PEO Surfaces

Figures 2-14 and 2-15 show the protein adsorption, as measured by XPS, as a function of grafting density for cytochrome-c, albumin, and fibronectin on each of the star PEO surfaces. Similar features can be seen to those outlined on linear PEG surfaces in Subsection 2.3.3.2. First, as with linear PEO, there is no region A-B due to the rapid grafting of the star molecules to the surface at low coupling concentrations. Second, region B-C is clearly defined for albumin and fibronectin, showing a rapid decline in adsorption, again at similar rates, on both star surfaces. In addition, the grafting densities for each star surface, marking points B and C, are approximately the same for both proteins, the same behavior as was seen on the linear PEG surfaces. Third, it is

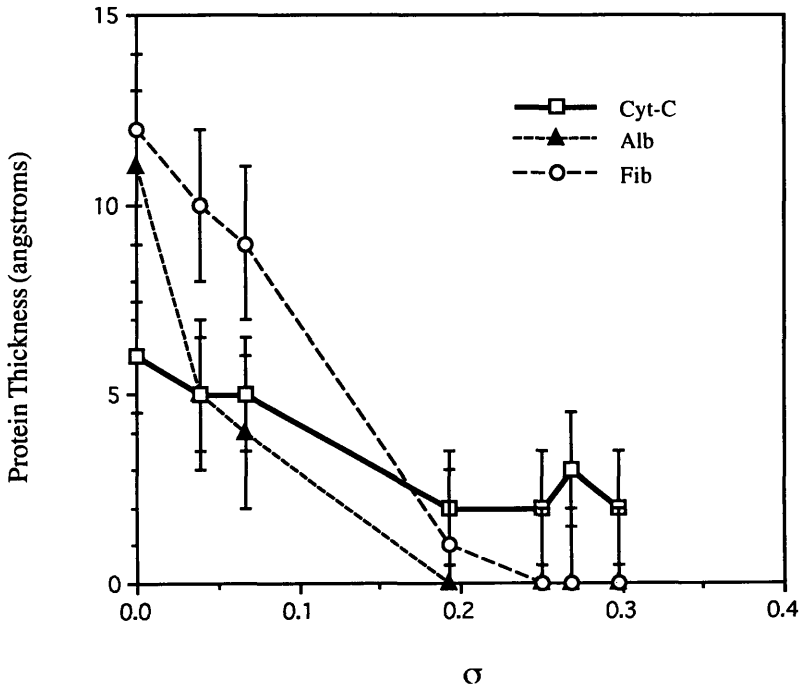


Figure 2-14: Protein adsorption, as measured by XPS, as a function of PEO star 228 grafting density.

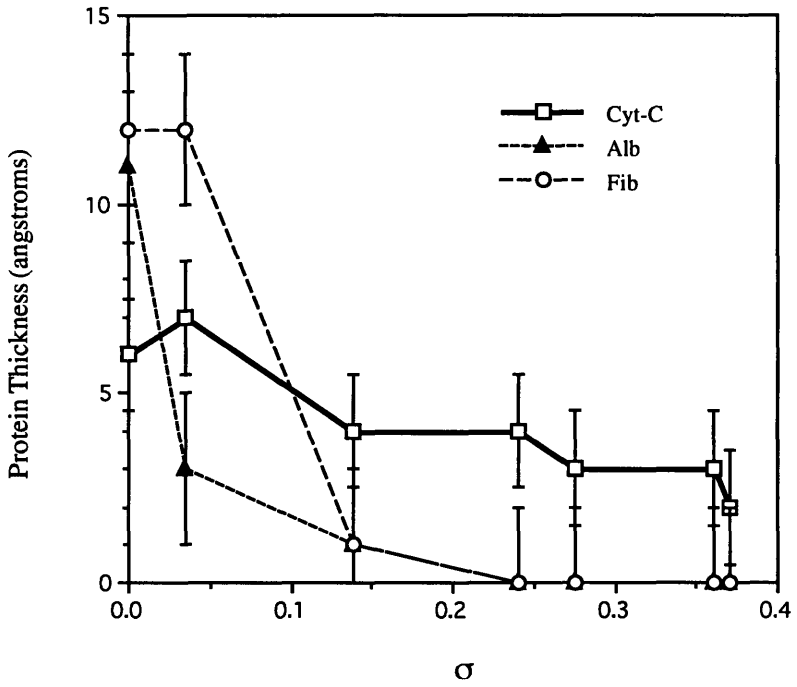


Figure 2-15: Protein adsorption, as measured by XPS, as a function of PEO star 3510 grafting density.

obvious from both figures that the most glaring feature of the protein adsorption on star surfaces is the continued adsorption of cytochrome-c at all grafting densities. The reason for this is discussed in-depth in Chapter 3, but it deals with the dense, hard-sphere characteristics exhibited by the star molecules, as opposed to the flexible, low-density character of the linear PEO random coil.

The ellipsometry results for the protein-adsorbed PEO star samples are shown in Figures 2-16 and 2-17. The same trends are seen as with the XPS results of Figures 2-14 and 2-15. Both fibronectin and albumin show a decline in adsorption with increasing grafting density, to nearly zero adsorption at the high grafting densities shown in the XPS data. Cytochrome-C is shown to continue to adsorb to the star surfaces at all grafting densities, in complete agreement with the XPS results.

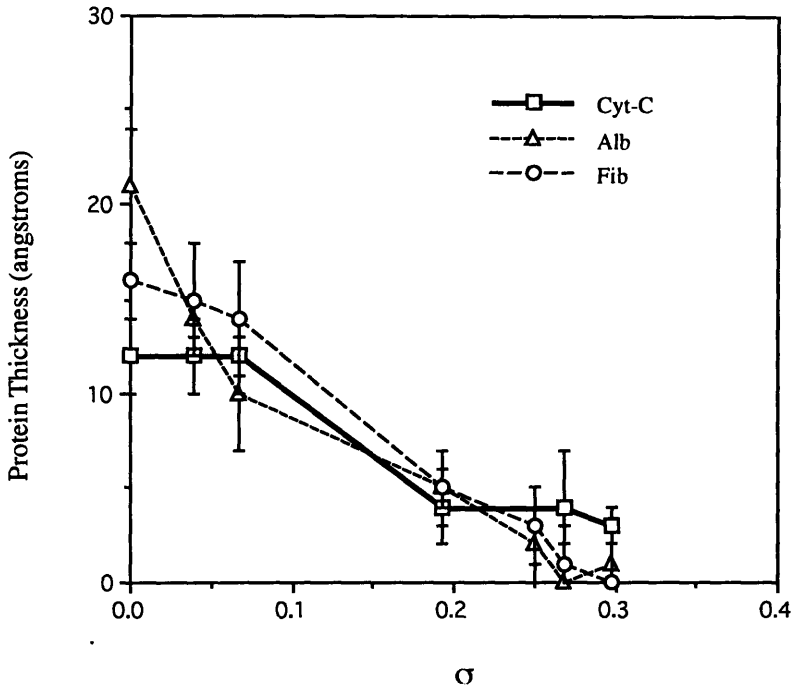


Figure 2-16: Protein adsorption on PEO star 228 surfaces as measured by ellipsometry.

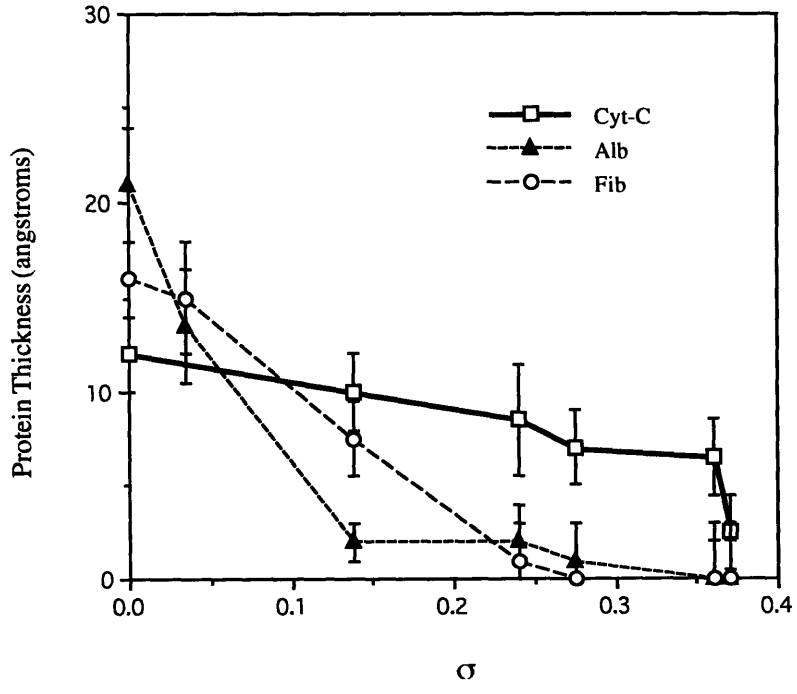


Figure 2-17: Protein adsorption on PEO star 3510 surfaces as measured by ellipsometry.

## 2.4 Conclusions

This chapter presented a method for creating well-defined, PEO grafted surfaces that were used and analyzed for protein adsorption analysis. Coupling the silicon surface with an aminosilane functionalized the surface with a high concentration of amines that were used as grafting sites for the tresylated PEO molecules. The grafting density of PEO on the surface was determined through the measurement of the dry thickness layer grafted to the surface. Finally, the protein adsorption of three proteins of different sizes was measured on the PEO surfaces possessing a range of PEO molecular weights, molecule types (linear or star) and grafting densities. The adsorption on the linear PEG was such that the range of grafting densities for maximum to minimum adsorption was approximately the same for the three proteins on a given PEG surface. In addition, the adsorption was indeed prevented for all three PEG surfaces at the highest grafting densities regardless of protein size. The adsorption on the star PEO surfaces showed similar behavior for both albumin and fibronectin, where both molecules were excluded from the surfaces at roughly the same grafting densities for a given star surface. Cytochrome-c continued to adsorb on both star surfaces for all grafting densities. This behavior is attributed to the hard-sphere characteristics of the star molecules, as discussed in greater detail in Chapter 3.

## 2.5 References for Chapter 2


1. K.L. Prime and G.M. Whitesides, *J. Am. Chem. Soc.*, 15, 10714 (1993).

2. C. Pale-Grosdemarge, E.S. Simon, K.L. Prime, and G.M. Whitesides, *J. Am. Chem. Söc.*, 113, 12 (1991).

3. E. Osterberg, K. Berstrom, K. Holmberg, J.A. Riggs, J.M. Van Alstine, T.P. Schuman, N.L. Burns, and J.M. Harris, *Coll. Surf. A: Phys. Eng. Aspects,* 77, 159 (1993).

4. K. Nilsson and K. Mosback, *Biochem. Biophys. Res. Comm.,* 102 (1), 449 (1981).

5. K. Nilsson and K. Mosback, *Methods Enzymology*, 104, 56 ()1984).

6. D.A. Stenger, J.H. George, C.S. Dalcey, J.J. Hickman, A.S. Rudolph, T.B. Nielsen, S.M. McCort, and J.M. Calvert, *J. Am. Chem. Soc.*, 114 (22), 8435 (1992).

7. P.E. Laibinis, C.D. Bain, and G.M. Whitesides, *J. Phys. Chem.*, 95 (18), 7017 (1991).

8. P.G. DeGennes, *Macromolecules*, 13 (5), 1069 (1980).

9. S.I. Jeon, J.H. Lee, J.D. Andrade, and P.G. de Gennes, *J. Colloid Interface Sci.,* 142, 149 (1991).

10. P. Flory, Principles of Polymer Chemistry, Cornell University Press, Ithaca, NY 1953.

11. A. Kopf, J. Baschnagel, J. Wittmer, and K. Binder, *Macromolecules*, 29, 1433 (1996).

12. B.J. Bauer, L.J. Fetter, W.W. Graessley, N. Hadjichristidis, and G. Quack, *Macromolecules*, 22, 2337 (1989).

13. M.S. Munro, A.J. Quattrone, S.R. Ellsworth, P. Kulkarni, and R.C. Eberhart, *Trans. Am. Soc. Artif, Intern. Org.*, 27, 499 (1981).

14. T.G. Grasel and S.L. Cooper, *J. Biomed. Mater. Res.*, 23, 311 (1989).

# CHAPTER 3

# A Model of Protein Adsorption on PEO-Grafted Surfaces

## 3.1 Introduction

As shown in Chapter 2, tresylated PEO in linear and star forms could be bound to silicon wafer surfaces, previously treated with aminosilane, in sufficient density to prevent the adsorption of cytochrome-c, albumin, and fibronectin in all but two cases: cytochrome-c on the star PEO 228 and 3510 surfaces. It was also noted that all three proteins were excluded from the surface in the same range of grafting densities for a given linear PEG, and that albumin and fibronectin were similarly excluded on the star PEO surfaces.

The following model is proposed to explain, qualitatively, the trends of observed protein adsorption on PEO grafted surfaces reported in Chapter 2. It is based only on the spatial arrangement of PEO molecules relative to one another. Energies of interaction between protein and PEO do not enter into it, although certain qualitative arguments can be made.

## 3.2 Model

### 3.2.1 Defining the Parameters

A surface is defined where the PEO molecules are bound in a 2-D lattice structure where a unit cell is defined to have length L. Therefore, $L^2$ is the area occupied by one hydrated molecule, including one-half the open space around it if it does not overlap with any other

molecules. (see Figure 3-1.) The diameter of the hydrated molecule is $d_{wet}$, defined to be twice the radius of gyration, $R_G$, of the linear PEO molecule, as calculated from Eq. 2-8. Therefore,

$$d_{wet}\,(\text{linear}) = 2\,R_G^{linear} \tag{3-1}$$

The value $d_{wet}$ for the star PEO molecules was determined using the empirical results set forth by Bauer et al.[1] for the radius of gyration of a star, as given by Eq. 2-13. Therefore,

$$d_{wet}\,(\text{star}) = 2\,R_G^{star} \tag{3-2}$$

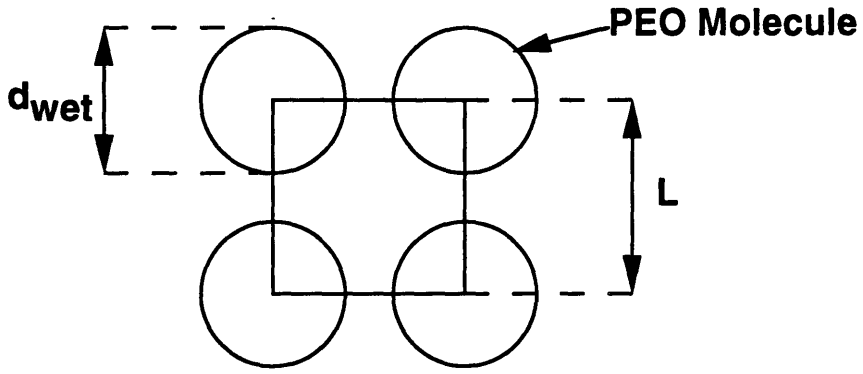


Figure 3-1: 2-D lattice model of PEO chains grafted on a surface.

We chose the radius of gyration to describe the size of the hydrated PEO molecules on the surface because $R_G$ is used extensivly in the literature to describe the conformation of grafted molecules in polymer brushes (which is essentially what these PEO surfaces are), both in theoretical[2-5] as well as experimental[6-8] studies. As seen in later discussion in this chapter comparing the model to the data, using readius of gyration to represent the size of the grafted PEO molecules, both star and linear forms, appears to be the appropriate size parameter to use.

The characteristic sizes of the proteins, $d_{prot}$, are well known, and all values of $d_{wet}$ and $d_{prot}$ are given in Table 3-1.

Table 3-1: Values of molecular weight, $d_{wet}$, and $d_{prot}$, for the proteins and linear and star PEO molecules.

| PEO | M(g/mol) | $d_{wet}$ (Å) | protein | M(kD) | $d_{prot}$ (Å) |
|---|---|---|---|---|---|
| 3400 | 3400 | 48 | cyt-c | 12 | 34, globular |
| 10K | 10,000 | 88 | alb | 68 | 72, globular |
| 20K | 20,000 | 128 | fib | 500 | 600 long, 25 wide |
| star 3510 | 350,000<br>Marm=5200 | 200 | | | rod-like, $R_G$=165 |
| star 228 | 200,000<br>Marm=10,000 | 160 | | | |

Note that due to the non-globular shape of fibronectin, a characteristic size of the protein was chosen to be its radius of gyration as calculated by:

$$R_G^2(\text{rod}) = \frac{l_r^2}{12} \tag{3-3}$$

where $l_r$ is the length of the rod.

To restate some of what was discussed in Chapter 2, the thickness of the dry PEO layer on the surface of the silicon wafer, h, as measured by ellipsometery and XPS, is an average value as if the layer were flat and uniform across the surface. This thickness was found to be directly related to the chain spacing by:

$$L = \left( \frac{M}{\rho_{dry} N_A h} \right)^{1/2} \tag{2-4}$$

with the assumption that when the hydrated PEO molecules dry on the surface, they dry to a constant density, $\rho_{dry}$ ($\rho_{dry}$ = 1g/cm$^3$ = 1g/10$^{24}$ Å$^3$). It was then found that the grafting density, $\sigma$, is also proportional to h, as well as to the PEO molecular weight.

$$\sigma \text{ (linear PEO)} = \left(\frac{a}{L}\right)^2 = \left(\frac{\rho_{dry} N_A h a^2}{M}\right) \qquad (2\text{-}5, 2\text{-}6)$$

$$\sigma \text{ (star PEO)} = \left(\frac{R_G^{star}}{L}\right)^2 = \left(\frac{\rho_{dry} N_A h \left(R_G^{star}\right)^2}{M}\right) \qquad (2\text{-}11, 2\text{-}12)$$

So for every dry thickness of PEO measured, a corresponding grafting density was calculated. These variables of $\sigma$, L, h, M, $d_{prot}$, and $d_{wet}$ can now be used in characterizing the PEO coverage on the surface and how it relates to protein adsorption.

### 3.2.2 PEO Chain Overlap

To characterize the PEO chain spacing on the surface, there are three key parameters that can be used to describe the degree of PEO chain overlap. The first parameter, $\nu$, is defined as,

$$\nu = \left(\frac{d_{wet}}{L}\right) \qquad (3\text{-}4)$$

$$= d_{wet}\left(\frac{\rho_{dry} N_A h}{M}\right)^{1/2} \qquad (3\text{-}4a)$$

and represents the degree of overlap of PEO chains along the sides of the unit cell. As depicted in Figure 3-2, there are three regimes of $\upsilon$:

$\upsilon < 1$ => No overlap, open space => protein adsorption

$\upsilon = 1$ => Start of PEO chain overlap => start of decreased adsorption

$\upsilon > 1$ => PEO chain overlap => decreased protein adsorption

A second parameter, $\upsilon_c$, is similar to $\upsilon$ and is defined as,

$$\upsilon_c = \frac{d_{wet}}{2^{1/2} L} = \frac{1}{2^{1/2}} \upsilon \tag{3-5}$$

where $2^{1/2} L$ is the distance between the attachment points of the two PEO molecules across the diagonal of the unit cell (see Figure 3-3). The space in the center of the unit cell is the largest open area in the 2-D lattice structure, and is important with respect to protein adsorption. Similar to $\upsilon$, there are also three regimes of $\upsilon_c$:

$\upsilon_c < 1$ => No overlap in center, open space => protein adsorption

$\upsilon_c = 1$ => Start of overlap in center => start of decreased protein adsorption

$\upsilon_c > 1$ => Overlap in the center => decreased protein adsorption

Note that $\upsilon_{c=1}$ is the point on the surface when all open space is first covered by PEO chains.

The final parameter of interest is $\varepsilon$, defined as:

$$\varepsilon = \frac{d_{prot}}{2^{1/2} L - d_{wet}} \quad \text{for } 2^{1/2} L > d_{wet} \tag{3-6}$$

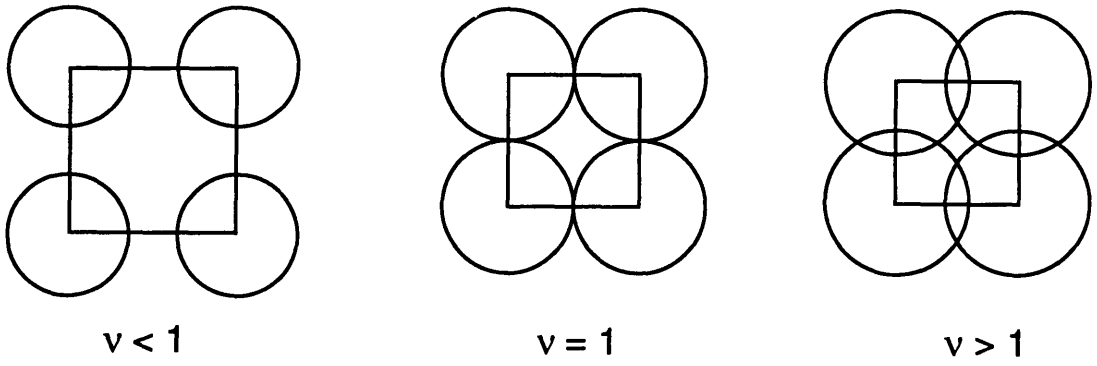


Figure 3-2: The degree of overlap of grafted PEO chains as defined by: (a) $\nu < 1$, (b) $\nu = 1$, and (c) $\nu > 1$.

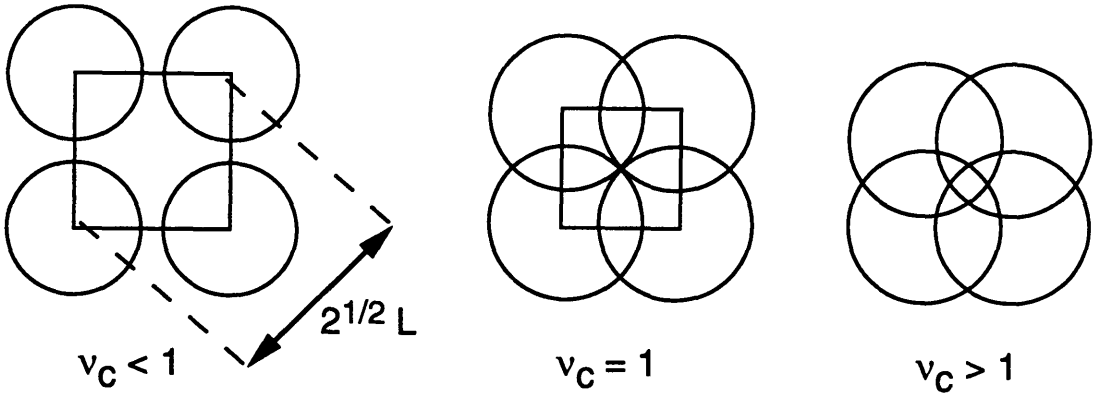


Figure 3-3: The degree of overlap of grafted PEO chains as defined by: (a) $\nu_c < 1$, (b) $\nu_c = 1$, and (c) $\nu_c > 1$.

This parameter $\varepsilon$ takes into account the size of the adsorbing protein and how it relates to the open space on the surface in the center of the unit cell, measured as $(2^{1/2} L - d_{wet})$. Again there are three regimes of $\varepsilon$, as depicted in Figure 3-4:

$\varepsilon < 1$ => Open space greater than $d_{prot}$ => protein adsorption

$\varepsilon = 1$ => Open space equals $d_{prot}$ => start of decreased adsorption

$\varepsilon > 1$ => Open space smaller than $d_{prot}$ => decreased protein adsorption

The condition $\varepsilon = 1$ can occur at any value of $\nu$, depending on the size of the PEO and size of the protein (see Figure 3-4). As will be outlined later, $\varepsilon$ is of key importance in explaining the protein adsorption on star PEO surfaces.

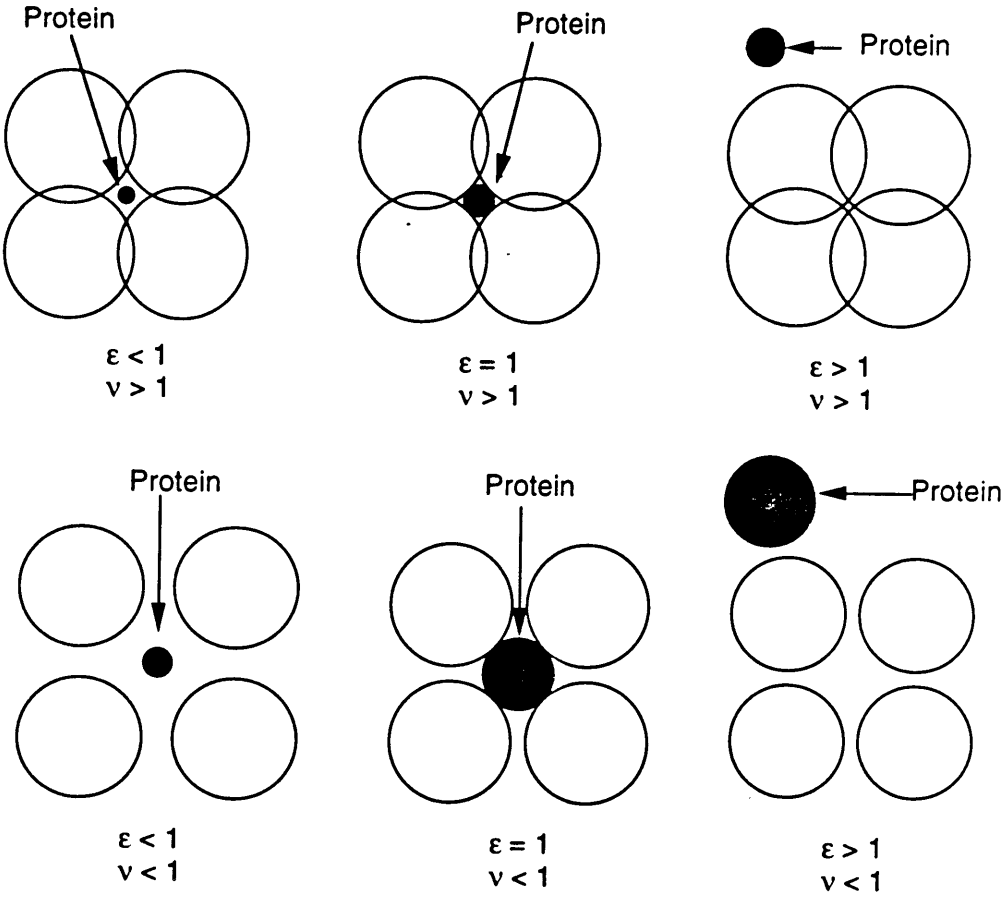


Figure 3-4: PEO chain spacing in how it relates to protein size, described by $\varepsilon < 1$, $\varepsilon = 1$, and $\varepsilon > 1$, at values of $\nu < 1$ and $\nu > 1$.

### 3.2.3 Protein Adsorption on Linear PEG Surfaces

When describing the protein adsorption on the linear PEG surfaces, we can correlate adsorption with grafting density by noting the values of $\sigma$ for where $\nu = 1$, $\nu_c = 1$, and $\varepsilon = 1$. As stated above, we expect a transition point in the adsorption behavior to occur somewhere in the vicinity of these points. From Eqs. 2-6 and 3-4a, the values of $\sigma(\nu = 1)$ and $\sigma(\nu_c = 1)$ were calculated and are given in Table 3-2. The values are small, at the low end of the grafting densities achieved on the PEG surfaces. This indicates that the surface rapidly becomes covered by PEO molecules. As seen from the data in Figures 2-8, 2-9 and 2-10, the protein adsorption is indeed starting to fall off at these low values of $\sigma$. However, just covering the surface with PEO is not sufficient to prevent proteins from reaching the surface, as seen by the high adsorption at these values of grafting density as well as the continued, although lower, adsorption at intermediate grafting densities.

Table 3-2: Values of $\sigma(\nu = 1)$ and $\sigma(\nu_c = 1)$ for linear PEG surfaces.

| PEG | $\sigma(\nu = 1)$ | $\sigma(\nu_c = 1)$ |
|---|---|---|
| 3400 | 0.00319 | 0.00638 |
| 10k | 0.00118 | 0.00236 |
| 20k | 0.00056 | 0.00112 |

Values of $\sigma$ when $\varepsilon = 1$, thus when the largest open spaces on the surface are becoming smaller than $d_{prot}$, can also be calculated. Table 3-3 gives the values of $\sigma(\varepsilon = 1)$ for the three proteins and the three PEG surfaces.

Table 3-3: Values of $\sigma(\varepsilon = 1)$ for linear PEG surfaces.

| | 3400 | 10k | 20k |
|---|---|---|---|
| cyt-c | 0.00274 | 0.00123 | 0.000694 |
| alb | 0.00127 | 0.000712 | 0.000454 |
| fib | 0.000401 | 0.000283 | 0.000211 |

Again, the values of $\sigma$ are at the low grafting densities, and, in general, the values are lower than the values of $\sigma(\nu = 1)$ and $\sigma(\nu_c = 1)$. Implicit in the parameter $\varepsilon$ is the assumption that protein adsorption cannot take place in the area occupied by a PEO chain. However, as seen in the data for the linear PEG surfaces, there is near-maximum adsorption at all values of $\sigma(\varepsilon = 1)$. The adsorption begins to decline only when the PEO chains start to overlap, at grafting densities greater than $\sigma(\nu_c = 1)$. Therefore, the important feature for linear PEG surfaces in preventing protein adsorption is PEO chain overlap on the surface, as described by $\nu$ and $\nu_c$.

Another feature to note in the adsorption on linear PEG surfaces is the point at which the onset of minimum adsorption occurs, signified by a marked decrease in slope (i.e., corresponding to point C in Figure 2-7). On each of the PEG surfaces, the adsorption of all three proteins becomes negligible at about the same value of $\sigma$, which is near the highest grafting density. An estimate of grafting density, represented by $\sigma^*$, at these minimum adsorption points are:

$\sigma^*(3400) \approx 0.014$, $\sigma^*(10k) \approx 0.0043$, $\sigma^*(20k) \approx 0.0022$ for each of the three linear PEG surfaces, respectively. In calculating the corresponding overlap (i.e., value of $\nu(\sigma^*)$), it turns out

to be about the same, that of $\nu^*(3400, 10k, 20k) \approx 2$. Therefore, significant chain overlap, to the point where PEO chains are roughly doubled up on the surface, is necessary for the prevention of protein adsorption. Furthermore, at this overlap, the chain spacing is approximately equal to the radius of gyration of the PEG molecule, $L \approx R_G^{linear}$. This exact spacing was theorized by de Gennes[2] and Alexander[3] in their theories on polymer brushes as marking the point on the surface where the excluded volume of the grafted chains would cause them to extend away from the substrate surface, resulting in chain stretching. It is therefore not surprising that, under these conditions, proteins cannot penetrate the PEO layer and reach the surface. If the chains are stretching in order to avoid themselves and surrounding chains, then it follows that they would rebel against being compressed by an approaching protein. In fact, at $\sigma^*$, additional PEG chains themselves begin to have difficulty penetrating the layer. This is indicated by the value of $\sigma^*$ for a given PEG surface lying in the "knee" of the curve of grafting density vs. coupling concentration (see Figure 2-5), marking the point where maximum grafting density is almost reached. If, in the process of coupling PEO to the surface, more PEO chains are having difficulty getting through the already existing brush layer, despite their ability to reptate by change of conformation, then globular proteins would surely have even more difficulty since they are rigid, nondeformable structures.

The above conclusion that chain overlap is critical on linear PEO surfaces for preventing protein adsorption possibly explains the lack of dependence in protein adsorption behavior with protein size. For example, given the large size of fibronectin, we would expect to see a rapid, early decrease in adsorption (i.e., at low grafting densities) compared to the other two smaller proteins, with fibronectin ultimately being the first to be excluded from the surface. The reason

why we do not observe this behavior, but rather we see the decline in adsorption for all three proteins occurring over the same range of protein densities, is that with the surface fully covered with a layer of PEO, there are no "holes" in which protein size would play a role. For a protein of any size to reach the surface, it would need to penetrate the PEO layer. This then results in steric repulsion by the compressed PEO chains. The larger the protein, the greater the hydrophobic attraction, but also the greater the area over which PEO chains are compressed, and thus the greater the repulsion.[9,10] Therefore, the influence of protein size is much reduced. The main feature governing protein adsorption in the PEO overlap regime is the degre of overlap, or the volume fraction of PEO in the layer. Increasing the grafting density greatly increases the steric repulsion as chains are compressed, and also serves to slightly decrease the hydrophobic attraction of the protein for the underlying substrate surface.[9,10]

At the point where the PEG surfaces are non-adsorptive (i.e., $\sigma^*$), the fact that the grafting density is lower for a larger molecular weight PEG is offset by the increase in height, H, of the hydrated PEG layer[2,8]

$$H = a\left(\frac{M}{M_o}\right)\sigma^{1/3} \qquad (3\text{-}7)$$

Therefore, H increases with increasing molecular weight and grafting density, with a greater dependence on molecular weight. At $\sigma^*$, estimations of the height of the PEG layer, H*, are: H*(3400) ≈ 56 Å, H*(10k) ≈ 112 Å, and H*(20k) ≈ 177 Å. The volume fraction of PEO, $\phi$, within the layer is also proportional to grafting density in the chain overlap regime: $\phi \cong \sigma^{2/3}$.[2] Therefore, at $\sigma^*$ on a surface for a given molecular weight PEG, the PEO layer is of a sufficiently high concentration and thickness to present an overall resistance to the proteins such

that they cannot reach the surface. Evidence of this is that the point $\sigma^*$ marks the same dry PEO thickness on all three PEG surfaces, that of h = 8-9 Å, corresponding to a PEO content of 80-90 ng/cm$^2$. This suggests that surface contents of linear, amorphous PEO chains equal to or greater than this content, when hydrated, would be sufficient to prevent protein adsorption.

The specific forces behind the protein adsorption behavior noted above can only be determined through a study of the energies of interaction between a protein molecule, the PEO layer, and the underlying substrate surface. This issue was investigated by Jeon et al.[9,10], who modelled the protein resistance of a grafted PEO surface through a combination of hydrophobic interactions, Van der Waals attraction between a protein and the substrate surface, and steric repulsion of the grafted PEO as it is compressed by an approaching protein. In their study, the authors conclude that "high surface density and long chain length of PEO are desirable for protein resistance [where] surface density has a greater effect than chain length".[9] These conclusions are in agreement with our experimental results. All three PEG surfaces prevented protein adsorption as long as they achieved a sufficient grafting density; larger PEG molecular weights served to decrease the necessary grafting density. It is noted, relative to the latter part of the quote above, that a PEG 20k grafted surface just at the onset of chain overlap (at the low grafting densities in Figure 2-10) has a similar PEO layer thickness as a PEG 3400 grafted surface with significant chain overlap ($H[20k] \approx R_G[20k] = 64Å^2$ vs. $H^*[3400] \approx 56$ Å), yet the PEO 20k surface adsorbed proteins whereas the PEG 3400 surface did not. The density of PEO within the PEG 20k surface was less than that of the PEG 3400 surface ($\sigma[20k] < \sigma^*[3400]$, and therfore $\phi[20k] < \phi[3400]$). This difference was therefore significant enough that proteins could get through the 20k layer and adsorb. This demonstrates the greater importance of PEO layer

density over PEO molecular weight in the prevention of protein adsorption. These conclusions agree with the findings of Pime and Whitesides,[11] where PEG oligomers of only 2-6 monomer units at high enough contents on the surface were sufficient to prevent protein adsorption.

Jeon et al.[10] also theorized the existence of "optimal" chain spacings for the rejection of proteins of various sizes, where the smaller the protein, the smaller the chain spacing (or grafting density) needed to prevent it from adsorbing. Our results do not support this claim, where we found that protein adsorption has little overall dependence on protein size. A possible reason for the discrepancy is that Jeon et al.[10] may not have correctly taken into account the hydrophobic interaction between the protein and the surface. Where they modelled the protein as an entirely hydrophobic entity facing the substrate surface, in reality, the protein has only small hydrophobic regions, and is free in solution such that these regions may or may not be facing the surface at any given moment in time. Therefore, the hydrophobic attraction, and its dependence on protein size, may have been overestimated. Jeon et al.[10] also concluded that these "optimal" chain spacings are independent of the length of the PEO chain by studying the effects of maintaining a particular value of PEO chain spacing while varying the PEO chain length. This claim is a bit misleading because the chain spacing and chain lengths they examined were within region C-D in Figure 2-7, where protein adsorption was already negligible. Increasing the PEO molecular weight in this region does not change the efficacy of the surface in rejecting proteins. Athought they identified the fact that a threshold exists, above which an increase in molecular weight does not effect the protein adsorption, our results demonstrate that when operating at chain spacings beneath this threshold, an increase in PEO molecular weight reduces protein adsorption.

### 3.2.4 Protein Adsorption and PEO Star Surfaces

The same analysis that was used for protein adsorption on linear PEG surfaces was applied to the PEO star surfaces. Values of $\sigma$ when $\nu = 1$ (start of the PEO star overlap), $\nu_c = 1$ (overlap of stars in the center of the unit cell such that all open space is covered with PEO), and $\varepsilon = 1$ (when the largest open space equals the size of the protein) are given in Table 3-4.

Table 3-4: Values of $\sigma$ when $\nu = 1$, $\nu_c = 1$, and $\varepsilon = 1$, for PEO stars.

| | | | | $\varepsilon = 1$ | |
|---|---|---|---|---|---|
| | $\nu = 1$ | $\nu_c=1$ | cyt-c | alb | fib |
| star 228 | 0.250 | 0.500 | 0.347 | 0.237 | 0.121 |
| star 3510 | 0.250 | 0.500 | 0.378 | 0.265 | 0.138 |

From these values, some insight into the degree of PEO star coverage on the surface and its effectiveness at preventing protein adsorption can be gained. From a comparison of the values of $\sigma(\nu = 1)$ to the data in Figures 2-14 and 2-15, it is clear that the initial point of star overlap was reached for both star surfaces, since the grafting densities of star 228 and 3510 reached and exceeded 0.250. (Note that at $\nu = 1$, $\sigma = (R_G^{star}/d_{wet})^2 = (1/2)^2$.) At this value ($\sigma = 0.250$), both fibronectin and albumin have nearly reached zero adsorption, whereas cytochrome-c still shows significant adsorption. The value of $\sigma(\nu_c = 1) = 0.500$ for star 228 and star 3510 indicates that neither star surface has reached full coverage of PEO, since the highest grafting densities achieved were only 0.289 for star 228 and 0.370 for star 3510. Of greatest interest are the values of $\sigma(\varepsilon = 1)$. First, it is seen that the open spaces on the surface become smaller than the size of

albumin at $\sigma \approx 0.237$ on star 228 and $\sigma \approx 0.265$ on star 3510, which closely correlates with the drop to zero adsorption at these grafting densities in the plots. This drop to zero at the point where $\varepsilon = 1$ and not at some later point (at $\varepsilon > 1$) indicates that the protein cannot easily move or compress the star PEO chains out of the way so as to diffuse into a space smaller than its size, whereas it can do this with linear PEG prior to the point $\sigma^*$. The PEO stars are severalfold more concentrated in PEO than linear PEO of the same effective diameter, dense enough to withstand the penetration of protein without the need for overlap, unlike for linear PEO.

Fibronectin does not reach zero adsorption at $\sigma \approx 0.121$ (star 228) or 0.138 (star 3510), as the values at $\varepsilon = 1$ indicate. However, as was observed earlier with the adsorption onto linear PEG surfaces, fibronectin seems to behave like a protein similar in size to albumin and not its radius of gyration, the latter from which the values of $\sigma(\varepsilon = 1)$ were calculated. As shown in Figures 2-14 and 2-15, fibronectin does reach zero adsorption at similar values of grafting density as that of albumin. There is an immediate decrease in adsorption of albumin and fibronectin at values of $\sigma$ less than $\sigma(\varepsilon = 1)$ on both star surfaces. One possible explanation for this is that since the star molecules behave as large, "hard" spheres, they define a rigid-wall pore whose diameter is on the order of the protein size, resulting in a great decrease in diffusion coefficient of the protein. There is much more flexibility in the "walls" of a space defined by linear PEO than stars. Therefore, the probability for reaching the surface drops quickly as the distance between star molecules decreases.

The value of $\sigma(\varepsilon = 1)$ for cytochrome-c on the star 228 surface is greater than the maximum grafting density achieved on the samples. Therefore, the condition where the open

spaces between star molecules are smaller than the size of cytochrome-c has not yet been reached. This explains the continued, although decreased, adsorption of cytochrome-c whereas albumin and fibronectin no longer adsorb. On star 3510 surfaces, $\sigma(\varepsilon = 1)$ for cytochrome-c just about equals the maximum PEO grafting density achieved. Thus the continued adsorption of cytochrome-c up to this point is possible, and if a value of $\sigma$ greater than 0.370 was obtained on the surface, then a drop in the cytochrome-c adsorption would probably be observed. Figure 3-4a is a possible picture of the star surface that describes the continued adsorption of cytochrome-c. Here, the entire space occupied by the star molecule is excluded to the protein. This is in contrast to that of a linear PEG surface, which could be described by Figure 3-3b,c, where the space occupied by the PEG molecule is not impenetrable to proteins until significant (approximately half) overlap is achieved.

The difference between the values of $\sigma(\nu = 1)$ and $\sigma(\varepsilon = 1)$ indicates an interesting feature of the protein adsorption: the rate of decay of adsorption with increasing grafting density (i.e., the slope of the decay). When values of $\sigma(\varepsilon = 1) < \sigma(\nu = 1)$, the rate of decay of protein adsorption is expected to be faster than when $\sigma(\varepsilon = 1) > \sigma(\nu = 1)$. The former signifies the decrease in size of open spaces to smaller than $d_{prot}$ at or before the onset of overlap, thus beginning to exclude the proteins at an early stage. The latter signifies that even though the molecules are overlapping, there are still open spaces on the surface larger than the protein, and thus it can still adsorb. It then follows that the greater the difference between $\sigma(\varepsilon = 1)$ and $\sigma(\nu = 1)$, the faster or slower the rate of decay. For example, if $\sigma(\varepsilon = 1) < \sigma(\nu = 1)$ for a given size protein (e.g., albumin), as protein size decreases, $\sigma(\nu = 1)$ remains unchanged while

$\sigma(\varepsilon = 1)$ increases, and thus the rate of decay should decrease. For both albumin and fibronectin, $\sigma(\varepsilon = 1) < \sigma(\nu = 1)$, and for cytochrome-c, $\sigma(\varepsilon = 1) > \sigma(\nu = 1)$. From Figures 2-14 and 2-15, the data agree with the model, where from maximum to minimum adsorption, the slope is much greater for albumin and fibronectin than for cytochrome-c, cytochrome -c not even reaching zero adsorption.

Overall, the protein adsorption of all three proteins was similar on both star 228 and star 3510 surfaces, despite the differences in their functionalities and arm molecular weights. This is probably because both stars are in the limit of behaving like hard spheres. Therefore, a protein perceives both surfaces similarly, where it can only adsorb in the open spaces between star molecules.

Complete coverage of the surface with star PEO of either kind was not achieved in the experiments presented here, but this is not to say that it cannot be achieved. As stated in Section 2.3.2.3, the highest coupling concentration for the stars was just at the point of chain overlap, which correlates well with the small chain overlap observed on the star-grafted surfaces. Higher concentrations would then force the molecules to interpenetrate. This would potentially increase the molecular overlap on the suface until the point where excluded volume effects prevent any closer packing on the surface, as was observed with linear PEG surfaces. Thefore, the potential exists for increased star coverage on the surface.

## 3.3 Haxagonal Lattice Structure and Hydrodynamic Radius

A hexagonal lattice structure was also considered in the construction of the model of PEO grafted chains on the surface (where a unit cell consists of the PEO molecules forming a triangle on the surface rather than a square). Only two parameters were considered, that of chain overlap, represented by $\nu$, and size of open spaces on the surface, represented by $\varepsilon$. The conclusion is that using a hexagonal lattice structure results in little difference in the values of $\sigma(\nu = 1)$ and $\sigma(\varepsilon = 1)$, which therefore means that the ultimate conclusions from the above analysis using a quadratic lattice structure still hold. In addition, using hydrodynamic radius to represent the size of the hydrated PEO molecules on the surface was also considered. For linear PEO, the hydrodynamic radius is approximately 70% the radius of gyration. The values of $\sigma(\nu = 1)$, $\sigma(\nu_c = 1)$, and $\sigma(\varepsilon = 1)$ therefore increase significantly. When comparing these values of $\sigma$ to the data, they no longer correlate. The lack of a correlation with the model with data also occurs when considering the star PEO surfaces. The hydrodynamic radius of a star molecule is approximately 1.291 times the radius of gyration, in keeping with the assumption that the stars are like hard spheres. This increase in the size of a star molecule causes a decrease in the values of grafting density at the transition points of $\sigma(\nu = 1)$, $\sigma(\nu_c = 1)$, and $\sigma(\varepsilon = 1)$, which no longer correlate with the data. Therefore, it appears that the use of radius of gyration to approximate the size of the grafted PEO molecules on the surface was the appropriate size parameter. In particular, with the star molecules, the radius of gyration seems to correctly approximate the region of these molecules that is resistant to penetration by proteins.

## 3.4 Conclusions

In conclusion, the model just presented accounts for the protein adsorption behavior of cytochrome-c, albumin, and fibronectin on PEG 3400, 10k, 20k, surfaces as well as on star 228 and 3510 surfaces. It explains the pertinent trends such as a relatively fast decay in adsorption observed for albumin and fibronectin on all surfaces, and a relatively slow to very slow decay for cytochrome-c on the linear PEG and star surfaces. It shows why complete coverage of the surface with linear PEG to the point where the chains are roughly half-overlapping (i.e., $L \approx R_G^{linear}$) is necessary for the non-adsorption of proteins on linear PEG surfaces, where this chain overlap appeared to be independent of PEO molecular weight and protein size (at least in the range of PEG molecular weights and protein sizes studied). The fact that much higher grafting densities for smaller molecular weight PEGs are necessary for the prevention of protein adsorption is a possible reason for why, with many polymer networks incorporating PEO presented in the literature, smaller PEO contents and molecular weights were insufficient in preventing protein adsorption and adverse biological reactions. With these networks, it is difficult to obtain high surface densities, especially when dealing with such heterogeneous surfaces. The results presented here, however, provide a possible guide that can help in targetting the design of a material in trying to obtain a sufficient PEO content on the surface to prevent protein adsorption and adverse biological reactions.

In contrast to linear PEO surfaces, open spaces can exist on PEO star surfaces and still achieve negligible adsorption of the larger proteins. The latter behavior is a consequence of the hard sphere characteristics of the PEO stars, which are much more concentrated in polymer segments than linear chains of equivalent molecular weight or equivalent radius of gyration.

Therefore, the star molecules themselves are sufficient on their own, without the need for overlap, in preventing proteins from adsorbing to a surface.

## 3.5 References for Chapter 3


1. B.J. Bauer, L.J. Fetters, W.W. Graessley, N. Hadjichristidis, and G. Quack, *Macromolecules*, 22 (5), 2337 (1989).

2. P.G deGennes, *Macromolecules*, 13 (5), 1069 (1980).

3. S. Alexander, *J. Phys. (Paris)*, 38, 977 (1977).

4. A. Kopf, J. Baschnagel, J. Wittmer, and K. Binder, *Macromolecules*, 29 (5), 1433 (1996).

5. S.T. Milner, T.A. Witten, and M.E. Cates, *Macromolecules*, 21, 2610 (1988).

6. J.B. Field, C. Toprakcioglu, R.C. Ball, H.B. Stanley, L. Dai, W. Barford, J. Penfold, G. Smith, and W. Hamilton, *Macromolecules*, 25, 434 (1992).

7. P. Auroy, L. Auvray, and L. Leger, *Macromolecules*, 24, 2523 (1991).

8. P. Auroy, L. Auvray, and L. Leger, *Phys. Rev. Lett.*, 66, 719 (1991).

9. S.I. Jeon, J.D. Andrade, and P.G. deGennes, *J. Colloid Interface Sci*, 142 (1), 149 (1991).

10. S.I. Jeon and J.D. Andrade, *J. Collard Interface Sci*, 142 (1), 159 (1991).

11. K.L. Prime and G.M. Whitesides, *J. Am. Chem. Soc.*, 15, 10714 (1993).

# CHAPTER 4

## Bonding of PEO to Polymer Surfaces Using Electron Beam Irradiation

### 4.1 Introduction

As was discussed in Chapter 1, much has been done in recent years in trying to engineer a purely PEO surface on a polymer substrate for biomedical application. Although some success has been achieved, a method has yet to be developed whereby the resulting surface is only PEO as seen by biological molecules. The process presented here may be the solution to this problem.

One method for the grafting of polymers and/or monomers is through irradiation using an electron beam. Under an electron beam, radicals are created whereby monomers can polymerize, polymers or monomers can graft to a surface, polymers can crosslink, or polymers can degrade. In the case of PEO, an aqueous solution of PEO will crosslink under an electron beam to form a hydrogel. In this reaction, the water molecules play an important role:[1,2]

$$2\,HOH \xrightarrow{e^-} 2\,{\cdot}OH + H_{2(g)}$$

$${\cdot}OH + -(CH_2\text{-}CH_2\text{-}O\text{-})_n \rightarrow HOH + -(CH_2\text{-}\dot{C}H\text{-}O\text{-})_n \qquad \text{(Scheme 4-1)}$$

Ultimately two radicals, each one along a different PEO chain, find each other and terminate, thus creating a tetrafunctional crosslink junction between the two chains. PEO hydrogels have been formed on various hydrophobic polymer surfaces (e.g., polyethylene) under the electron beam in this way, but these hydrogels are not stable on the surface. They can be scraped cleanly from the

surface rather easily, or will delaminate if kept in an aqueous environment. The PEO has a much higher affinity for binding to itself than to the polymer substrate. This may partly be due to the inherent hydrophobic/hydrophilic difference between PEO and the polymer. Also, if the surface is not wet by water, the hydrogel radicals created by the radiation may not be effective in creating radicals on the surface to which PEO radicals can couple.

It was hypothesized that PEO would bind to a polymer surface if the surface was made hydrophilic. In order to achieve this, a hydrophilic monomer, methacrylic acid (MA) ($CH_2$=C($CH_3$)COOH), was chosen to be grafted first to the polymer surface, and was chosen for two important reasons. First, MA has already been successfully grafted to various polymer surfaces using the electron beam.[3] Second, when PEO is placed in an aqueous solution of poly(acrylic acid) (PAA) or poly(methacrylic acid) (PMAA), the ether oxygens of PEO immediately hydrogen bond to the hydrogen in the acid groups of PAA or PMAA, and the resulting complex that is formed is no longer water soluble.[4-6]

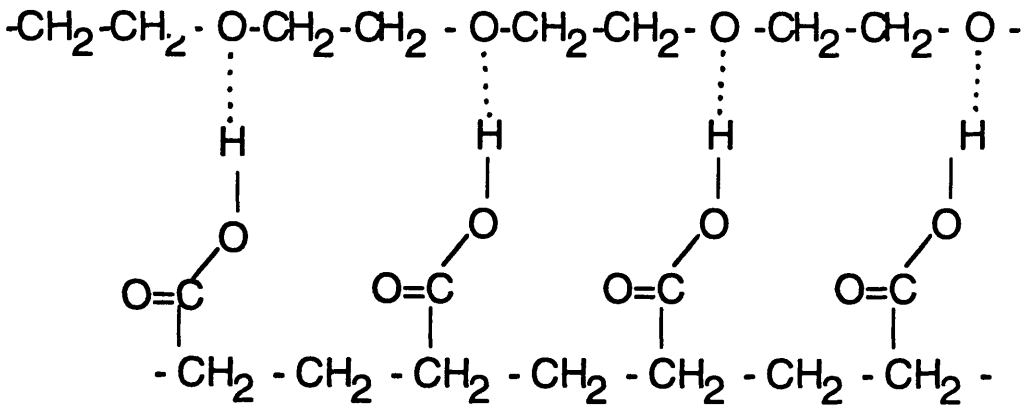

(Scheme 4-2)

The hydrogen bonds are broken and the polymers resolubilized only through the addition of base, which displaces the hydrogen ion with a sodium or other counter-ion. Utilizing this fact, by

grafting a layer of methacrylic acid (MA) to a polymer surface, a close association of the PEO to the surface is promoted, and would potentially help in leading to the binding of PEO to the surface under the electron beam.

The following results prove that by grafting methacrylic acid to a polymer surface first, PEO will form stable grafts to the surface under the electron beam. This method has several advantages over others that have been tried in the past. First, full PEO coverage would be more easily achieved in this manner since it is the body of the polymer that is binding to the surface, not just the chain ends. Second, there is extreme versatility where either monolayers or multilayers of any thickness could be made. A monolayer of PEO can be created simply by rinsing away any non-hydrogen bonded PEO from the MA-treated surface before grafting the PEO; multilayers can be created by maintaining a finite layer of PEO solution on the MA-treated surface before e-beaming. Multilayers are also of unique importance in that by using a low molecular weight linear PEO (e.g., 5000 - 25 000 g/mol), or using a star-shaped PEO, there would be a high concentration of hydroxyl groups on the surface available for the attachment of a ligand to create a surface catered towards a specific biological purpose.

This chapter focuses on the synthesis of the MA and MA-PEO surfaces, their characterization, and stability on polymer surfaces, in particular on polystyrene and low-density polyethylene. The remaining polymers that are mentioned in Section 4.2 were mainly tested for their ability to graft on methacrylic acid (as the subsequent grafting of PEO would follow), and are dealt with briefly at the end of this chapter. Chapter 5 then addresses the effectiveness of the modified polystyrene surfaces at preventing non-specific adsorption of proteins, focussing mainly on PEO monolayers.

## 4.2 Experimental

### 4.2.1 Materials

Polystyrene (PS) low-density polyethylene (LDPE), polymethyl methacrylate(PMMA), and polyethylene terephthalate (PET) sheets (ca. 1 mm thick) were obtained from Goodfellow, Inc. (Berwyn, PA) and used as received. Polypropylene (PP) dishes were obtained from Fluoroware Inc. (Chaska, MN, H22 series) and used as is. Membrane pieces of poly(vinylidene fluoride) ($PVd_2F_2$) (GVX 0508 V304) and poly(ether sulfone) (PES) (lot BM 12 0392 C) were obtained from Millipore Corp. (Bedford, MA). Poly(dimethyl siloxane) (PDMS) was obtained from General Electric Corp (Albany, NY, product SE30). Polyvinyl chloride (PVC) powder was obtained from Pechiney St. Gobain (mass polymerized grade Rucon® B34), and plasticized PVC was Tygon® tubing. Poly(ethylene oxide) samples of molecular weights 8000, 100 000, 600 000, $1x10^6$, $5x10^6$ g/mol, were obtained from Polysciences, Inc. (Warrington, PA), and PEO of molecular weight 35 000 g/mol was obtained from Fluka Chemical (Ronkonkoma, NY). PEO star 3510 was a gift, as mentioned previously in Section 2.2.1. Methacrylic acid, acrylic acid, and 2-vinyl-n-pyrrolidinone monomers were obtained from Aldrich Chemical (Milwaukee, WI) and used without further purification.

### 4.2.2 Electron Beam Irradiation

Radiation grafting was performed using a 3 million electron volt Van de Graaff generator (MIT High Voltage Research Lab, see Figure 4-1). Polymer pieces (LDPE and PS), 2 $cm^2$, were

placed in a glass dish and immersed in a solution of freshly mixed[†] 20% (w/v) methacrylic acid in water (the solution not exceeding a layer of 1-2 mm over the samples so as to ensure maximum beam dosage). The samples were covered with 1.5 mm thick glass, so as to impart a dosage to the target materials' surface to within ±10% of the intended dosage, and passed under the electron beam for a total dose of 2 megarads (one pass, 2 Mrad/pass, one rad of absorbed dose = 100 ergs per gram of irradiated matter, 1 megarad = 1 million rads). The total dose delivered was controlled by the beam current in microamperes, the voltage (generally 2.5-3.0 million eV), the speed of the belt on which the samples were placed to pass under the beam, and the number of times the samples were passed under the beam. In all experiments, the dose rate was between 50 000 and 100 000 rads per second.

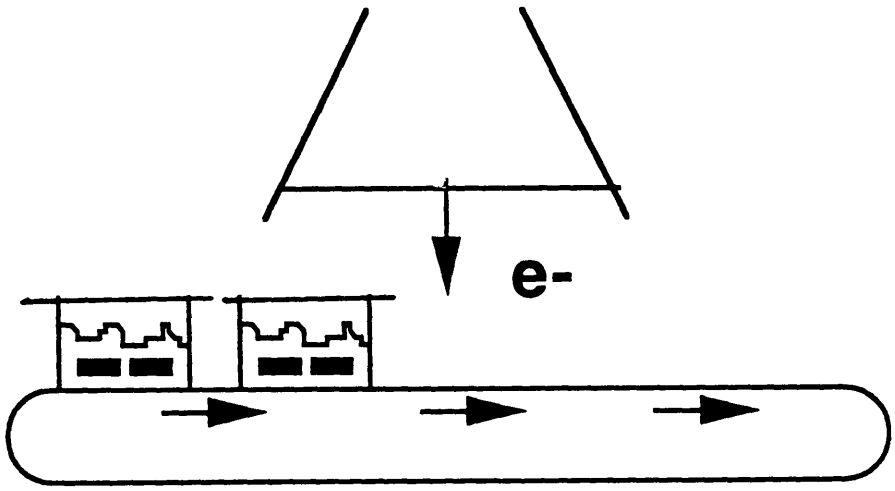


Figure 4-1: Schematic of apparatus for electron beam irradiation.

[†] It was noted that MA and MA/water solutions that had been exposed to air and left standing for more than 24 hrs did not graft as effectively as fresh solutions. This could be due to an increased dissolved oxygen content which depleted much of the beam dose.

After exposure to the beam, samples were removed from the dish, rinsed thoroughly with water, and placed in an aqueous solution of PEO. At constant PEO concentration (4% w/v), the molecular weight of the linear PEO ranged from 8000 to 5 x $10^6$ g/mol. At constant linear PEO molecular weight (35 000 g/mol), concentrations ranged from 0.05% to 15% (w/v). The concentration of the star solution was 2% (w/v). For monolayer formation, after soaking in PEO solution for 10 minutes, pieces were rinsed thoroughly with water, placed in a dish, immersed in water, covered, and passed under the electron beam for a total dose of 2 Mrad. For multilayer formation, after 10 minutes in the PEO solution, excess PEO solution was drained from the samples, the samples placed in a dry dish, covered, and exposed to the electron beam (while still wet) for a total dose of 2 Mrad. All samples were rinsed with water after the second irradiation.

### 4.2.3 Surface Analysis

All surfaces were analyzed using a Surface Science Inc. SSX-100 XPS spectrometer. High resolution scans of the carbon 1s photoelectron (as described in Section 2.2.2.2) were taken to detect the bonding character of the carbon on the top ~50Å of the surface, where the acid peak from the methacrylic acid and the ether peak from the PEO were detected and analyzed. Samples were also critically examined by eye for a qualitative assessment of their wettability with water.

## 4.3 Results

### 4.3.1 MA-Treated Surfaces

Methacrylic acid treated surfaces were dried in air and analyzed by XPS. Figures 4-2 and 4-3 show the high resolution carbon 1s scans of untreated and MA-treated LDPE and PS materials.[†] The presence of the MA is evident through the appearance of a new, higher energy peak shifted 4 eV from the main alkane carbon peak, which is indicative of acid carbon, COOH (also the same shift for ester carbon). Two other intermediate peaks are also present, one shifted 1.5 eV from the main peak, indicative of ether/alcohol carbon (C-O), and one shifted 2.7 eV from the main peak, possibly a carbonyl carbon or an ether carbon with some strong secondary effects from neighboring carbons (e.g., a neighboring ester/acid). To ascertain as to whether the two intermediate peaks were due to the actual involvement of the MA grafting to the surface or if they were secondary reactions involving only the MA with itself while under the electron beam, some of the 20% methacrylic acid solution that had been exposed to a 2 Mrad dose (now consisting of monomer and polymer) was placed on a glass slide, allowed to dry in air in a chemical fume hood, and the residue (mainly PMAA) analyzed in XPS. The high resolution carbon scan in Figure 4-4 clearly shows only two peaks, the alkane carbon peak and the acid peak shifted 4 eV from it, with the relative peak areas of 78% and 22% being close to those of the theoretical prediction of 75% and 25%, respectively. Therefore, the two additional peaks present in Figures 4-2b and 4-3b are due to the mechanism of binding the MA to the polymer surface, the details of which are not currently known and cannot be determined from only an XPS scan.

[†] Both sides of the samples yielded the same scan, indicating that the pieces were thin enough to cause a negligible change in the effective beam dose as it passed through the sample.

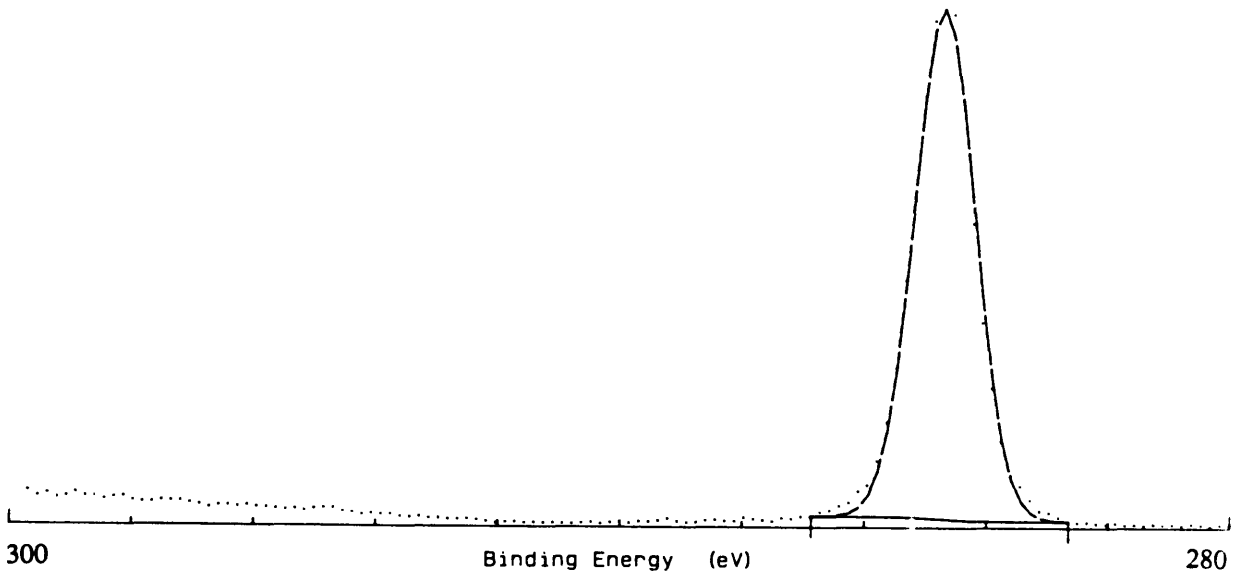


(a)

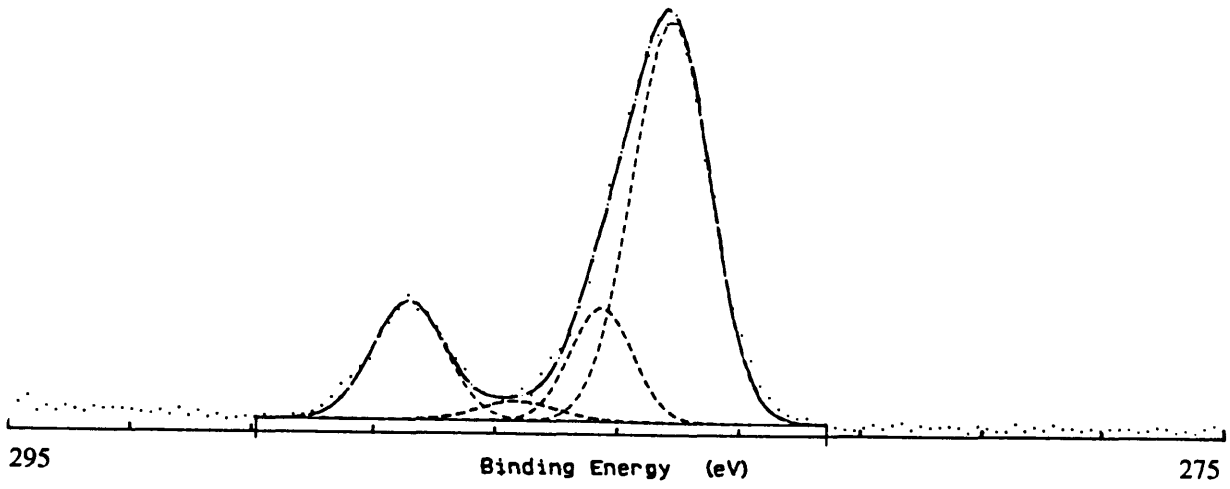


(b)

Figure 4-2: XPS high resolution carbon scans of: (a) untreated LDPE, and (b) MA-treated LDPE.

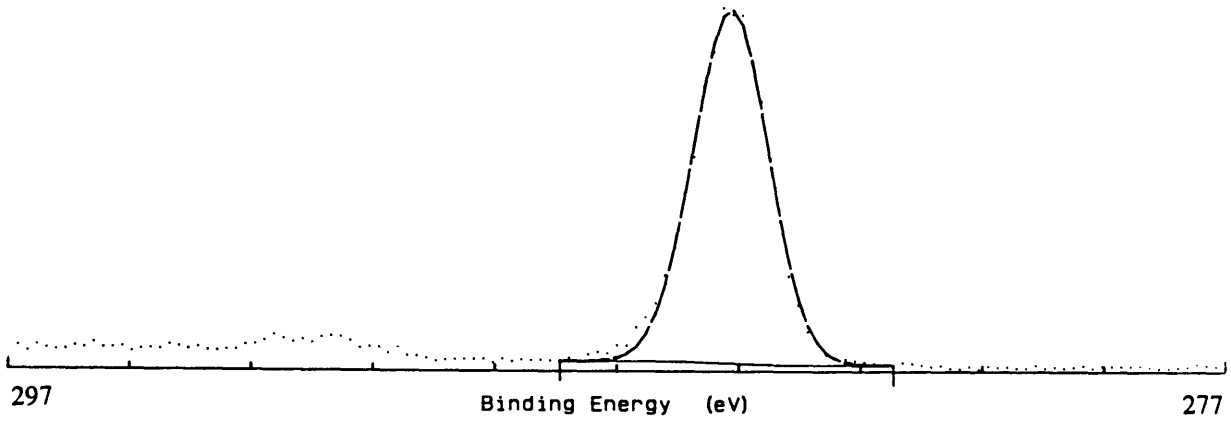


(a)

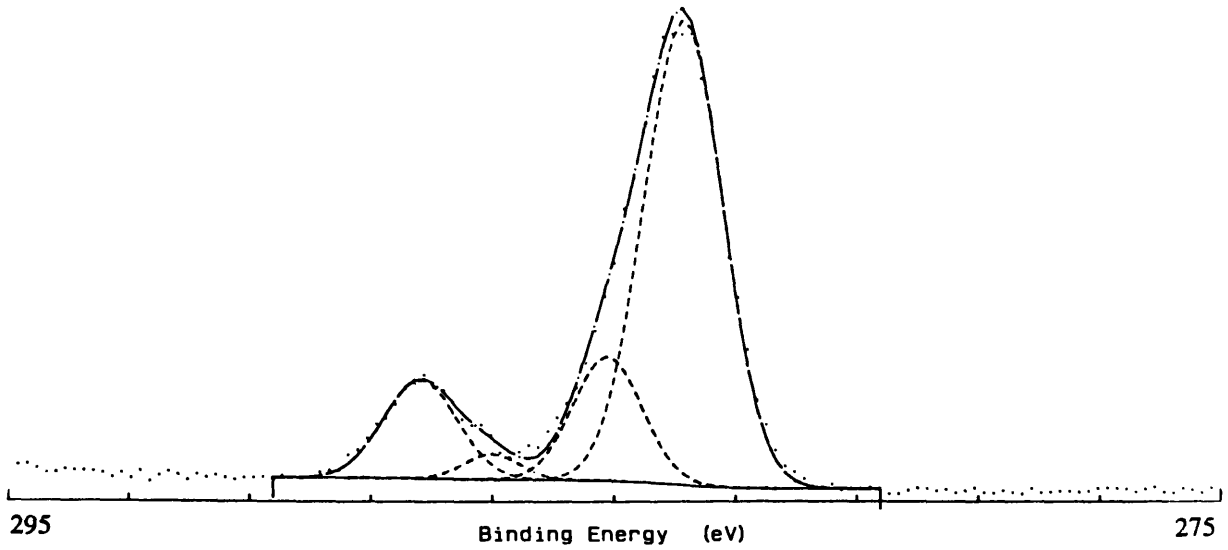


(b)

Figure 4-3: XPS high resolution carbon scans of: (a) untreated PS, and (b) MA-treated PS.

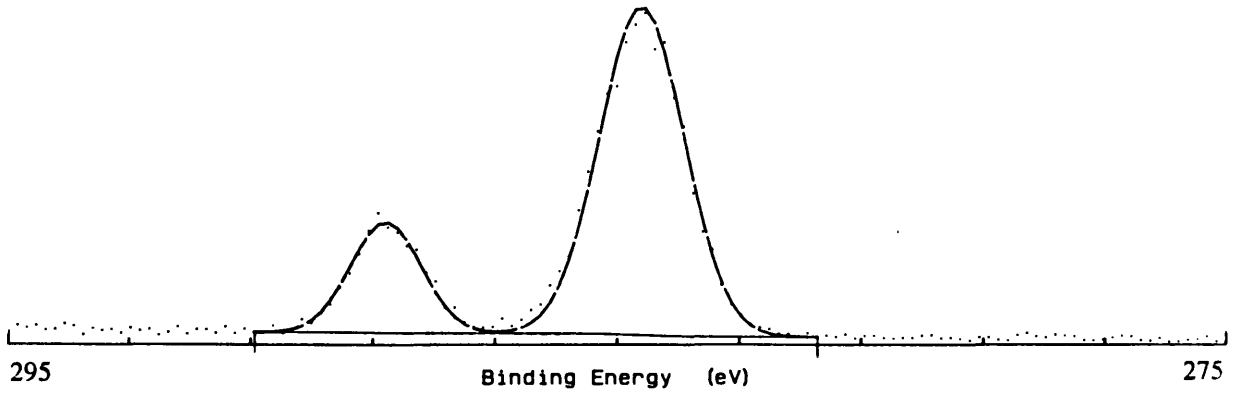


Figure 4-4: XPS high resolution carbon scan of MA soution residue after exposure to 2 Mrad.

Further evidence of the MA on the surface is the extreme wettability these samples possess after MA grafting. Whereas before treatment the samples were extremely hydrophobic so that water beaded up as spherical drops, after MA grafting, the samples held a continuous film of water on their surface. The surfaces thus made hydrophilic could not be made hydrophobic again by extensive rinsing with water, methanol, or ethanol. This wettability was retained even after five days soaking in water (0.03% w/v sodium azide as bacteriostat). Additional evidence of MA on the surface was in the presence of sodium in an XPS survey scan after an MA-treated sample was placed in 1M NaOH for one hour and rinsed thoroughly with water. This treatment replaced the $H^+$ counterion on the acid groups with $Na^+$. It was found that the ratio of sodium to non-acid carbon from the survey scan, %Na / (%C-%Na), nearly equalled the ratio of the peak areas of acid to non-acid carbon from the high resolution carbon scan, giving values of 0.041 vs. 0.046 respectively. Therefore, almost all acid carbon on the surface was indeed COOH, unchanged from e-beaming, whose $H^+$ was replaced by an $Na^+$ counterion.

It should be noted here that both polystyrene and low density polyethylene react similarly to the grafting of MA and PEO to their surfaces. Therefore, all results throughout the remainder of this chapter can be applied to either LDPE or PS.

### 4.3.2 PEO-Grafted Monolayers

A typical XPS high resolution carbon scan showing a grafted linear PEO monolayer (MW = 35 000 g/mol) on the surface of PS or LDPE is shown in Figure 4-5a. Of main importance is the change in area of the second peak, the ether/alcohol carbon peak, showing an increase in the relative peak area (i.e., percent of total carbon signal) from 15-18% for MA-treated surfaces to 25-29% for the PEO surface. The increase in the ether peak was expected since PEO consists entirely of ether carbon. Figure 4-5b shows the high resolution scan for a star monolayer grafted onto a MA-treated surface. A larger increase in the ether peak is observed, increasing from 15-18% for MA-treated surfaces to 38-43% for the star PEO surface. This larger increase for star PEO monolayers is not surprising considering these molecules are denser in PEO than linear molecules, thus increasing the PEO signal on the surface.

In order to learn more about the grafted PEO monolayer, variations were made in the adsorbing PEO solution, changing the concentration, molecular weight, and time the MA-treated samples were in contact with the solution. Figure 4-6 shows the relative peak area ratios of the ether to alkane carbon peaks (C-O/C-C) and ether to acid carbon peaks (C-O/COOH) as a function of PEO concentration. As can be seen, there is no dependence on concentration of the amount of PEO adsorbed/grafted in the monolayer for both star and linear PEO. If more PEO were adsorbing in the monolayer, an increase in both the (C-O/C-C) and (C-O/COOH) ratios would be seen. Similarly, there is no dependence of the adsorbed monolayer on the molecular weight of the PEO, shown by the plots in Figure 4-7 of (C-O/C-C) and (C-O/COOH) as a function of molecular weight, where the ratios of (C-O/C-C) and (C-O/COOH) for the star PEO are shown as a single point. The peak area ratios for the PEO stars are greater than those of the

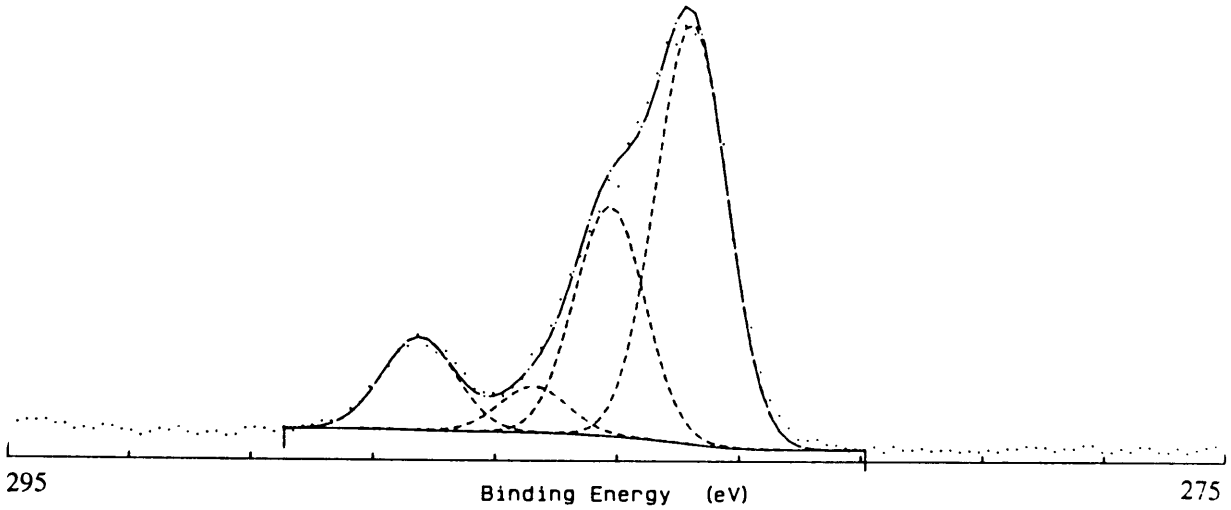


(a)

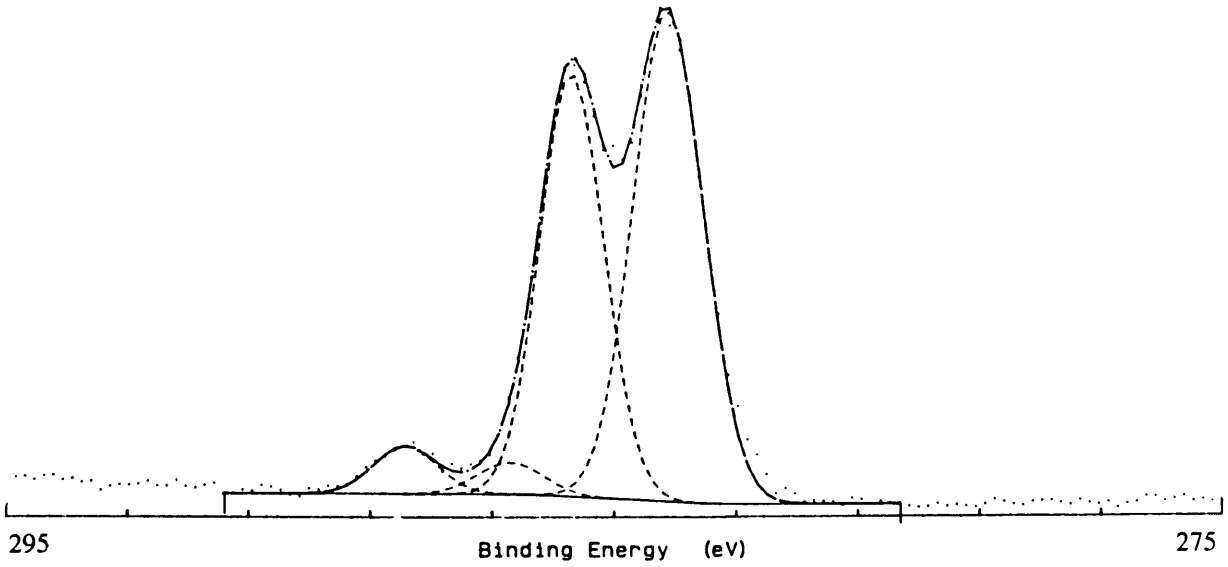


(b)

Figure 4-5: XPS high resolution carbon scans of grafted monolayers of: (a) linear PEO 35k, and (b) star PEO 3510.

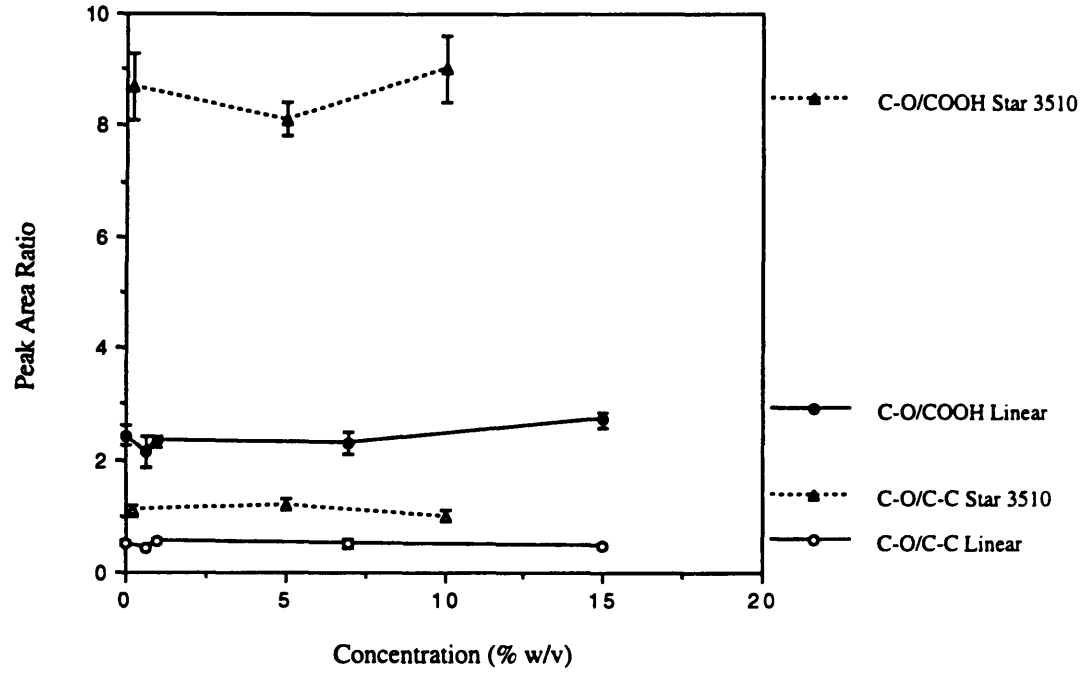


Figure 4-6: Ether/alkane (C-O/C-C) and ether/acid (C-O/COOH) relative peak area ratios of PEO grafted monolayers as a function of PEO concentration.

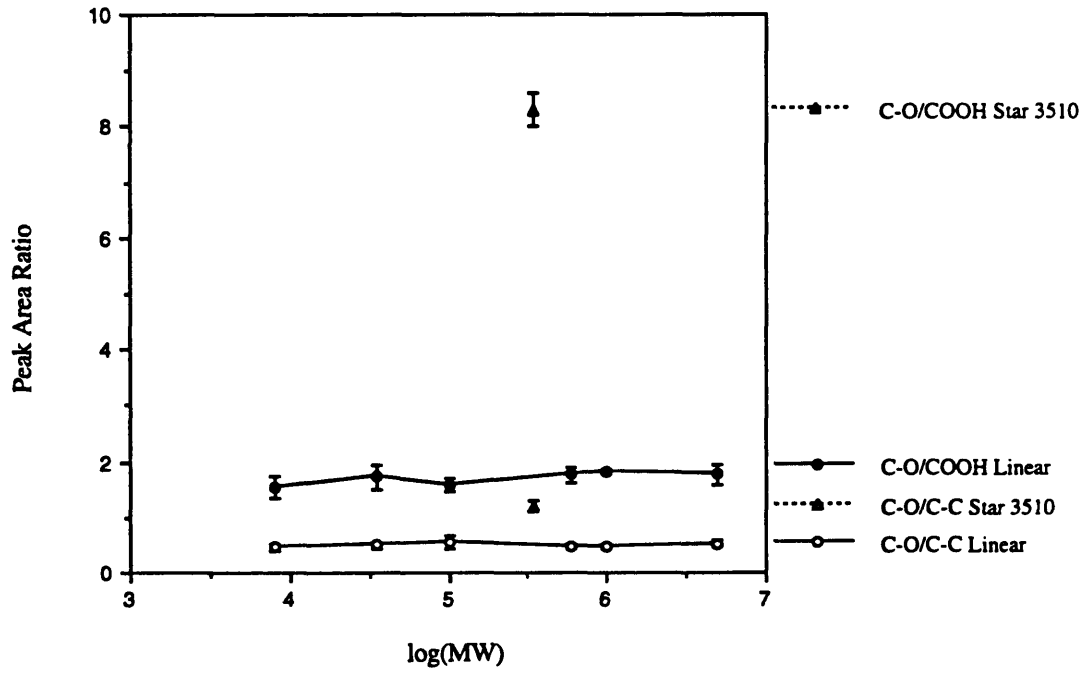


Figure 4-7: Ether/alkane (C-O/C-C) and ether/acid (C-O/COOH) relative peak area ratios of PEO grafted monolayers as a function of PEO molecular weight.

linear in all cases. This is as one would expect given the dense nature of the star molecules attenuating the underlying signals to a greater degree than linear PEO. In addition, the differences between the linear and star (C-O/C-C) ratios in Figures 4-6 and 4-7 are not as great as the differences between the linear and star (C-O/COOH) ratios. The reason for this is that the carbon in the DVB cores of the star molecules is contributing to the C-C signal, thus making the ratio lower than expected.

In addition to the independence of the adsorbed monolayer on concentration and molecular weight, the amount of time that the samples were in contact with the adsorbing PEO solution also had no effect on the PEO monolayer. This was observed when MA-treated pieces that had been in the adsorbing solution for 10 minutes showed the same adsorption as those that had been in solution for 3 hours (both XPS scans identical to the one in Figure 4-5a). In fact, XPS scans of linear PEO monolayers were observed to be nearly identical to each other despite the variations made in the adsorbing PEO solution. The relative peak areas of the four peaks shown in Figure 4-5a would vary by only a few percent from sample to sample. These results lead to the conclusion that when the PEO is adsorbing to the MA-treated surface through hydrogen bonding, it adsorbs immediately and strongly, with no exchange with the molecules in the surrounding solution over time. The majority of adsorbed chains are most likely lying down on the surface with few loops or tails, drawn down by the hydrogen bonding. This is quite feasible considering the strong, almost instantaneous complexation that takes place when PEO is put in aqueous solution with PAA or PMAA, resulting in an insoluble precipitate.

It would be interesting to know exactly how much PEO is in this monolayer, but this is difficult to determine. One estimate can be made by looking at the attenuation of the acid and/or

alkane carbon peak intensities, and using Eq. 2-14 to calculate the thickness, d, of the dry PEO overlayer (an average thickness as if it were a uniform layer). If this is done with the data obtained in all the high resolution carbon scans of PEO monolayers, both the attenuation of the acid peak and the alkane peak give a similar answer: 5 ± 2 Å for linear PEO monolayers and 17 ± 2 Å for star PEO monolayers. Both thicknesses are lower than the maximum thicknesses achieved on silicon wafer for linear PEG (all three molecular weights) and star 3510 (see Figure 2-4). Since it was found in Chapter 2 that protein adsorption was prevented only at the highest PEO contents achieved on the surface, then we can speculate that the grafted PEO monolayers presented here may not be sufficient to completely prevent protein adsorption. The proof of this statement is presented in Chapter 5.

### 4.3.3 Stability of PEO Layer

In order for these PEO surfaces to be utilized for biomedical applications, it is important to determine that the PEO layer is stable and covalently bound to the MA-treated surface. This was done in two ways. First, a PEO hydrogel was grafted to a MA-treated surface. These MA-PEO surfaces were then gently scraped to remove excess hydrogel. As seen in the scan in Figure 4-8a, the majority of the surface is still PEO. If the MA were not present on the surface, the hydrogel would cleanly scrape off the surface, leaving the bare hydrophobic polymer, and only a single (C-C) peak would be detected. These PEO grafted, scraped samples were then placed in a 0.5 M NaOH solution for 10 minutes, rinsed thoroughly with water and air dried. If the PEO was only hydrogen bonded to the surface, then the NaOH would break the H-bonding and the PEO would come cleanly off the surface, leaving only the MA surface. As seen in Figure 4-8b, after the

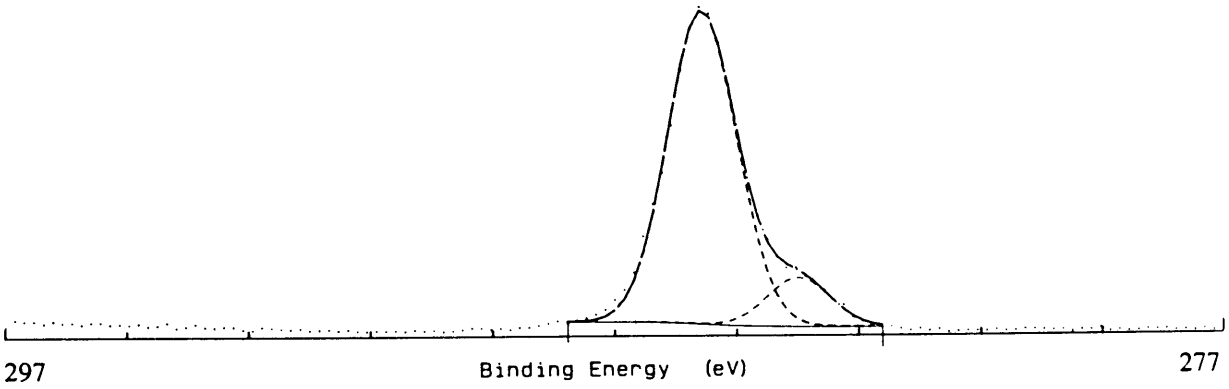


(a)

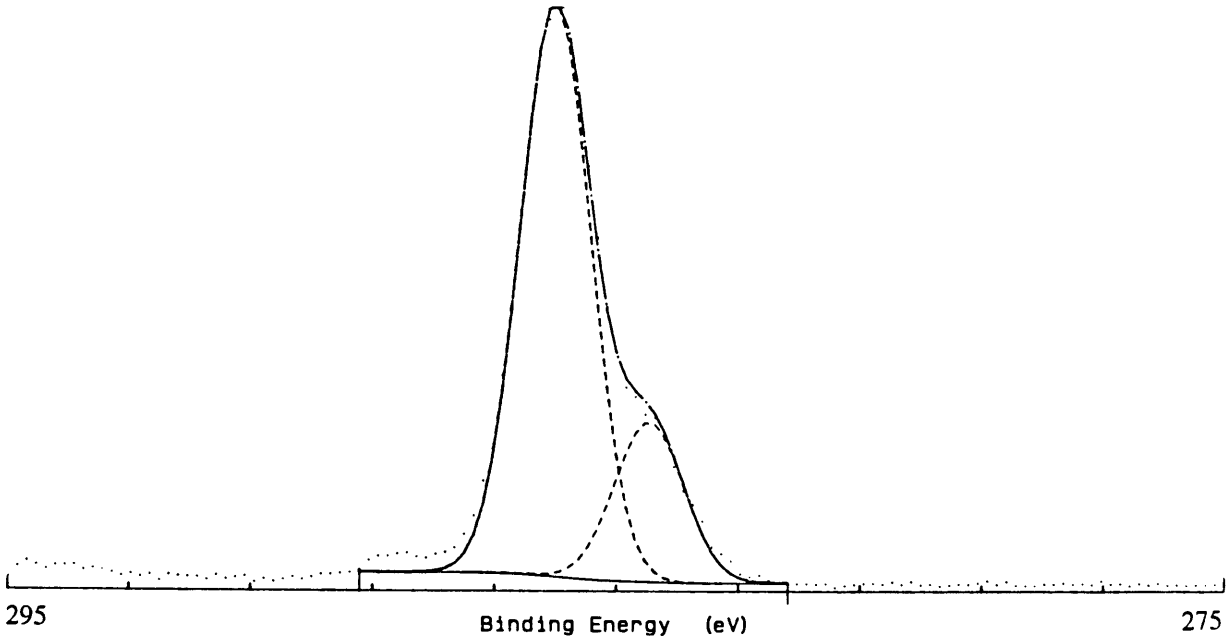


(b)

Figure 4-8: High resolution carbon scans of a PEO grafted hydrogel surface: (a) after excess hydrogel was scraped from the surface, (b) after scraped and soaked in NaOH.

treatment with base, the surface remains unchanged, with PEO still being the dominant material on the surface. To prove that base does indeed remove ungrafted, H-bonded PEO, Figure 4-9 shows scans of three surfaces: an MA-treated surface, a surface with an adsorbed, ungrafted, PEO monolayer, and the monolayer surface after the sample was rinsed in 0.5 molar NaOH for several minutes. As can be seen, the base does effectively remove the adsorbed PEO from the surface; Figure 4-9c looks identical to Figure 4-9a. In terms of long-term stability, a PEO hydrogel was grafted to MA-treated polystyrene and immersed in phosphate buffered saline solution, pH 7.4 ( with 0.03% sodium azide as bacteriostat), for one month. After that time, the hydrogel was still present in a stable layer the polymer surface.

### 4.3.4 PEO Multilayers

The thickness of a grafted multilayer can be controlled in several ways. The viscosity of the PEO solution can be varied by varying either the concentration or molecular weight of the PEO. Figure 4-10 shows high resolution carbon scans of three surfaces with a grafted PEO layer created by simply draining excess PEO solution from the surface before grafting. As can be seen, at constant concentration (4%) with increasing molecular weight from 35 000 g/mol to 100 000 g/mol to 1 million g/mol, the PEO layer on the surface increases. Analyzing the attenuation of the alkane carbon (C-C) peak (using Eq. 2-14) reveals dry layer thicknesses of approximately 5 Å, 9 Å, and 46 Å, respectively. In addition, the method of how the PEO solution is applied to the surface will also vary the resulting multilayer thickness. Spraying the surface with solution would result in a thinner layer than if the sample were dipped in solution where only the excess solution was allowed to drain from the surface. Two difficult aspects of grafting multilayers onto

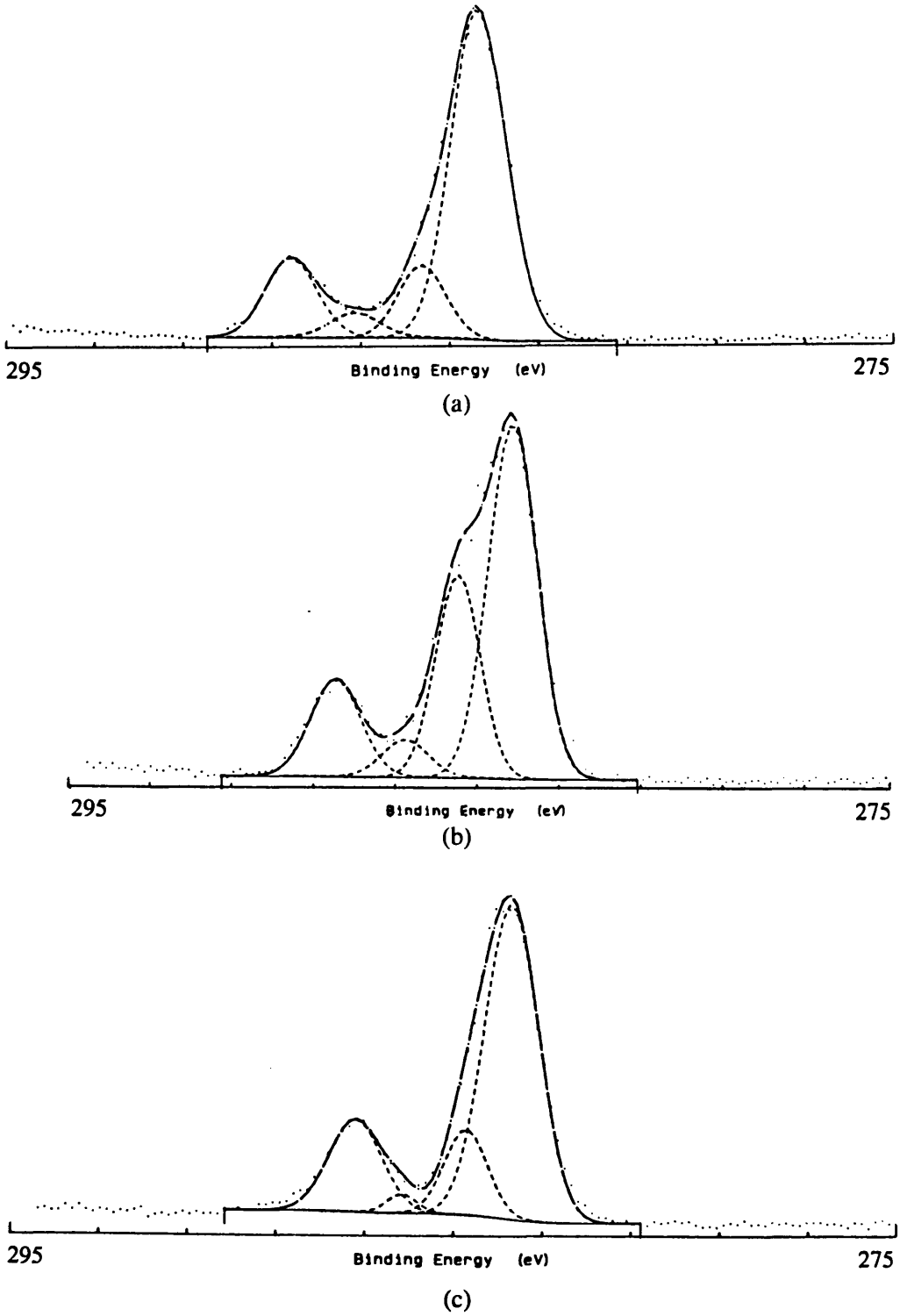


Figure 4-9: High resolution carbon scans of: (a) MA-treated surface, (b) MA-treated with adsorbed, ungrafted linear PEO monolayer, (c) monolayer surface after rinse with NaOH.

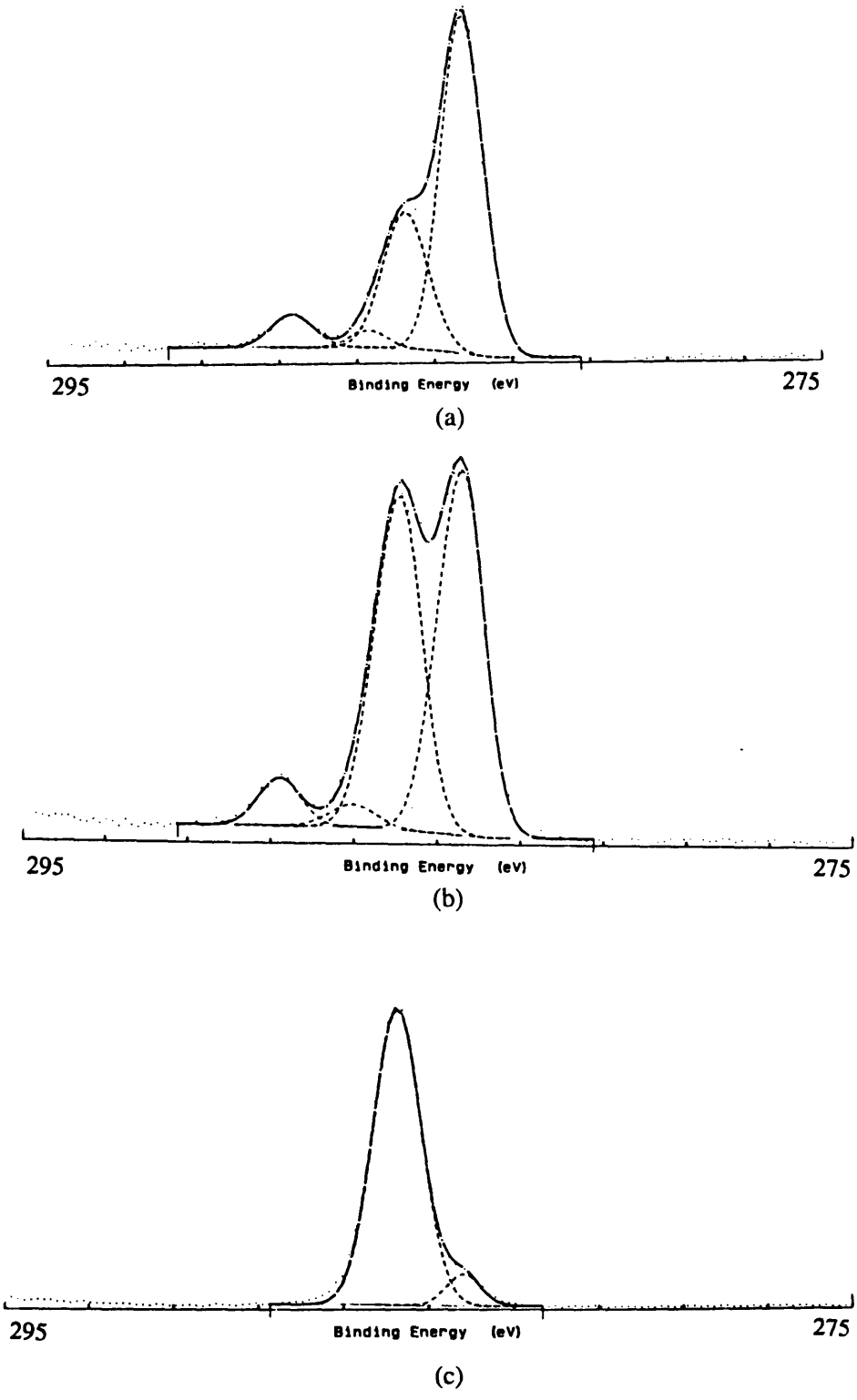


Figure 4-10: High resolution carbon scans of grafted linear PEO multilayers: (a) 8k linear, (b) 35k linear, and (c) one million linear molecular weights from 4% solutions.

MA-treated surfaces are, first, preventing the surface from drying out in the time between applying the PEO solution and irradiating, and second, obtaining a uniform layer on the surface. These two issues are addressed Chapter 6.

### 4.3.5 Other Monomers, Polymer Substrates, and Irradiation Conditions

As stated in the experimental section of this chapter, other polymer materials were obtained and tested for the ability of methacrylic acid to be grafted to the surface. The test of whether MA had grafted or not to the surface was simply a qualitative assessment of the wettability of the surfaces after irradiation. It was found that different materials require roughly the same conditions for grafting methacrylic acid, in looking at changes in the concentration of MA monomer in solution and/or changes the irradiation dose. Table 4-1 shows the results of the study with various polymers, giving the conditions required for a specific material to obtain good/excellent wettability (defined as holding a film of water on the surface).

Table 4-1: Optimal conditions for grafting MA monomer to various polymer materials.

| Polymer | Dose (Mrad) | % MA in solution (w/v) |
|---|---|---|
| Polystyrene | 2 or 4 | 20 |
| Polyethylene | 2 or 4 | 20 |
| Poly methylmethacrylate | 4 | 10 |
| | 2 or 4 | 20 |
| Poly vinylidene fluoride | 2 | 20 |
| Plasticized PVC | 4 | 20 |
| Poly vinyl chloride | 2 | 20 |
| Poly propylene | 2 or 4 | 20 |
| Poly ethylene terephthalate | 2 or 4 | 20 |

The dose requirement was kept at a minimum so that any beam effects on the bulk polymer were also kept to a minimum. Irradiation doses of less than 2 Mrad total dose did not graft MA sufficiently on any polymer (wettability was poor). The concentration of MA monomer in solution was kept at 10-20% since in some cases 20% or greater the monomer would start to dissolve into the polymer. For example, with PMMA, the surface would become soft at concentrations greater than 20% or if kept in 20% solution longer than 10-15 minutes. Two materials onto which MA would not graft were poly(ether sulfone) and poly(dimethyl sulfoxide), and poly(tetrafluoroethylene) breaks down under an electron beam.

Two other monomers were investigated for their grafting to polymer surfaces. Acrylic acid (AA) monomer was tried in a range of concentrations similar to those of MA and was found not to graft to the surfaces. It was interesting to observe that where AA would not graft to surfaces, it readily grafted to itself, where it would produce a cross-linked hydrogel after only a 4 Mrad dose. Methacrylic acid, on the other hand, readily grafted to many polymer surfaces, as seen in Table 4-1, but did not cross-link to form a gel, even after doses up to 10 Mrad. Therefore, although the exact mechanism is not known, the presence of the methyl group on MA must play a key role in the grafting reaction of MA to other polymer materials, PEO included.

The second monomer tried was 2-vinyl-n-pyrrolidinone (NVP). NVP was found to create a very wettable surface only on PMMA (30% NVP or greater in water, 2 Mrad or greater doses), but was found not to graft PEO. A PEO hydrogel grafted onto an NVP-PMMA surface was easily scraped from the surface. Therefore, the property of a surface being wettable is not sufficient for the grafting of PEO. There is obviously something very specific about methacrylic acid that lends it to have extremely high grafting capabilities towards materials other than itself.

## 4.4 Conclusions

It has been shown that the problem of delamination of PEO layers from polymer surfaces that were grafted through electron beam irradiation can be solved by the grafting of an intermediate layer of methacrylic acid. It was found that MA monomer is unique in its ability to graft onto many different polymer materials, including PEO, and that a wettable surface alone is not sufficient to graft PEO. The covalent attachment and stability of the PEO layer was proven through its retention on the surface after extensive washing with water, contact with basic solution, and mechanical scraping of the surface.

PEO monolayers formed on the surface have been shown to be independent of PEO molecular weight, PEO concentration, and time the MA-treated samples are in contact with the PEO solution before being grafted to the surface. This leads to the conclusion that once the MA-treated samples are placed in the PEO solution, the PEO immediately hydrogen bonds to the surface with no exchange taking place with molecules in solution, the adsorbed molecules lying flat with few loops or tails. The monolayer is then grafted on in this conformation. Star molecules are indicated to create a slightly thickner monolayer than linear PEO, as evidenced by the greater attenuation of the underlying acid peak in the high resolution carbon scans.

PEO multilayers, on the other hand, can be varied and controlled through the variation of PEO concentration, molecular weight, and how the solution is applied to the surface before grafting. Multilayers of low molecular weight linear PEO, or of PEO star molecules, are important in that they provide a large number of free hydroxyl groups for the attachment of a ligand such that a specific biological function can be imparted to the surface. PEO layers on

polymeric surfaces provide a completely inert front to a biological environment such that they have extensive potential use in the biomedical field.

## 4.5 References for Chapter 4


1. P.A. King and J.A. Ward, *J. Poly. Sci. Part A-1*, 8, 253 (1970).
2. J.W. Stafford, *Die Makromol. Chemie*, 134, 57 (1970).
3. Dr. Ed Ellis, Polymer Technology Corporation (Wilmington, MA), private communication.
4. K.L. Smith, A.E. Winslow, and D.E. Peterson, *Indust. Eng. Chem.*, 51, 1361 (1959).
5. S. Nishi and T. Kotaka, *Macromolecules*, 18, 1519 (1985).
6. H Adachi, S. Nishi, and T. Kotaka, *Polymer J.*, 14, 985 (1982).

# CHAPTER 5

## Protein Adsorption on Electron Beam-Grafted PEO Surfaces

### 5.1 Introduction

Chapter 4 provided the details of a new method for grafting PEO to polymer surfaces using electron beam irradiation. Through the initial grafting of methacrylic acid monomer, it was found that PEO would very stably graft to polystyrene and low density polyethylene, with the potential to bind to many other polymer materials since the methacrylic acid will graft to a wide variety of polymer surfaces. The method also provides considerable flexibility in varying the PEO layer being grafted, where both monolayers and multilayers can be made.

In this chapter, the effectiveness of the PEO grafted surfaces at preventing protein adsorption is investigated. Since it is already well known and accepted that proteins and cells do not adhere to PEO cross-linked hydrogels, the emphasis of the following study was on the PEO grafted monolayers. As was previously seen, XPS scans consistently showed the presence of the PEO in the monolayers, but whether the PEO is grafted in a sufficiently dense layer to prevent the adsorption of proteins is a question that still needed to be answered. As seen in Chapters 2 and 3, the density of the PEO in the layer is key in the creation of a non-adsorbing surface.

Monolayers of both linear and star PEO on polystyrene were tested for the adsorption of proteins. Two methods of analysis were used. One was the measuring of gamma counts from adsorbed protein that had been radiolabelled with 125-I isotope; two experiments were performed

using this method. The first involved the adsorption of the same three proteins used previously, those of cytochrome-c, albumin, and fibronectin. The second involved the adsorption of fibronectin only. The second method of analysis was measuring the nitrogen intensity from adsorbed fibronectin in an XPS scan, where the nitrogen detected is primarily from the amide bonds in the protein. In contrast to the aminosilane treated surfaces described in Chapter 2, the only source of nitrogen in these experiments was from adsorbed protein.

## 5.2 Experimental

### 5.2.1 Synthesis of PEO-Grafted Surfaces

All samples were made using the materials and methods described in Section 2.2. Monolayers of 35k and 1 million molecular weights linear PEO (solution concentration 4% w/v in water), as well as PEO star 3510 (solution concentrations 0.2%, 5%, 7%, 15% w/v in water), were grafted onto MA-treated polystyrene pieces (surface area $2.0 \pm 0.2$ cm$^2$). Some samples of MA-PS were put aside as controls. Samples were exposed to 2 Mrad for the grafting of the methacrylic acid monomer (20% w/v in water), and 2 Mrad for the subsequent grafting of the PEO. They were rinsed thoroughly with water after each step in the synthesis. In addition, cross-linked hydrogels of 1 million molecular weight linear PEO and star 3510 PEO were made with an irradiation dose of 4 Mrad (2 Mrad/pass, 2 passes). In all, there were a total of ten sample types:

| | | |
|---|---|---|
| 1. | PS: | Polystyrene control |
| 2. | PS-MA | Polystyrene-methacrylic acid controls |
| 3. | PS-MA-35k | PS-MA with monolayer of 35k linear PEO |
| 4. | PS-MA-1mil | PS-MA with monolayer of 1 million linear PEO |
| 5-8. | PS-MA-3510 | PS-MA with monolayer of star 3510 from adsorbing solutions: 0.2%, 5%, 7%, and 15% |
| 9. | 1 mil gel | Hydrogel of 1 million linear PEO (from 4% solution) |
| 10. | 3510 gel | Hydrogel of star 3510 (from 7% solution) |

For each experiment, there were three PS pieces for each of the ten sample types being tested for each protein, with the exception of the two hydrogels, in which there were only two gel pieces per gel type.

### 5.2.2 Experiment 1: Adsorption of all Three 125-I Proteins

Polystyrene pieces of PS, PS-MA, PS-MA-35k, PS-MA-1 mil, and PS-MA 3510 (5%) were rehydrated in PBS solution, pH 7.4 (after being dessicated and stored at -10°C), and placed in the protein solutions of cytochrome-c, albumin, and fibronectin. For each protein solution, 200 µl of 125-I labelled (hot) protein were added to 20 ml unlabelled (cold) protein in PBS. The specific activities and concentrations of the hot protein, as well as the final concentrations of the adsorbing protein solutions, are given in Table 5-1.

Table 5-1: Specific activities and concentrations of protein solutions.

| Protein | Specific Activity (µCi/µg) | Concentration (hot only, µg/ml) | Concentration (hot+cold, mg/ml) |
|---|---|---|---|
| Cytochrome-c | 0.576 | 39 | 1.0 |
| Albumin | 0.218 | 642 | 1.0 |
| Fibronectin | 0.718 | 101 | 0.1 |

The samples were incubated in the protein solution for 24 hrs at 25 °C. They were then rinsed three times with 2 ml PBS, with one additional rinse for 24 hrs in 2 ml PBS. Measurements of the gamma counts were made after the first, third, and 24 hr rinses. Counts on all samples after the 24 hr rinse were referenced to PS after the first rinse.

### 5.2.3 Experiment 2: Adsorption of 125-I Fibronectin Only

Polystyrene pieces of PS, PS-MA, PS-MA-1mil, and PS-MA-3510 (0.2%, 7%, 15%) were rehydrated in PBS, and placed in a solution of fibronectin in PBS, pH 7.4, along with pieces of the 1 mil gel and 3510 gel. The protein solution consisted of 80 μl of 61.62 μg/ml 125-I fibronectin (specific activity measured at 3.99 μCi/μg) added to 15 ml of 0.1 mg/ml, fibronectin solution. The pieces were incubated for 24 hrs in the protein solution at 25 °C. They were then rinsed three times with 2 ml PBS, and one final time in 2 ml PBS for 24 hrs. The gamma counts were measured after the first and 24 hr rinses, and the counts after the 24 hr rinse were referenced to those of PS after the first rinse.

### 5.2.4 Experiment 3: Adsorption of Fibronectin After Base Treatment

Polystyrene samples of PS-MA, PS-MA-1mil, and PS-MA-3510 (7%) were rehydrated in water and placed in a solution of 1M sodium carbonate buffer (pH ≈ 12) for 30 minutes. They were then removed, rinsed thoroughly for 10 minutes in water, and placed in 0.1 mg/ml fibronectin solution in PBS, pH 7.4, along with samples of PS controls and PS-MA, PS-MA-1mil, and PS-MA-3510 samples not contacted with base. After 24 hrs at 25°C, the samples were removed from the protein solution and rinsed three times with 1.5-2 ml PBS solution each rinse, and one final time with pure water. They were then dried in air and analyzed by XPS. The intensity of the nitrogen signal was measured on each sample (resolution 4, spot 600 μm, window 20eV, two to three spots per sample) and referenced to the intensity measured on the PS controls.

### 5.2.5 Gel Permeation Chromatography

The solution of irradiated methacrylic acid was analyzed using gel permeation chromatography (GPC). A 100 μl volume of 0.3% (w/v) solution was injected into a Waters 150C GPC (Waters Corp, Bedford, MA). The mobile phase was 0.03% sodium azide in water (from the Milli-Q purification system), and the columns were TSK-Gel 4000PWxL and 6000PWxL (Varian Corp, Sunnyvale, CA) in series with a guard column. The flow rate was 0.5 ml/min. The chromatogram from the refractive index (RI) detector was collected on a CUI 486 personal computer.

## 5.3 Results and Disucssion

### 5.3.1 125-I Protein Adsorption

The results from the experiments using the 125-I labelled proteins are shown in Figure 5-1. The most obvious feature of the results is that none of the monolayer surfaces are of sufficient PEO density to completely prevent the adsorption of proteins. The underlying substrate surface must be somehow accessible to the protein solution, causing the observed adsorption. There are, however, some interesting differences betweeen the three monolayers tested.

For all three proteins of cytochrome-c, albumin, and fibronectin, there is a consistent downward trend in moving from PS-MA on the left to PS-MA-3510 on the right. The star monolayer is clearly the least adsorptive surface, with the monolayer of 1 million linear PEO being a close second, and 35k linear PEO being the most adsorptive. This is not so surprising if one looks at the structural differences between these three molecules. The 35k linear PEO is the smallest, shortest molecule, so when it is hydrogen bonding to the MA on the surface during the

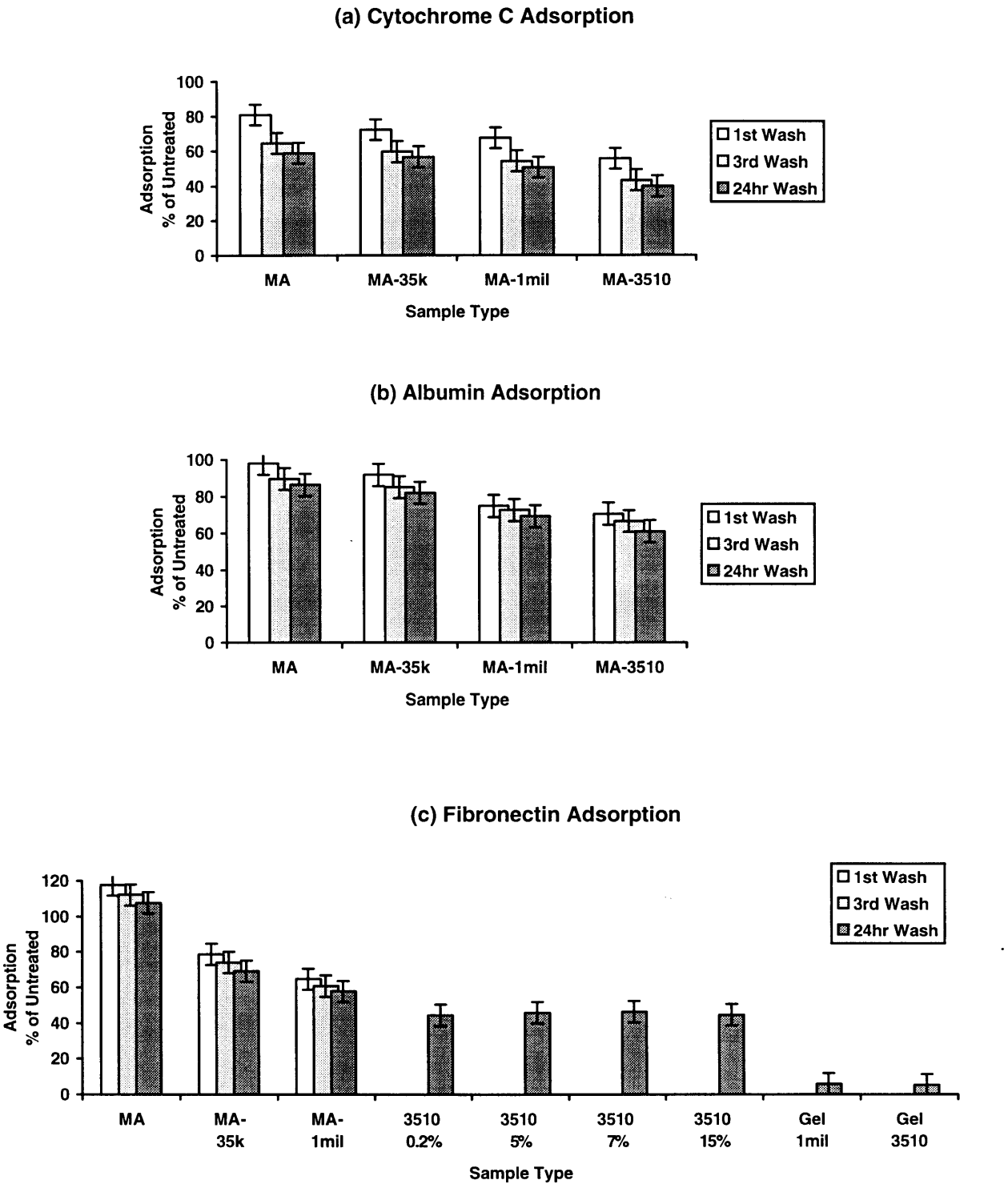


Figure 5-1: Protein adsorption on PEO monolayers relative to that on polystyrene as measured by 125-I labelled proteins.

initial adsorption, it probably is pulled down the tightest to the surface. Therefore, a large number of molecules probably adsorbed, thus causing some reduction in adsorption, but they adsorbed so closely that there were few, if any, loops or tails left free off the MA surface to act in completely preventing the proteins from reaching the surface. The one million molecular weight PEO, on the other hand, is a much larger molecule, so when it adsorbs, the whole molecule does not get pulled down so tightly. With loops and tails free off the surface, there is more of a barrier for the proteins to encounter in trying to reach the surface.[1] So less molecules of a million molecular weight adsorb than 35k PEO, but these are, in effect, a better barrier due to the looser structure on the surface (In Chapter 4, XPS scans showed an equal presence of PEO on the surface for both 35k and one million PEO). The star molecules are similar to the one million linear PEO, in that they are also very large molecules, but where the one million PEO had free loops and tails, the star molecules have free, non-hydrogen bonded arms that act as a barrier to the proteins. Combined with the fact that star molecules are more dense in PEO than a linear, randomly coiling molecule of equivalent molecular weight or size, the stars are even more effective at keeping proteins off the surface than the one million linear PEO.

One other interesting feature of the data is that in the adsorption of cytochrome-c and albumin, the 35k monolayer shows similar adsorption to that of the methacrylic acid alone, whereas for fibronectin, the difference is much larger. This difference for fibronectin is probably due to the fact that fibronectin has a heparin-binding domain. Therefore, it has an affinity for negatively charged groups. This explains its greater adsorption on PS-MA than on PS alone, as well as the significant drop in adsorption on the 35k monolayer, since on these samples the PEO is now hydrogen bonded or covalently bonded to many of the acid groups on the surface. Albumin,

in general, shows greater adsorption overall than the other two proteins. This is probably due to the hydrophobic character of albumin such that it has a greater affinity for the underlying polymer substrate than the other two proteins.

Also shown in Figure 5-1 are the results of the adsorption of fibronectin on the two hydrogels as well as the star 3510 monolayers formed from star solutions of differing concentration. As expected, the amount of protein on the hydrogels is extremely small, where the protein present is most likely not adsorbed, but rather has either managed to diffuse part way into the hydrogel, or it was carried along with the excess solution as the hydrogels were treated with the washes. The occurrence of diffusion into the gels was minimized by using a larger irradiation dose in making the hydrogels, to increase the cross-link density within the gel, and also by adsorbing with the largest protein, fibronectin. Therefore, a grafted hydrogel would very effectively remain clean of protein deposits, as expected.

The results from the adsorption on the star 3510 monolayers show equal adsorption on all four surfaces. This result proves the fact that the amount of PEO adsorbed in a monolayer is independent of the concentration of PEO in the adsorbing solution, as was seen from the XPS results on linear PEO monolayers presented in the previous chapter. The available space on the surface is rapidly and stably adsorbed to, such that changes in the PEO solution have little effect on how much PEO sits on the surface.

### 5.3.2 Fibronectin Adsorption on Base-Treated Surfaces

One way to determine that it was the underlying substrate surface of the grafted methacrylic acid, not effectively covered by the PEO layer, that was causing the protein adsorption seen in Figure 5-1 was through exposing the surfaces of PS-MA and PS-MA-PEO to strong base. The premise behind this experiment was that fatty acids in the body exist in the sodium salt form, $-COO^-Na^+$. Therefore, this form must be more "biocompatible", fully accepted by biological entities, than the acid form of -COOH. Based on this, by exposing treated surfaces to sodium carbonate buffer, the $H^+$ on the free acid groups on the surface, unbound by PEO, are effectively replaced with $Na^+$. It would then be expected that there would be reduced protein adsorption if the acid groups have been interacting with the proteins.

Figure 5-2 shows the results from the XPS scans measuring the intensity of nitrogen on the surface as referenced to adsorbed PS controls. For each condition of PS-MA, PS-MA-1mil,. and PS-MA-3510, there is a consistent drop of 20-25% in adsorption from the non-base treated to the base-treated surfaces. This proves two things: first, that the grafted methacrylic acid was indeed exposed to the protein solution and thus affecting adsorption; second, that the sodium salt of the acid groups is without question more "biocompatible", as the adsorption was significantly reduced from that of the COOH surfaces.

### 5.3.3 Molecular Weight of the Grafted Methacrylic Acid

One aspect of the methacrylic acid grafted surfaces that, based on the above results, is probably having significant influence on the grafting of a PEO layer is the resulting molecular weight of the grafted MA on the surface (for not only is the monomer grafting to the surface, it is

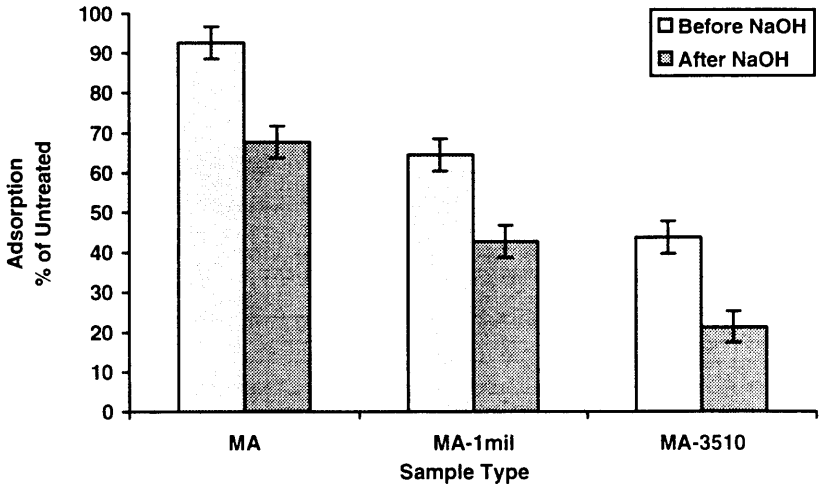


Figure 5-2: Effect of base treatment on protein adsorption to grafted surfaces.

also polymerizing out from the surface). An estimate of this molecular weight was obtained by doing GPC on a sample of MA solution that was exposed to a radiation dose of 2 Mrad. The chromatogram was obtained, shown in Figure 5-3, and the elution volume of the poly(methacrylic acid) polymer (PMAA) peak (ca. 18 ml) was correlated to a calibration curve for the GPC columns based on PEO standards.

$$\log(M_{PEO}) = 9.9423 - 0.30023\ EV \qquad (5\text{-}1)$$

where EV is the elution volume (in milliliters) of where the peak appears in the chromatogram. The corresponding molecular weight of PEO was then found to be ~34,000 g/mol. The molecular weight of the PMAA was finally calculated using a combination of the Mark-Houwink empirical

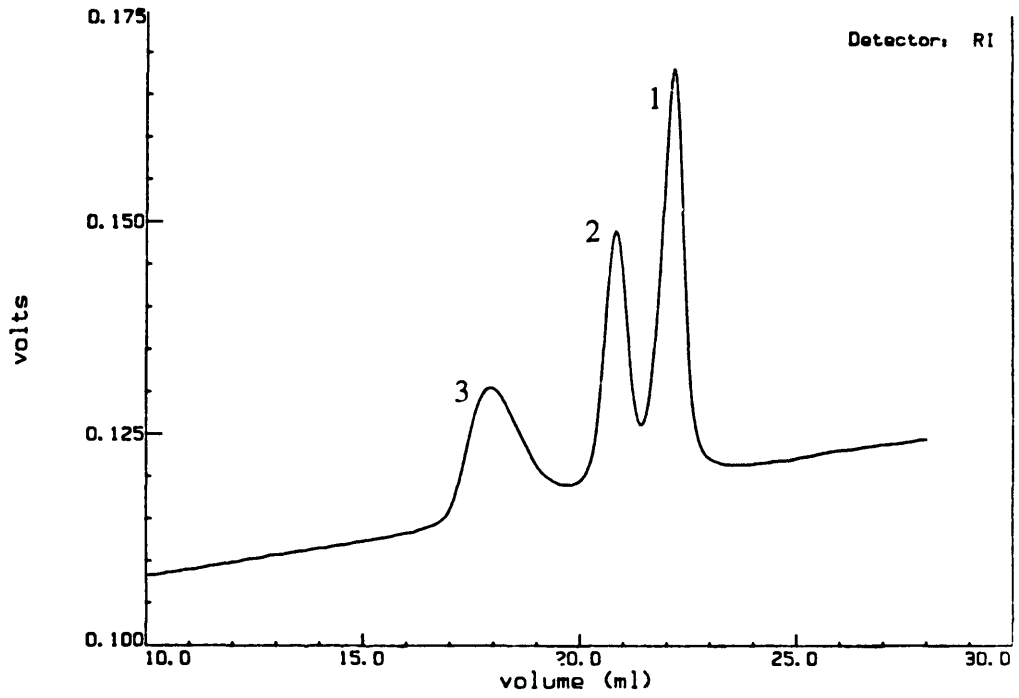


Figure 5-3: GPC chromatogram of methacrylic acid polymer and monomer after exposure to a radiation dose of 2 Mrad. peak 1: sodium azide salt, peak 2: MA monomer, peak 3: MA polymer.

relation for intrinsic viscosity, [n], of a linear randomly coiling molecule[2], and universal calibration[2-4]

$$\text{Mark-Houwink} \qquad [\eta] = k M^{a} \tag{5-2}$$

$$\text{Universal Calibration} \qquad [\eta] M = \text{constant} \tag{5-3}$$

where k and a are empirical constants for a given polymer. Therefore, combining Eqs. 5-2 and 5-3, we get

$$M_{PMAA} = \{(k_{PEO}/k_{PMAA})\, M_{PEO}^{(1+aPEO)}\}^{1/1+aPMAA} \tag{5-4}$$

$$= \{(0.0121/0.066)\, M_{PEO}^{1.784}\}^{1/1.5}$$

filling in for k and a for PEO in water at 30 °C and PMAA in 0.001 M HCl at 30 °C.[5]

We then find that the approximate molecular weight of the PMAA chains is 80,000 g/mol.

An important implication of this result is that it explains quite well the continued adsorption of proteins on the PEO grafted monlayer surfaces. Considering the methacrylic acid chains have a considerable molecular weight, the adsorbing PEO does not layer over the surface; it actually becomes incorporated into it. Therefore, to ensure that the methacrylic acid is fully covered by PEO, the PEO layer must be a grafted multilayer.

## 5.4 Conclusions

The effectiveness of the PEO grafted monolayers on polystyrene at preventing protein adsorption was tested and found to be, at best, ~ 60% effective. The underlying substrate surface was not fully covered with a dense enough layer of PEO to block the proteins from reaching the surface. The acid groups of the methacrylic acid, in particular, were found to contribute considerably to the adsorption. Considering that the molecular weight of the grafted PMAA was found to be approximately 80,000 g/mol, the PEO is not layering over the surface, it is becoming incorporated into it. Star PEO monolayers were the most effective at preventing protein adsorption, considering their numerous free arms, considerable size, and dense structure. The one million molecular weight linear PEO was nearly as effective as star PEO, probably due to its large, randomly coiling size lending it to have a loose, grafted structure with free loops and tails serving as a barrier to the proteins. The 35k linear, on the other hand, was bound more tightly to the surface such that its effectiveness at preventing proteins from reaching the surface was minimal. This is especially true when considering that the approximate molecular weight of the grafted PMAA on the surface is roughly twice the molecular weight of the 35k PEO. It is also interesting to note that, despite the fact that the amount of PEO that adsorbs in a monolayer is independent

of PEO molecular weight and concentration (see Chapter 4), how it adsorbs and grafts definitely has a molecular weight dependence.

## 5.5 References for Chapter 5


1. E.W. Merrill and E.W. Salzman, *ASAIO*, 6, 60 (1983).

2. P.J. Flory, Principles of Polymer Chemistry, Cornell University Press, Ithaca, NY, 1953.

3. W.W. Yau, H.J. Stoklosa, and D.D. Bly, *J. App. Poly. Sci.*, 21, 1911 (1977).

4. H. Guixian and S. Mingshi, *Polymer Testing*, 10, 59 (1991).

5. Polymer Handbook, J. Brandrup and E.H. Immergut, eds., John Wiley & Sons, New York, 1989.

# CHAPTER 6

## Summary and Future Work

### 6.1 PEO Grafted Silicon Surfaces

#### 6.1.1 Summary

In Chapters 2 and 3, much was learned about the grafting densities achieved when coupling linear and star PEO molecules to amine-functionalized silicon surfaces. For linear PEO, there was a rapid rise in grafting density followed by a quick leveling off when plotted as a function of the PEO coupling concentration. In these cases, the maximum concentrations were well above the critical concentration marking the start of chain overlap, thus inducing significant chain overlap on the surface to the point where steric hindrance and excluded volume effects prevented any more chains from penetrating the layer to bind to the surface. The grafting densities achieved were a strong function of PEO molecular weight, with PEG 3400 having the highest grafting densities and PEG 20k the lowest. The PEO star molecules, on the other hand, did not reach a maximum grafting density on the surface, but rather continued to show a positive slope at the higher coupling concentrations. The highest coupling concentration was 15% (w/v) for both stars, which is just at $c_{crit}$ for star 228 and slightly above $c_{crit}$ for star 3510. Therefore, only minimal overlap was achieved on the surface, making it possible to achieve higher grafting densities by using higher coupling concentrations until steric repulsion and excluded volume effects prevent tighter packing on the surface.

The dependence of protein adsorption on PEO grafting density and molecule type (star or linear) was analyzed through the development of a model based on the spatial arrangement of PEO molecules on the surface. The two key parameters were the degree of chain overlap, and the size of

open spaces on the surface relative to the size of the proteins. For linear PEG surfaces, it was found that total coverage of the surface with PEO occurred at low graftng densities, and that significant overlap of the chains was necessary to prevent the adsorption of proteins. For all three PEGs, this critical overlap was found to be approximately the same, where a given chain was roughly half-overlapped with its neighbors (i.e., the chain spacing approximately equaled the radius of gyration of the PEO molecule) before protein adsorption was prevented. Furthermore, at this point of zero protein adsorption on all three PEG surfaces, the same total PEO content was present, that of 80-90 ng/cm$^2$. It is possible that this PEO content on the surface marks the point where steric repulsion exceeds hydrophobic attraction to such an extent that the probability of a protein reaching the underlying surface drops to zero. This point also marked the occurrence of when the maximum grafting densities of PEO on the surface were being reached. If more PEO chains could not get through the layer, then it follows that proteins would not either. The point of non-adsorption also appeared to have little dependence on protein size, but the decline of adsorption as grafting density increased did; the larger the protein, the greater the drop-off in adsorption. Therefore, for linear PEG grafted surfaces, the prevention of protein adsoprtion was found to depend on both PEG molecular weight and grafting density, where the two are intimately coupled.

Star PEO grafted surfaces showed very different behavior than that of linear PEG. The star surfaces did not reach total coverage of the surface, nor did they achieve much chain overlap, yet protein adsorption was prevented for the larger proteins: albumin and fibronectin. This is because the repeat units (-$CH_2CH_2O$-) within the domain of a single star molecule are dense enough to prevent protein adsorption without the need for overlap. Therefore, the only places on the surface for adsorption to occur were in the open spaces between the star molecules. When these spaces, at a

certain grafting density as approximated by the model, became smaller than the size of the protein, protein adsorption was prevented. For the smallest protein of cytochrome-c, however, high enough grafting densities were not achieved on the surface such that the cytochrome-c was excluded. Therefore, the protein continued to adsorb for all grafting densities achieved.

The results of PEO grafted to silicon wafers are important in that they can be used to target the design of materials in which PEO is incorporated into the surface for the purpose of preventing protein adsorption.

### 6.1.2 Future Work

There are several areas where more could be done to learn additional information about PEO grafting densities and protein adsorption. First, the curves in Chapter 2 could more fully be filled in by testing a larger number of PEO grafting densities within the existing range. This could possibly point out any subtleties in the adsorption that are not clear from the exisitng data. Secondly, an even larger range of linear PEG molecules could be studied, going lower than 3400 g/mol and higher than 20,000 g/mol, as well as studying a wider range of PEO star molecules with other variations in functionality and arm molecular weight. Third, higher coupling concentrations of star molecules (greater than 15%) could be used to create surfaces of higher grafting density, and these surfaces then tested for the adsorption of proteins, particularly small ones like cytochrome-c. It would be interesting to see if the point where the adsorption drops to zero agrees with that predicted by the model. Fourth, surfaces with varying amine concentraitons would also be interesting to test to see if better control of grafting density could be obtained.

## 6.2 PEO Grafted Polymer Surfaces Via Electron Beam Irradiation

### 6.2.1 Summary

A new method for binding PEO to polymer surfaces was developed of potential industrial and biomedical interest. By first grafting methacrylic acid to polymer surfaces via electron beam irradiation, it was found that PEO would stably graft to the polymer surface. The PEO layer was found to be stable after extensive washing in water, soaking in strong base, and mechanical scraping.

There is a large amount of flexibility in the surfaces being created using this method. First, monolayers as well as multilayers of PEO can be made. The amount of PEO in a monolayer was found to be independent of PEO molecular weight as well as concentration of the adsorbing solution. This was probably due to the immediate, strong adsorption that takes place when the methacrylic acid sample is first contacted with the PEO solution. Multilayers, on the other hand, can be controlled by varying the viscosity of the PEO solution, as well as by varying the method in which the PEO layer is applied. A second advantage of this method is that methacrylic acid will graft to a large variety of polymer substrates. This makes it possible to create PEO layers on a large number of materials, including the commodity polymers: polyethylene, polystyrene and poly(vinyl chloride). This is important from the standpoint where different applications usually require different polymer materials. Third, methacrylic acid monomer was found to be unique in the range of polymers to which it could be grafted, whereas other monomers such as acrylic acid and 2-vinyl-n-pyrrolidinone failed in either grafting to a polymer surface, or in grafting to PEO. More than surface hydrophilicity is required for the grafting of PEO to polymer surfaces through electron beam irradiation.

Protein adsorption sutdies with cytochrome-c, albumin, and fibronectin showed that grafted PEO monolayers were of insufficient PEO coverage to prevent protein adsorption. The underlying

methacrylic acid was found to be exposed at the surface and significantly affect protein adsorption. Certain trends, however, were seen between monolayers of 35k and one million molecular weight linear PEO, and monolayers of star PEO. The star monolayers were most effective at preventing adsorption, at best reducing adsorption by 60% from untreated polystyrene. This was due to the dense, hard sphere character of the stars, as well as the protection served by the free arms not bound to the surface. The monolayers of the one million molecular weight PEO were a close second to the star PEO monolayers, for the reason that because the molecule is so large, a large number of free loops exist on the surface that act as a barrier to the proteins. The 35k monolayers were the least effective at preventing protein adsorption, probably due to the fact that because these molecules are small, they become closely bound to the surface in the initial adsorption, with few loops or tails free to act as a barrier between the proteins and the underlying surface. Ultimately, to be fully effective at preventing protein adsorption, the PEO must be grafted on in a multilayer, thus sufficiently covering the underlying substrate surface.

### 6.2.2 Future Work

Several areas of this method of grafting PEO to polymer surfaces using electron beam irradiation could be investigated in order to improve the process. First, the molecular weight of the grafted poly(methacrylic acid) could be decreased from its current approximate value of 80,000 g/mol in order to reduce the exposure of the PMAA chains to the surface. One possible way this could be done is by adding a small amount of mercaptoethanol, or similar chain transfer agent, to the MA monomer solution. This would induce chain transfer during the grafting reaction and result in smaller overall degrees of polymerization of PMAA. A second area that needs investigation is in creating

uniform multilayers on a substrate surface. One problem was in the surface drying out, or partially drying out, before the second irradiation could be performed. This could be solved by obtaining a chamber where the humidity could be controlled. Of course, this chamber must be able to pass under the electron beam, and one would have to make sure to account for the difference a layer of humid air over the samples would have in affecting the intended dose to the samples as opposed to a layer of dry air. The problem of non-uniform layers could also possibly be solved by laying over the surface, coated with PEO solution, a thin film of polyethylene, or some other hydrophobic material. This would serve to keep the solution spread out over the surface as well as preventing it from drying out. The PEO will not bind to the PE directly, so after irradiation, the PE film could be removed by soaking in water.

Another line of investigation on PEO star monolayers, as applied to both methods of grafting described in this thesis, would be determining what fraction of the arms on the bound star molecules could be utilized as leashes to hold specific bioactive polymers. In view of the process of quantitative XPS, one would look for enhanced nitrogen content if the bioactive polymer were peptide or protein. It seems unlikely that more than about half the arms of the star molecules would be accessible for binding such molecules after the stars have been grafted to the surface.

# APPENDIX A

## XPS Analysis of Polymer Surfaces After Exposure to an Ammonia Plasma and Binding of PEO Star Molecules

### A.1 Introduction

The modification of polymer surfaces is a popular area of study for many reasons, some prominent ones being for the varying adhesion properties, altering wettability, or improving biocompatibility. The latter of these reasons was the motivation behind the study presented here.

Despite the great strides that have been made in the biomedical field in the area of artificial devices, there still remains the problem of achieving a high level of biocompatibility with artificial polymeric surfaces, especially for those used in contact with blood. Problems of protein and platelet deposition, platelet activation and thrombus formation, complement activation, etc., still exist in the use of current biomaterials. Many researchers are searching for a "better" biomedical material.

An end to this search may lie with poly(ethylene oxide) (PEO). For reasons not yet clearly understood, proteins, and thus cells, do not adhere to PEO surfaces.[1] Nor does PEO induce any adverse biological reactions, such as platelet activation leading to thrombus formation or complement activation leading to an immune response.[2] The problem lies in that PEO, as a cross-linked hydrogel, is extremely fragile, and when not cross-linked, is infinitely soluble in aqueous solution. Thus, for PEO to be used effectively in surface modification, it must be covalently linked to another polymer. End-linking linear PEO by one end[3] or by both ends forming a

network[1,4-7] has been studied by various groups. This study focuses on the formation of a covalently bound monolayer of PEO on the surface, but the PEO in this case being in a star-shaped form, not linear (Figure A-1). These star molecules consist of a central core of poly(divinyl benzene) with linear PEO "arms" radiating outward from this core.[8,9] The reason for the use of star-shaped molecules is three-fold. First, in solution, star molecules are much more dense in polymer segments per unit volume than their linear counterparts having the same molecular weight, thus potentially providing a more effective barrier between the substrate surface and a biological environment. Second, star molecules have a larger number of chain ends (up to 200) per molecule than their linear molecular weight equivalents. This property provides a higher probability of binding a star molecule to a substrate surface through those chain ends, and allowing for multiple, and thus stronger, binding as well. In addition, a second benefit to the large number of chain ends per molecule is the opportunity of creating a biologically active surface. This can be achieved by the subsequent binding of biological molecules (e.g., an enzyme) to the chain ends of the stars already bound to the substrate surface.

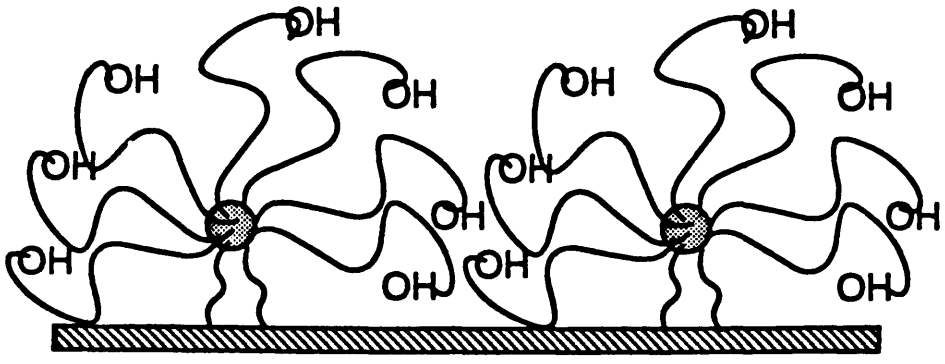


Figure A-1. PEO star monolayer bound to a polymer surface.

In the following study, the means by which the polymer substrate was first "activated" for the subsequent binding of the star molecules was through plasma enhanced chemical vapor deposition (PECVD), in which an ammonia plasma was used to deposit primary amines on a polymer surface. PECVD allows for only interaction with the immediate substrate surface while leaving the bulk material unchanged. PEO star molecules were then activated by reacting the hydroxyl groups on the PEO chain ends with tresyl chloride. When both the plasma treated material and the tresylated star molecules are placed together in aqueous buffered solution, the tresylated ends react with the primary amines, thus binding the star molecules to the surface. The substrate surfaces, after each step of the procedure, were analyzed using X-ray photoelectron spectroscopy (XPS). Chemical derivatization using pentafluorobenzaldehyde (PFB) was used to estimate the primary amine content on the polymer surface after ammonia plasma treatment.[10] The PFB reacts with primary amines in a Schiff's base reaction, shown in Figure A-2, thus tagging primary amines with five fluorine atoms. These can then be quantified in an ESCA survey scan. The percentage of nitrogen that is primary amine is then calculated by the formula

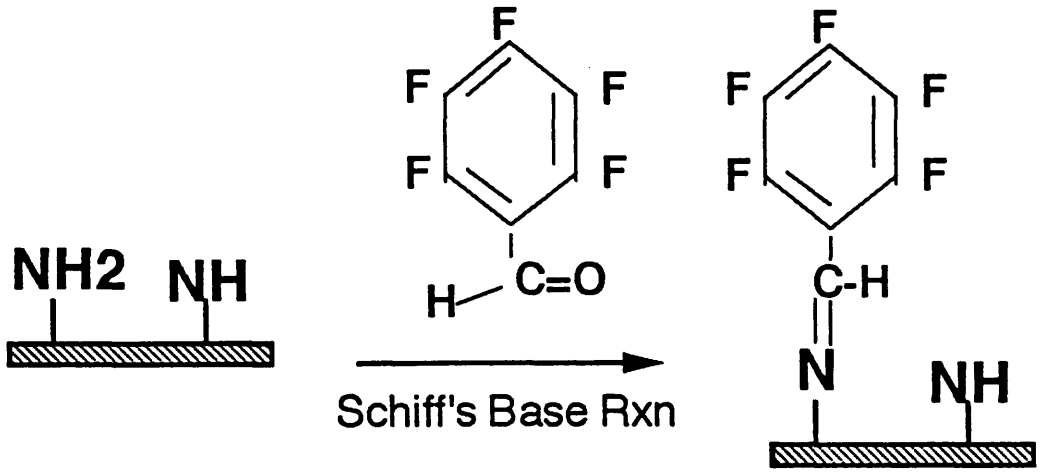


Figure A-2: Schiff's base reaction binding pentafluorobenzaldehyde to primary amines

% $NH_2$ = [(F/5) / N] x 100, where F is the percent fluorine on the surface after reaction with PFB, and N is the percent nitrogen on the surface after exposure to ammonia plasma.

## A.2 Experimental

### A.2.1 Plasma Enhanced Chemical Vapor Deposition

Films of low density poly(ethylene) (LDPE) and poly(ethylene terephthalate) (PET) were obtained from Goodfellow Corp. (Berwyn, PA). Pieces of ca. 1 $cm^2$ were washed extensively in methanol before use. The PECVD was achieved using a Plasma Therm Inc. 700 Series RIE/PECVD (Jacksonville, FL). A schematic of the chamber is shown in Figure A-3. Samples were treated under plasma conditions of 350 mTorr ammonia, an ammonia flow rate of 20 sccm, radio-frequency (rf) power of 25 Watts, for a reaction time of 2.5 minutes. The reaction chamber was evacuated to a pressure of $10^{-6}$ Torr for 10 minutes after the samples were placed inside, then flushed and evacuated three times with nitrogen before ammonia was introduced. After an ammonia flush of 5 minutes, the final reactant pressure was reached, and the rf turned on. When the reaction was complete, the rf was turned off, the chamber evacuated, and a series of flush and evacuations with nitrogen performed before the chamber was brought to atmospheric pressure and the samples removed. Samples were reacted with tresylated stars, PFB, or analyzed under XPS within 48 hours after plasma exposure.

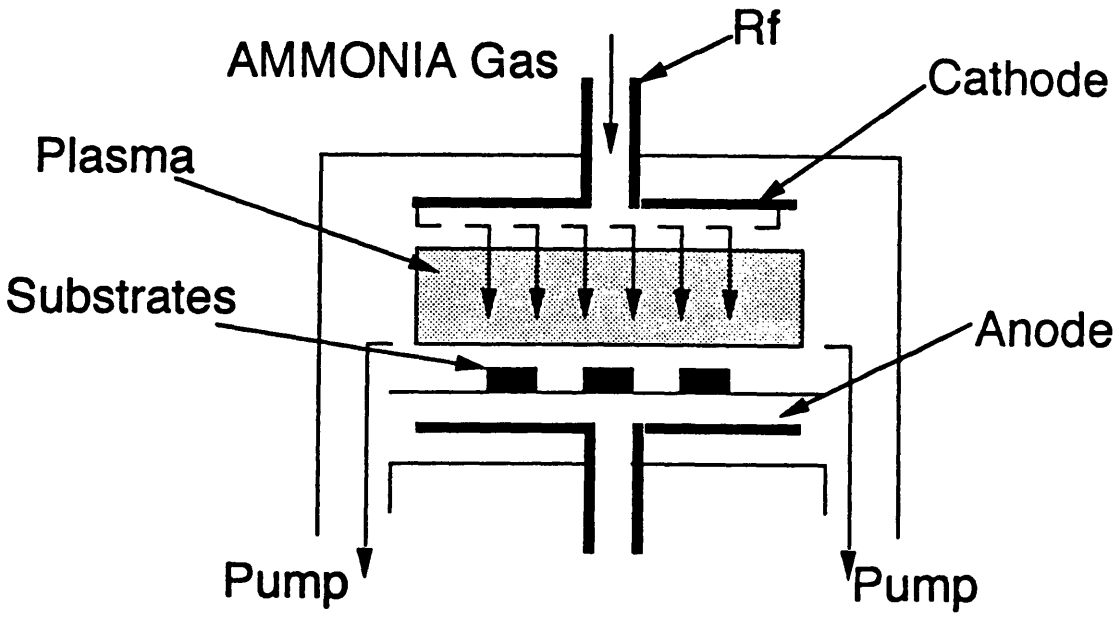


Figure A-3. Schematic of PECVD reaction chamber.

A.2.2 Tresylation and Coupling of PEO Stars

PEO stars were obtained from Dr. Paul Rempp of the Institut Charles Sadron in Strasbourg, France. The weight average molecular weight was determined to be 550,000 via batch light scattering, with an arm molecular weight of 10,000 (calculated from stoichiometry during synthesis). Therefore, the average functionality of these stars is 55 arms per molecule. The PEO stars were tresylated using the procedure of Nilsson and Mosbach,[11] the tresyl chloride obtained from Aldrich Chemical Co. Elemental analysis on PEO linear standards revealed a yield of 75% tresylation of hydroxyl groups. For coupling, the tresylated stars were dissolved in an aqueous 0.02 molar carbonate buffer solution at pH 9.5. The polymer samples were then added and reaction took place overnight at 4 °C. The samples were rinsed several times in water before being set to dry in a dessicator.

### A.2.3 Chemical Derivitization with PFB

Pentafluorobenzaldehyde was obtained from Aldrich Chemical Co. and used as received. Five to ten plasma treated samples were placed in a small glass container with 1 $cm^3$ of PFB, not in physical contact. The container was sealed and the reaction took place for 8 hours at 45 °C. The samples were then removed and placed under vacuum overnight.

### A.2 4 XPS Analysis

The XPS machine used was an SSX-100 by Surface Sciences Inc. with an Al Kα x-ray source. The take-off angle was 35 degrees. Flood gun was set at 5 eV, and a nickel wire mesh was placed over the sample holder to help dissipate charge. Both survey scans (spot size 1000 μm, resolution 4) and high resolution carbon 1s scans (spot size 600 μm, resolution 2) were performed. A peak-fitting program was used to resolve the high resolution scans into their component peaks, with the lowest energy carbon peak set to 285 eV. For all XPS analyses, there were three samples for each experiment, two spots analyzed on each sample. All values given below are averages from these data sets.

## A.3 Results and Discussion

### A.3.1 XPS of Plasma Treated Samples

After samples of LDPE and PET were exposed to the ammonia plasma, XPS survey scans showed there to be, on average, 9.1 atom percent and 8.5 atom percent nitrogen deposited on the surface, respectively. High resolution carbon 1s scans before and after plasma treatment are shown in Figure A-4 for LDPE. As expected, the LDPE high resolution scan for the

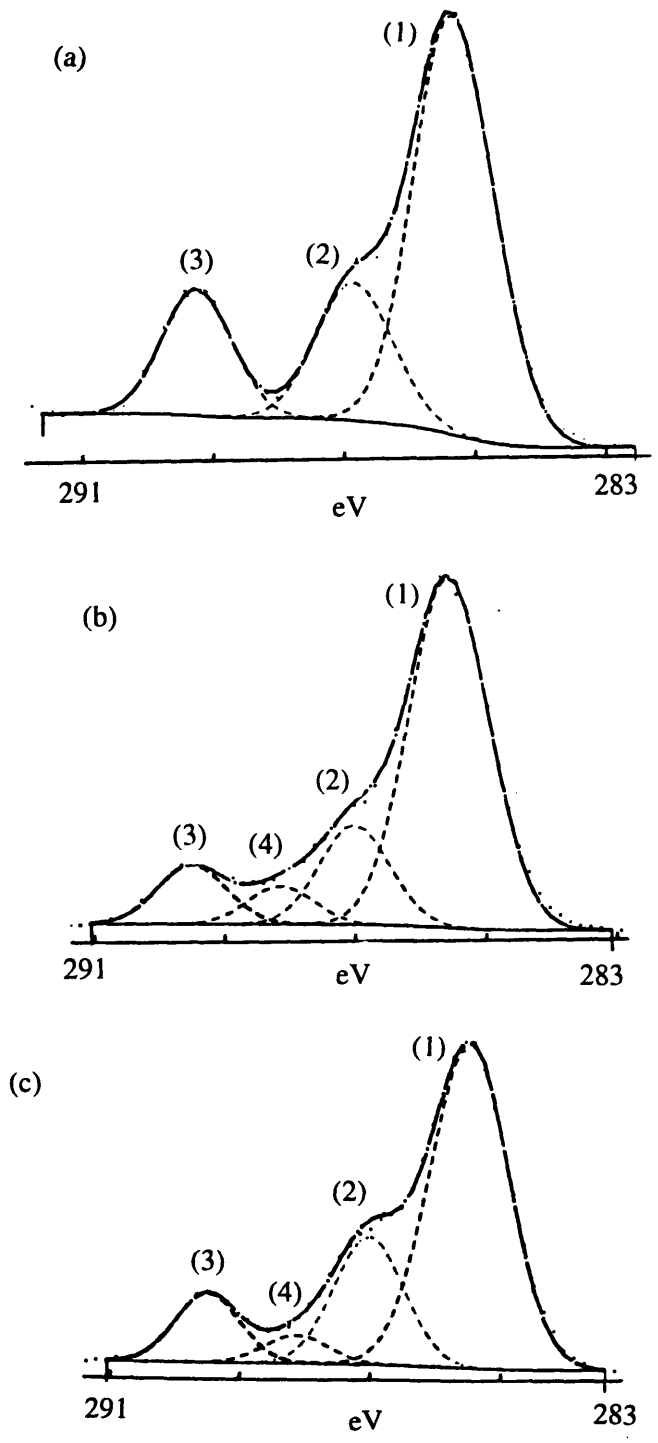


Figure A-4. High resolution carbon 1s scans of PET before (a) and after (b) exposure to an ammonia plasma, and (c) after exposure to tresylated PEO stars.

untreated control shows only one peak at 285 eV. After plasma treatment, two additional higher energy peaks, one shifted 1.2 eV from the main peak, indicative of C-N type bonding, and the other shifted 3 eV, indicative of C=N type bonding. In addition, during the plasma treatment, 4-5 percent oxygen was incorporated into the surface, so the two additional peaks could also be due to some C-O and C=O type bonding as well.

Figure A-5 shows the high resolution scans for PET. The PET control shows the three expected peaks: the largest, lowest energy peak representing C-C type bonding; the next peak shifted 1.5 eV from the main peak representing C-O type bonding; the highest energy peak shifted 4.0 eV representing O-C=O type bonding. After exposure to ammonia plasma, there is the addition of a fourth peak at an energy shift of 3.0 eV. Now that nitrogen is incorporated into the surface, this fourth peak is representative of either C=O or C=N type bonding; the second peak also now includes C-N type bonding, with the third peak possibly incorporating some form of C, N, and O bonding, such as O=C-N. Since nitrogen bound to carbon results in similar energy shifts as oxygen bound to carbon, it is not possible to distinguish between their relative contributions in the carbon 1s scan.

### A.3.2 PFB Derivitization Results

To determine the amount of nitrogen present that is primary amine, plasma treated surfaces were reacted with PFB. In XPS survey scans, the amount of fluorine bound to the surface was found to be 9.5 percent for LDPE and 11.1 percent on PET. Given the amount of

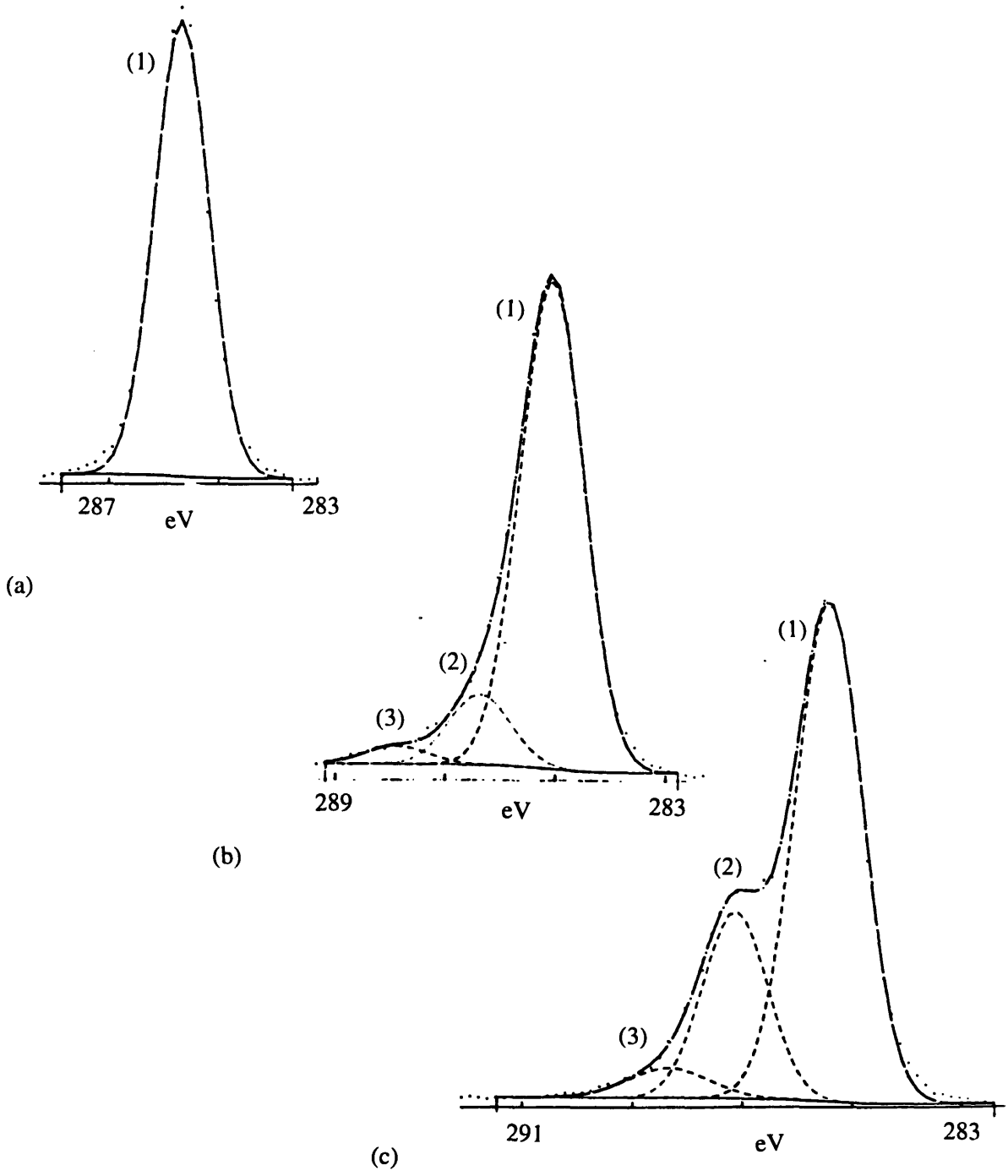


Figure A-5. High resolution carbon 1s scans of LDPE before (a) and after (b) exposure to an ammonia plasma, and (c) after exposure to tresylated PEO stars..

nitrogen deposited by the ammonia plasma, it was then calculated that of the total amount of nitrogen deposited, 24 percent was primary amine on LDPE, and 30 percent was primary amine on PET. Considering the density of polymer to be $1 g/cm^3$, and figuring in the molecular weight of a monomer unit, lead to the approximate density of primary amine to be 1.2 $NH_2/nm^2$ on LDPE and 0.8 $NH_2/nm^2$ on PET. From static light scattering experiments, the root-mean-square radius of gyration of the star molecules was found to be 15 nm when fully hydrated. Therefore, the density of primary amines on the surface should be sufficient for achieving complete monolayer coverage of stars bound to the surface.

### A.3.3 PEO Star Surfaces

High resolution carbon 1s scans were used to determine, qualitatively, the amount of PEO stars bound to the polymer surface. This was accomplished by noting an increase in peak (2), since PEO is entirely ether-type carbon. Figure A-4(c) shows the high resolution scan for LDPE, and the presence of the PEO stars is clearly seen by the increase in size of the second peak, as expected. This peak is shifted 1.6 eV from the main peak, indicative of the C-O type bonding. A common method for tracking changes in surface bonding character is through a peak area ratio of the higher energy peaks with the main C-C peak at 285 eV. Therefore, comparing the peak area ratio of peak (2) to peak (1), C-O/C-C, the ratio after star treatment is now more than double that from the plasma treated control, 0.37 compared to 0.14.

The presence of the PEO stars is not so evident in the case of PET, as shown in Figure 5(c). There is a slight increase in the second peak, the C-O/C-C peak area ratio being 0.34, an

increase from 0.25 in the plasma treated control. Considering the amount of primary amine known to be on the surface, and the extent of tresylation achieved, it is surprising that a larger PEO signal was not evident. What was also surprising was the large drop in nitrogen content on both PET and LDPE star treated surfaces from the plasma treated controls when so little PEO was detected. Nitrogen content dropped by as much as 60 percent on the PET surface, from 8.5 atom percent to 2.5 atom percent. These facts, among others stated below, lead to the hypothesis that the polymer surface is fragmenting during plasma treatment, and that these, now polar, fragments are washing off in the aqueous solution during the coupling reaction.

### A.3.4 Surface Fragmentation Study

During the course of the study, several observations were made where it became evident that the surface was likely breaking up in the ammonia plasma. In addition to the two reasons given above concerning loss of nitrogen and lack of PEO on the surface, there were several others. First, when plasma treated samples were dipped in water for several seconds, the surface was extremely wettable and held a film of water. If the rinsing was continued for 2-3 minutes, the wettability was lost. Secondly, further evidence arose during the PFB experiments. Placing the samples under vacuum to remove any adsorbed PFB was found not to be sufficient in that a small amount of fluorine (< 1 percent) was found on untreated controls. Therefore, a step was added where the samples were rinsed briefly in acetone once they were removed from vacuum. This action not only decreased the fluorine content on the surface, it also markedly decreased the

nitrogen content as well. As a result of the above findings, the following study was carried out and is outlined in Figure A-6.

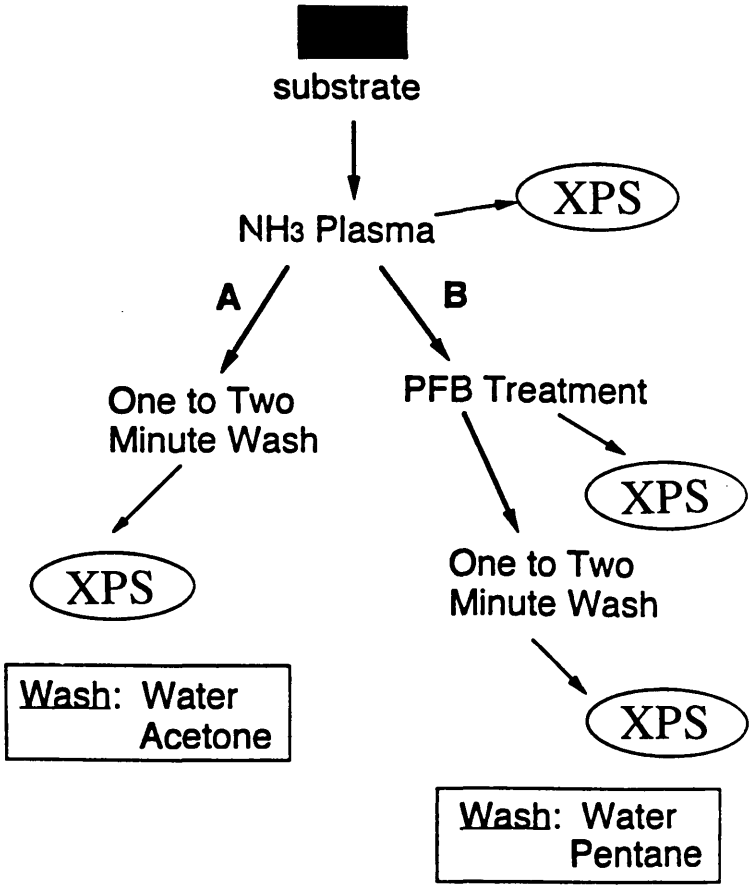


Figure A-6. Procedure used to verify surface fragmentation after exposure to ammonia plasma.

Washed samples of both LDPE and PET were exposed to an ammonia plasma under the same conditions as before, and several were set aside for XPS analysis. The remaining samples were either rinsed in water or acetone for 2-3 minutes, or treated with PFB. The PFB samples

were then either rinsed in water or pentane for 2-3 minutes, or simply set aside after vacuum treatment. In all cases, the samples were analyzed in XPS for surface composition changes. The reason for the pentane rinse was due to the fact that the liquid phase reaction for PFB[12] takes place in pentane, and since it is a non-polar solvent, it was of interest to see what its effect would be on the plasma-treated, now polar, polymer surfaces.

Figure A-7 outlines the results of the study for PET. For the samples with no PFB treatment, the loss of nitrogen was significant after washes with acetone and water, showing decreases in nitrogen content of 55 and 65 percent, respectively. For the PFB treated samples, the changes were even more dramatic. There is an initial drop in nitrogen content of approximately 17 percent following the reaction with PFB. This can be attributed to the PFB now on the sample surface blocking part of the signal from the nitrogen. Following a wash with

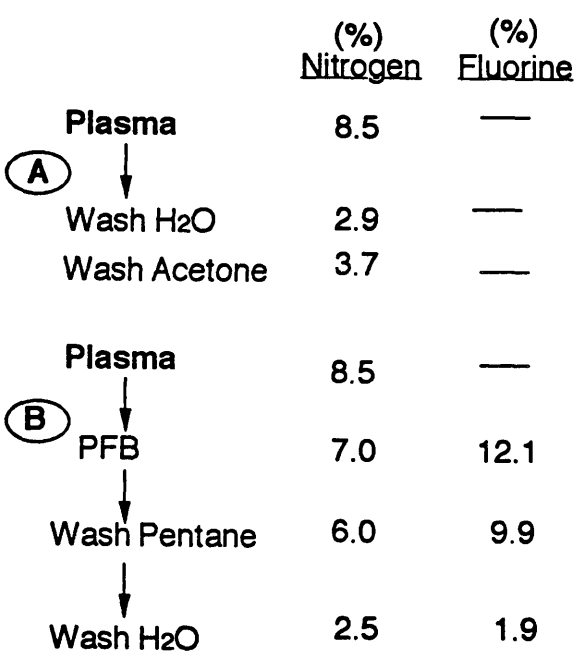


Figure A-7. XPS results of wash study on PET.

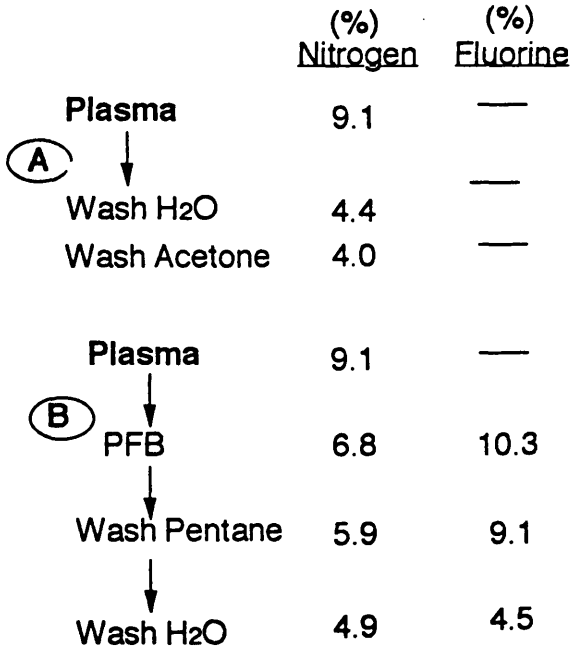


Figure A-8. XPS results of wash study on LDPE.

pentane, nitrogen levels dropped to 29 percent of their original value, fluorine content dropped to 18 percent. When these samples were then rinsed with water, the losses increased markedly, reaching 70 percent for nitrogen and 85 percent for fluorine.

The results from the study for LDPE are shown in Figure A-8. Non-PFB treated samples showed a loss in nitrogen content of 50 percent and 56 percent for water and acetone washes, respectively. For the PFB treated samples, there was again an initial drop in nitrogen due to the PFB coverage on the surface. When washed with pentane, losses of 11 percent fluorine and 35 percent nitrogen resulted. Losses again increased after washes with water to 46 percent and 56 percent of the original nitrogen and fluorine values, respectively. It should be noted that rinsing samples in water for 24 hours resulted in the same surface composition changes as the 2-3 minute washes.

The above results clearly indicate polymer surface fragmentation resulting from exposure to an ammonia plasma. The fragments, being polar, mainly wash away in polar solvent, with only some losses occurring in non-polar solvent. Nitrogen and fluorine losses occurred to a lesser extent for LDPE than PET, indicating that LDPE is more stable than PET in the plasma. This is also supported by the fact that LDPE showed a significantly greater presence of PEO stars on the surface than did PET. Surface fragmentation from ammonia plasma exposure has also been found with other polymer types such as poly(methyl methacrylate),[13] polycarbonates,[13,14] and polystyrene.[14]

## A.4 Conclusions

The primary conclusion to be drawn from the above study is that PECVD using an ammonia plasma is not suitable as a means to deposit primary amines on polymer surfaces where these surfaces are then used in aqueous solution. It is clear from the XPS scans that a large amount of nitrogen is deposited on the surface, and from PFB studies that a significant amount of this nitrogen is the desired primary amine. However, as important as it is to functionalize the surface, it is imperative that these surfaces also be stable, especially when in contact with aqueous solution. The lack of PEO stars binding to the surface, and the loss of surface nitrogen after exposure to polar solvent, makes the procedure unsuitable as a way to obtain monolayer coverage of PEO star molecules for the purpose of increased biocompatibility. A different means of functionalizing polymer surfaces with primary amines needs to be found, resulting in stable surfaces, before the remainder of the procedure can be tested for its truest potential.

## A.5 References for Appendix A


1. Verdon, S.L., Chaikof, E.L., Coleman, J.E., Hayes, L.L., Connolly, R.J., Ramberg, K., Merrill, E.W., and Callow, A.D., *Scanning Microscopy*, 4, 341 (1990).

2. Merrill, E.W. and Salzman, E.W., *Am. Soc. Artif. Intern. Organs*, 6, 60 (1983).

3. Nagoaka, S., Mori, Y., Takuchi, H., Yokota, K., Tanyawa, H., and Nishiumi, S., *Polymer Preprints*, 24, 67 (1983).

4. Brush, J.L. and Uniyal, S., *J. Poly. Sci.*, 66, 377 (1979).

5. Furusawa, K., Shimura, Y., Otobe, K., Atsumi, K., and Tsuda, K., *Kobanshi Ronbunshu*, 34, 309 (1977).

6. Mark, J.E., Elastomers and Rubber Elasticity, J.E. Mark and J. Lal, eds., Washington DC, American Chemical Society, ACS Symposium Series 193, 1982.

7. Desai, N.P. and Hubble, J.A., *Biomaterials*, 12, 144 (1991).

8. Lutz, P. and Rempp, P., *Makromol. Chem.*, 189, 1051 (1988).

9. Gnanou, Y., Lutz, P., and Rempp, P., *Makromol. Chem.*, 189, 2885 (1988).

10. Nakayama, Y., Takahagi, T., Tusami, S., Hatada, K., Nagoaka, S., Suzuki, J., and Ishitani, A., *J. Poly. Sci., Poly. Chem.*, 26, 559 (1988).

11. Nilsson, K. and Mosbach, K., *Meth. in Enzymol.*, 104, 56 (1984).

12. Gombotz, W.R. and Hoffman, A.S., *J. Appl. Poly. Sci.*, Applied Polymer Symposium 42, 285 (1988).

13. Lub, J., Vanvroonhoven, F.C.B.M., and Benninghoven, A., *J. Poly. Sci., Poly. Chem.*, 27, 4035 (1989).

14. Lub, J., Vanvroonhoven, F.C.B.M., Bruninx, E., and Benninghoven, A., *Polymer*, 30, 40 (1989).

# APPENDIX B

## Estimation of Inter-Detector Lag in Multi-Detection Gel Permeation Chromatography

### B.1 Introduction

In recent years, the use of multiple detectors for gel permeation chromatography (GPC) has become more common. Probably the two most common detectors coupled with the traditional differential refractive index (DRI) detector are the differential viscometric (DV) detector and the light scattering (LS) detector. An advantage of coupling either or both of these detectors to the DRI (or some other concentration sensitive) detector is the ability to identify the molecular mass of a polymer in each elution volume increment. However, accurate determination of these absolute molecular masses requires a precise estimation of the inter-detector lag such that the concentration and LS or DV signals corresponding to any elution slice are correlated correctly. Several methods for estimating this lag have been reported in the literature[1-5] that are based on a variety of experimental techniques or analyses. We present here a different method for estimating the detector lag between a concentration detector and a second detector in which the signal is dependent on the molecular weight of a polymer sample. This straightforward method is analytical in its approach and does not require any knowledge about the MWD of the polymer sample used in the analysis.

### B.2 Theory

In GPC, the elution volume of a polymer molecule depends on its hydrodynamic size, not its mass. In most cases, the sample injected in GPC contains molecules of the same class, e.g., linear, star, comb, so that the sizes of molecular species increase as the molecular weights increase. Thus, in general, increasing elution volumes correlate with decreasing molecular

weights (exceptions being non-homogeneous samples, such as those containing mixtures of both linear and branched polymer molecules). In a multi-detection GPC run, one signal (e.g., DRI) depends only upon the concentration of the solute molecules, while the molecular weight dependent signal (LS or DV) is a function of both the concentrations as well as the molecular weights of these eluting molecules. Therefore with increasing elution volumes, the molecular weight dependent signal will generally peak before the concentration signal because of the constantly decreasing contribution from the molecular weights of the eluting solute molecules. Consequently, the peaks corresponding to these two signals would be offset even if the two detectors were at the same position in the flow system. In reality, different detectors are at different positions in the flow system which leads to a lag between their signals.

B.2.1 Light Scattering Detector

If we consider the case of the LS detector, we have the signal measured from any elution slice as being proportional to the excess Rayleigh ratio, $R_\theta$

$$R_\theta = Kc[MP(\theta) - 2A_2cM^2P^2(\theta)] \qquad \text{(B-1)}$$

where c is the concentration of the polymer of molecular weight M in that elution slice, and $A_2$ is the corresponding second virial coefficient. $P(\theta) = 1 - 2\mu^2\langle r_g^2\rangle/3!+...$ is commonly termed as the structure factor (where $\mu = (4\pi/\lambda)\sin(\theta/2)$, $\lambda$ being the wavelength of the incident light, and $r_g$ the radius of gyration) and K is an optical constant.

In a GPC experiment, realistic upper estimates for the concentration are approximately $10^{-4}$ -- $10^{-5}$ g/cc at the peak of the concentration chromatogram, and generally $A_2$ = $10^{-3}$ -- $10^{-4}$ mol cc/$g^2$. As a result, the $A_2$ term in Eq. B-1 can usually be neglected for GPC-LS calculations. Therefore, for our purposes, Eq. B-1 can be written as:

$$R_\theta = KcMP(\theta) \qquad \text{(B-1a)}$$

(although this simplification does not have an effect on the final outcome of our analysis).

For further simplifying the analysis, we would like to set $P(\theta) \approx 1$. If $P(\theta) \neq 1$, then the analysis becomes slightly more complex since $P(\theta)$ is a function of $r_g$, and $r_g$, in turn, varies with

the elution volume. For a low-angle laser light scattering (LALLS) detector, since $\theta$ is small, $P(\theta) \approx 1$ in any case. For a MALLS detector, $P(\theta) \neq 1$ for higher angle detectors unless $r_g << \lambda$ (i.e., the scattering molecules are small). However, it is preferable, if possible, to use LS signals from a higher angle detector (such as 90°, for example) since they are less susceptible to noise due to extraneous scatterers. Therefore, when this analysis is applied to MALLS detectors, the preferred strategy is to use higher angle LS signals from scatterers small enough such that $P(\theta) \approx 1$.

With the assumption of $P(\theta) \approx 1$, the dependence of the LS signal on the elution volume, v, can be written as:

$$\frac{dR_\theta}{dv} = \frac{\partial R_\theta}{\partial c}\frac{dc}{dv} + \frac{\partial R_\theta}{\partial M}\frac{dM}{dv} \qquad \text{(B-2)}$$

From Eq. B-1, we obtain $\frac{\partial R_\theta}{\partial c} = KM$ (B-3a)

and $\frac{\partial R_\theta}{\partial M} = Kc$ (B-3b)

The elution dependence of polymer molecules from GPC columns can generally be written as an equation of the general form:

$$\text{Log } M = B - D\,v \qquad \text{(B-4)}$$

$$\Rightarrow \frac{dM}{dv} = -2.303\,D\,10^{B-Dv} = -2.303\,D\,M \qquad \text{(B-5)}$$

The concentration peak occurs at $\frac{dc}{dv} = 0$, while the LS peak occurs at $\frac{dR_\theta}{dv} = 0$.

From Eq. B-2, we see that for $\frac{dR_\theta}{dv} = 0$, $\quad \frac{\partial R_\theta}{\partial c}\frac{dc}{dv} = -\frac{\partial R_\theta}{\partial M}\frac{dM}{dv}$

$$\Rightarrow KM\frac{dc}{dv} = -Kc\frac{dM}{dv} \qquad \text{(B-6)}$$

Using Eq. B-5, we rewrite the above condition as:

$$\left[\frac{dc}{dv}\right]_{\frac{dR_\theta}{dv}=0} = 2.303\,D\,c \qquad \text{(B-7)}$$

Since all quantities on the right hand side of Eq. B-7 are finite (even though small), we can conclude that under practical GPC conditions, $\frac{dc}{dv} \neq 0$ when $\frac{dR_\theta}{dv} = 0$ (unless the sample is perfectly monodisperse). Thus the peaks of the concentration and the LS chromatograms generally cannot be matched to get the detector lag since they both do not represent the same elution slice.

Given all this, in order to find the inter-detector lag, we need to find the elution slice on the concentration chromatogram that should correspond to a known slice on the LS chromatogram. We choose, as our reference slice, the peak of the LS signal. Referring to Eq. B-7, we see that the elution slice corresponding to $\frac{dR_\theta}{dv} = 0$ is the slice on the concentration curve (at elution volume v*) where

$$\frac{1}{c}\frac{dc}{dv} = 2.303\,D. \qquad \text{(B-7a)}$$

The quantity on the left hand side is easily evaluated by fitting the peak portion of the concentration chromatogram with a smooth curve, and then calculating the fractional slope as a function of elution volume. The offset between the peaks of the concentration and the LS signals is given by $v_{\text{peak concentration}} - v^*$. The inter-detector lag then is the difference between the $v_{\text{peak LS}}$ and v* for the data as it is received by the collection instrument (since $v_{\text{peak LS}}$ and v* would coincide if there was no lag).

Once the concentration and LS chromatograms have been obtained for the sample being utilized in the lag estimation procedure, a value for D (the slope of the log molecular weight vs. elution volume curve for this polymer-column combination) is required. It is possible to determine the true value of D independently from a traditional GPC calibration procedure, such as the peak calibration method[6]; this true value of D should directly yield, in one step, the correct detector lag using Eq. B-7a. However, the availability of the true value of D is not a requirement; some reasonable estimate of D can be used as an initial value in an iterative procedure. The first calculation yields a first estimate of the detector lag. At this point, the GPC-LS calculations should be carried out for the sample with this value of detector lag. These

calculations will yield an estimated molecular weight vs. elution volume plot for this sample. The slope of this plot should be entered as the next estimate for D in a new iteration of the above procedure to yield another detector lag value and hence another apparent molecular weight vs. elution volume plot. These iterations should be carried out until the detector lag converges to a constant value. With this value, the slope of the molecular weight vs. elution volume plot is the true D for this polymer-column combination. The final convergence value does not depend on the initial estimate of D. It should be noted here that this iterative procedure is more cumbersome given the necessity of careful evaluations of D from the sample data.

### B.2.2 Differential Viscometry Detector

In a viscometric detector, the signal being measured is the pressure drop of the fluid as it flows through a capillary tube. This pressure drop is proportional to the viscosity of the fluid. For polymer solutions, the intrinsic viscosity, $[\eta]$, is evaluated by the equation:

$$\frac{\ln\left(\frac{\eta_s}{\eta_o}\right)}{c} = [\eta] + k''[\eta]^2 c \qquad \text{(B-8)}$$

where the subscript "o" refers to the solvent, and "s" refers to solution containing the polymer at concentration c. k" is referred to as the Kraemer constant. For low concentrations (typical in GPC experiments), $k''[\eta]^2 c << [\eta]$. Therefore, the pressure drop measurement, p, of any elution slice allows the evaluation of the intrinsic viscosity of that slice through the relationship:

$$[\eta] = \frac{1}{c} \ln \frac{p}{p_o} . \qquad \text{(B-9)}$$

This intrinsic viscosity is dependent upon the polymer molecular weight as $[\eta] = K'M^{\alpha}$, where K' and $\alpha$ are the Mark-Houwink constants for a polymer. Substituting for $[\eta]$ from the Mark-Houwink equation and rearranging:

$$\ln \frac{p}{p_o} = c\, K'\, M^{\alpha} \qquad \text{(B-10)}$$

Differentiating, we get

$$\frac{d\left(\ln \frac{p}{p_o}\right)}{dv} = K' c \frac{d(M^{\alpha})}{dv} + K' M^{\alpha} \frac{dc}{dv} \qquad \text{(B-11)}$$

Substituting from Eq. B-4 and setting $\frac{d\left(\ln \frac{p}{p_o}\right)}{dv} = 0$,

$$K' M^{\alpha} \frac{dc}{dv} = - K' c \frac{d(10^{\alpha(B - Dv)})}{dv}$$

$$= 2.303 D \alpha K' c (10^{\alpha(B - Dv)}) \qquad \text{(B-12)}$$

Thus the elution slice on the concentration curve corresponding to $\frac{d\left(\ln \frac{p}{p_o}\right)}{dv} = 0$ is given by :

$$\frac{1}{c} \frac{dc}{dv} = 2.303 D \alpha \qquad \text{(B-13)}$$

The detector lag can then be evaluated in a method similar to that mentioned in part A. However, in this analysis, the constant $\alpha$ needs to be pre-determined in order to carry out the calculations. One could either use a polymer sample for which $\alpha$ is available in the literature, or use narrow standards of the polymer to determine $\alpha$ from intrinsic viscosity experiments.

## B.3 Experimental

Experiments were carried out on the DAWN-F (Wyatt Technologies, Santa Barbara, CA, USA) MALLS detector ($\lambda = 6328$ Å) coupled to a 150-C (Waters, Milford, MA, USA) GPC system. The chromatography was carried out using a combination of Waters Ultrahydrogel 500 and 2000 columns, with a guard column, at 25 °C. The mobile phase was water (containing 0.02% $NaN_3$ as a bacteriostat) with a flow rate of 0.92 ml/min. The analyses were performed using Lotus 1-2-3 (Lotus, Cambridge, MA, USA) and the Astra program provided with the DAWN-F. Curve fitting was carried out with Microsoft Excel (Microsoft, Redmond, WA, USA). Polymers utilized in the studies were narrow MWD polyethylene oxide (PEO) standards, molecular weights ranging approximately from 50,000 to 900,000 (Toyo Soda, Japan), and a

broad MWD PEO sample, nominal molecular weight 200,000 (Polysciences, Warrington, PA, USA). The detector lag estimation analyses were carried out on the DRI signals from narrow MWD PEO samples of molecular weight less than 100,000. The $v_{peak\ LS}$ for each sample was evaluated from the 90° LS detector signal. The resulting mean value of the detector lag was then used in subsequent molecular weight calculations with the GPC-LS data.

## B.4 Results and Discussion

The analyses on the low molecular weight polymer samples yielded an estimated detector lag of $0.124 \pm 0.009$ ml. The elution behavior of a number of different PEO samples was then obtained using the mean value of the detector lag in the molecular weight calculations. The elution behavior, thus obtained, for the broad and narrow MWD PEO samples overlapped, as they should. Figure B-1 shows the data for the elution dependence of the broad MWD sample.

As pointed out elsewhere[2], the slope of the elution curve is sensitive to the inter-detector lag. Too high a value of detector lag leads to an artificially flat elution curve, while too low a value leads to too steep a curve. (This is especially noticeable for narrow MWD samples, since changing the value of the detector lag leads to significant changes in the polymer concentration assigned to any elution slice. Calculations for broad MWD samples are generally less susceptible to this problem since their concentration chromatograms are spread out.) Therefore, we can use the slope of the elution curve as the parameter to ascertain the accuracy of our method. For this purpose, the absolute reference elution curve was obtained from a traditional GPC peak calibration method using only the DRI detector with narrow MWD standards (of the same polymer as the samples used for the analysis). Shown in Figure B-1 is the elution depedence (linear over the evaluation range) corresponding to such a GPC peak calibration method using the narrow MWD PEO standards. Examination of Figure B-1 shows that the elution curve obtained by using the estimated detector lag correlates well with the peak calibration data. Since the detector lag obtained by our analysis yields (from the GPC-LS data)

an elution curve for a polymer-column combination that agrees with the reference curve, the value of the lag must be correct.

The methods described by Balke et al.[4] and Kuo et al.[5] determine the inter-detector lag (for GPC-LS and GPC-DV systems, respectively) by comparison with reference data obtained from calibration with narrow MWD standards. In a sense, the philosophical underpinnings of our one-step method (i.e. utilizing the slope from a reference curve directly for the calculation of the inter-detector lag) are similar to these methods, the major difference being that they obtain the inter-detector lag through an empirical approach, while we use an analytical one. On the other hand, our iterative method, though not as simple, obviates the necessity of the reference data for obtaining the inter-detector lag.

Some points should be noted here:

1. It is easier to carry out the lag estimation with reasonably narrow MWD samples since they provide high $\frac{dc}{dv}$ values. However, broad distribution samples are also utilizable, as long as the peak slices can be easily identified. If the iterative procedure is being followed, the intermediate estimates of D (from the sample data) must be evaluated carefully since the data range is small.
2. The calculation for the offset of the two peaks are carried out on the concentration curve. Generally concentration detectors have a less noisy signal than molecular weight sensitive (mainly dust). Still, the calculations of the fractional slope must be accurate, since the accuracy of the method depends on this quantity directly.
3. If we use the D value from a previous iteration in the next iteration of the analysis, the effects of column dispersion do not bias our values. This is consistent with the fact that one cannot expect the detector lag to be a function of the column efficiency.
4. Since the method described here utilizes GPC columns in-line, both the concentration and molecular weight dependent signals have lower noise by virtue of the columns eliminating most extraneous scatterers in the flow field (particularly important for aqueous systems) as well as suppressing the pressure fluctuations due to the pump.

5. This analysis assumes the elution curve to be linear over the elution volume range under consideration. Generally, this should hold, especially for narrow MWD samples, but if this linearity condition does not hold, the analysis would need to be modified if it is to be utilized.

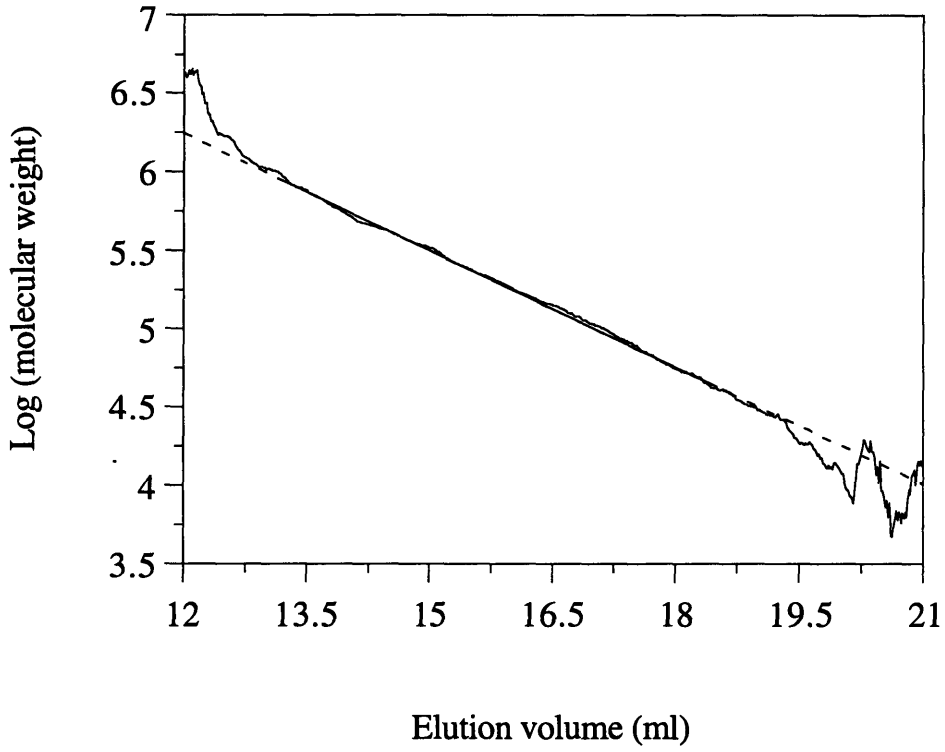


Figure B-1. Data showing elution behavior of broad MWD PEO samples using GPC-LS with the detector lag value obtained by this method (rough line) and elution curve for traditional peak calibration method using narrow MWD PEO samples (smooth line). The reference elution curve is extrapolated for clarity (dashed line).

## B.5 References for Appendix B


1. D. Lecacheux and J. Lesec, *J. Liq. Chromatogr.* , 5 , 2227 (1982).

2. T. H. Mourey and S. M. Miller, *J. Liq. Chromatogr.* , 13 , 693 (1990).

3. J. Billiani, I. Amtmann, T. Mayr and K. Lederer, *J. Liq. Chromatogr.*, 13 , 2973 (1990).

4. S. T. Balke, P. Cheung, R. Lew and T. H. Mourey, *J. Appl. Poly. Sci. Appl. Poly. Symp.*, 48, 259 (1991) .

5. C.-Y. Kuo, T. Provder, M. E. Koehler and A. F. Kah, in T. Provder (Editor), *Detection and Data Analysis in Size Exclusion Chromatography* (*ACS Symposium Series*, No. 352), American Chemical Society, Washington, DC, 1987, p. 130.

6. W. W. Yau, J. J. Kirkland and D. D. Bly, Modern Size-Exclusion Liquid Chromatography: Practice of Gel Permeation and Gel Filtration Chromato-graphy, John Wiley & Sons, New York, 1979.